Deliverable D3.5 – Feasibility analysis of dynamic *en-route* charging technical report

Project acronym & number:	UNPLUGGED
Project Number	314 126
Project title:	Wireless charging for Electric Vehicles
Status:	Draft
Authors:	UNIFI
Contributors:	CIRCE, CRF, UNIFI, VTEC, CONTI, IDIADA (TfL, CIRCE Reviewers)
Due date of deliverable:	31/10/2014
Document identifier:	UNPLUGGED-D3.5 Feasibility analysis of dynamic en-route charging APP v150728.01.docx
Revision:	Rev.06
Date:	28/07/2015

Unplugged

UNPLUGGED: Wireless charging for Electric Vehicles

UNPLUGGED project aims to investigate how the use of inductive charging of Electric Vehicles (EV) in urban environments improves the convenience and sustainability of car-based mobility. In particular, it will be investigated how smart inductive charging infrastructure can facilitate full EV integration in the urban road systems while improving customer acceptance and perceived practicality. UNPLUGGED will achieve these goals by examining in detail the technical feasibility, practical issues, interoperability, user perception and socio-economic impacts of inductive charging. As one special variant, inductive *en-route* charging will be investigated thoroughly.

As part of the project, two smart inductive charging systems will be built, taking into consideration requirements from OEMs, energy utilities and end users. The systems will be innovative and will go beyond the current state of the art in terms of high power transfer, allowing for smart communication between the vehicle and the grid, as well as being in line with the latest inductive charging standards and considering interoperability. These innovative inductive charging systems designed and built as part of the project will then be tested and assessed in order to understand their potential impacts on urban mobility and the acceptance of e-mobility. Application in an *en-route* charging scenario in particular will be examined for different vehicle types, ranging from cars to buses.

It is anticipated that UNPLUGGED will provide clear evidence on and demonstrate whether the use of smart inductive charging infrastructure can overcome some of the perceived barriers for e-mobility, such as range and size of on-board energy storage, and practical difficulties associated with installing traditional charging post infrastructure.

Project Consortium

- fka Forschungsgesellschaft Kraftfahrwesen mbH Aachen , Germany
- ENIDE SOLUTIONS .S.L , Spain
- CENTRO RICERCHE FIAT SCPA, Italy
- UNIVERSITA DEGLI STUDI DI FIRENZE, Italy
- VOLVO TECHNOLOGY AB, Sweden
- Continental Automotive GmbH, Germany
- Hella KGaA Hueck & Co., Germany
- VRIJE UNIVERSITEIT BRUSSEL, Belgium
- IDIADA AUTOMOTIVE TECHNOLOGY SA, Spain
- TRL LIMITED, United Kingdom
- COMMISSARIAT A L ENERGIE ATOMIQUE ET AUX ENERGIES ALTERNATIVES, France
- ENDESA SA, Spain
- ENEL DISTRIBUZIONE S.P.A., Italy
- FUNDACION CIRCE CENTRO DE INVESTIGACION DE RECURSOS Y CONSUMOS ENERGETICOS, Spain
- POLITECNICO DI TORINO, Italy
- TRANSPORT FOR LONDON, United Kingdom
- BAE Systems (Operations) Ltd, United Kingdom

More Information

Coordinator: Axel Barkow (coordinator)

Mail: barkow@fka.de Tel +49 241 8861 185 - Mobil +49 163 7027833 - Fax +49 241 8861 110

Forschungsgesellschaft Kraftfahrwesen mbH Aachen

Steinbachstr. 7 - 52074 Aachen - Germany

info@unplugged-project.eu - www.unplugged-project.eu

Dissemination Level

PU	Public	X
PP	Restricted to other program participants (including the Commission Services)	
RE	Restricted to a group specified by the consortium (including the Commission Services)	
CO	Confidential, only for members of the consortium (including the Commission Services)	

Change History

Version	Notes	Date
V141103	Creation of the Draft (UNIFI)	03/11/2014
V141203	Final version of the contributions (CIRCE, CONTI, CRF,IDIADA, UNIFI, VTEC)	3/12/2014
V141210	Revisions from involved partners and final draft(UNIFI)	10/12/2014
V141230	Internal review process (TfL, CIRCE)	30/12/2014
Final	Submitted document (UNIFI)	03/12/2015
V150728	Conclusion added (correction request) (UNIFI)	28/07/2015

Abbreviations

EM	Electrical Machine
ESS	Energy Storage System
ICE	Internal Combustion Engine
AC	Alternating Current
ADC	Analog to digital converter
DC	Direct Current
DSP	Digital Signal Processor
EV	Electric Vehicle
EVSE	Electric Vehicle Supply Equipment
FS	Full Scale
PF	Power Factor
RMS	Root Mean Square
SAR ADC	Successive Approximation ADC
WPT	Wireless Power Transfer
BMS	Battery Management System
FEV	Full Electric Vehicle
PHEV	Plug-in Hybrid Electric Vehicle
RESS	Rechargeable Energy Storage System
EDLC	Electrical Double Layer Capacitor
ECU	Electronic Control Unit
BEV	Battery Electric Vehicle
CPM	Charging Point Manager
EVSA	Electric Vehicle Supplier Aggregator
BRT	Bus Rapid Transit

Table of Contents

1 Executive Summary (UNIFI)

This document has the aim to provide a preliminary study on the feasibility of dynamic wireless charging: taking into account the vehicle, infrastructure, business model and driver interaction with the system.

First part of this document is dedicated to the analysis of the technical needs of energy storage systems that have to be used with dynamic charging. Firstly, an analysis of the market ready solutions is given and then the impact on the general architecture of the vehicle is analyzed. Personal vehicles and commercial or people movers ones are analyzed separately: this because different weights, space and load conditions generate different needs. On the vehicle side, also the topic of communication system has been taken into account in order to have a complete picture of the vehicle needs.

In the second part, the document analyzes the infrastructure side. Firstly, an overview over possible technical solutions to enable wireless charging and then an analysis on the monitoring strategies of power absorption is provided. In particular, for the first part seven possible solutions to ensure wireless recharge is presented, characterized by different coil size, positioning and connection. These have been tested using as input the real world data acquired from the public transportation of the city of Firenze. Second part, focuses on a benchmark with pros and cons using a market ready energy meter, giving also a procedure of the measurement points over the UNPLUGGED proposed device.

Last part of the document focuses on two feasibility analysis, firstly a research study over drivers' attitude to correctly align the vehicle on the recharge infrastructure and secondly on scenario and business model development for a possible application on the city of Firenze: this city has been chosen as case study because it is member of the Advisory Board. The drivers' behavior has been investigated both with a simulator-based approach and on a real instrumented vehicle.

2 Analysis of energy storage systems for dynamic charge: Vehicle (CRF, VTEC, CONTI)

In this chapter, an analysis of the storage systems that could be installed on passenger and freight vehicles has been made. Initial idea was to perform an analysis about the driving dynamic when the vehicle is over the electrified line due to the coupling forces between infrastructure and the vehicle itself. However, during the static analysis CRF recognized that these magnetic coupling forces are not influential: any driver could recognize the magnetic coupling force. So, the activity of CRF has been turned to study the differences between static and dynamic energy storage systems.

2.1 Analysis of energy storage systems for dynamic charge (CRF)

With respect to energy storage systems, dynamic charging introduces a different management of recharging than the static or *en-route* case. In particular, it is necessary to take into account need to manage possible current/power peaks during the activation/deactivation of the wireless charging system, while a vehicle is moving over different primary side segmented coils. Current/power peaks on the vehicle DC bus depend on the primary side configuration. As described in [1], for dynamic charging scenario, a real Korean application is experiencing different primary track, with different segment lengths and controls. In this application, only part of the track is powered and the primary side is buried in the ground in order to optimize energy transfer and reduce costs. From the vehicle point of view, it becomes very important to guarantee maximum power transfer for a short time slot. New solutions for energy storage could be explored, taking into account wireless charging technology aims to significantly reduce the energy content of battery.

2.1.1 Lithium battery developments, ultra-capacitor integration and new technologies

In the last years, research has been widely active on the development of new lithium battery technologies and ultra-capacitors, trying to get better performance as well as to integrate components to get benefits of each technology. A possible system improvement could be the integration of energy-downsized battery packs, as described in Deliverable D3.1, into hybrid solutions that integrate the ultra-capacitors with the DC bus, in order to enhance the high power acceptance for a limited time range, maximizing the power transfer. Furthermore, with this solution, an improvement of system regenerative braking capacity might be reached. Below is a list of under-development and test technologies [2]:

- **Carbon Nanotube Electrode Lithium**: MIT (Massachusetts Institute of Technology) is developing a cathode able to accept and release many more positive ions than standard lithium batteries. This could see energy densities and power flows increased up to ten times that of current on-the-market technology. These new cathodes could also improve solid-state capacitors, or enable a combination of battery-capacitor. The estimated time for having this technology available for EV is about ten years.
- **Copper Nanowire Cathode Lithium**: Colorado State University is developing a new cathode using microscopic thin copper wires in substitution of graphite electrode. These wires can accept and release ions on the entire surface increasing the capacity and power of conventional lithium batteries.
- **Lithium Air Carbon**: Li-air batteries are based on a metal-air chemistry. They use lithium oxidation at the anode and oxygen reduction at the cathode to induce a current flow. The lithium-air couple has a theoretical energy density that can reach up to about 10000 Wh/kg [3]. However, this battery technology is not expected to be available on the market for electric cars until 2020.
- **Lithium Silicon:** Northwestern University is actively researching the use of silicon electrodes to substitute carbon ones. The development of more flexible electrodes would allow an increase in energy content and power, reducing charging time.
- **Carbon Foam Capacitor Hybrid**: Michigan Tech is working on a power storage device to combine benefits of chemical battery (energy density) and of solid-state capacitor (power peak management). This technology is called asymmetric capacitor: On the capacitor side, energy is stored by electrolyte ions that are physically attracted to the charged surface of a carbon anode. Combined with a battery-style cathode, this design delivers nearly double the energy of a standard capacitor. A unique carbon

foam is used as a cathode to increase the storage capacity. The hybrid battery-capacitor not only weighs less than a conventional lithium battery, but it also delivers more of its charge than a typical capacitor. The unit can be recharged thousands of times without showing performances degradation.

- **Lithium Silicon Polymer**: Lawrence Berkeley National Laboratory is working on this polymer. The technology is a tailored polymer that conducts electricity and binds closely to lithium-storing silicon particles, even as they expand to more than three times their volume during charging and then shrink again during discharge.
- **Lithium Sulphur Carbon Nanofibre**: Stanford University is researching the integration of carbon nanofibers on anode. Carbon nanotubes coated on the inside with sulphur allow batteries to store up to ten times the energy of conventional lithium batteries. Sulphur is a more environmentally friendly (and cheaper) electrode coating, because it is readily available and non-toxic
- **Lithium Manganese Composite/Silicon Carbon Nanocomposite**: Envia's primary development is a proprietary cathode material based on manganese, an abundant metal that is stable when used in the battery. Manganese is also less expensive than the more common cobalt-based cathode material.

Additional research activities related to battery development are on going. In particular, activities linked with **graphene** technology [4]. Graphene batteries are made by enhancing existing Li-Ion batteries. Improvement in battery performance is reached by enriching the electrodes with graphene; it changes chemical and physical properties of batteries, allowing better results in charge-discharge rate characteristics as well as improved capacity. Graphene is a promising material for energy storage, also for high performance supercapacitors. For high power applications, it is critical to have high specific capacitance with fast charging time at high current density. Graphene-based supercapacitors exhibit high stability and significantly improved electrical double layer capacitance and energy density with fast charging and discharging time at a high current density, due to enhanced ionic electrolyte accessibility in deeper regions. Some tests on supercapacitor cells demonstrate high value of their capacitance after 10,000 cycles, suggesting stable performances of supercapacitors at high current rates. That means they are suitable for fast charging-discharging applications. High performances are assured by the highly porous nature of grapheme.

Japanese scientists are working on graphene nanosheets (GNS), analyzing the lithium storage properties of GNS materials as high capacity anode materials for rechargeable lithium batteries [5]. Graphite is a practical anode material used for lithium batteries, because of its capability for reversible lithium ion intercalation in the layered crystals, and the structural similarities of GNS to graphite may provide another type of intercalation anode compound. While the accommodation of lithium in these layered compounds is influenced by the layer spacing between the graphene nanosheets, control of the intergraphene sheet distance through interacting molecules such as carbon nanotubes (CNT) or fullerenes (C60) might be crucial for enhancement of the storage capacity.

Other European research projects this subject include Autosupercap (project ended in the first half of 2014). The aim of the project was to develop supercapacitors of both high power and high energy density, affordable for automotive industry. High power and sufficient energy density are required for both the performance of the power system but also to reduce the target weight of supercapacitors. Some target performance levels have been established in the FP7-GC Workprogramme including 20 kW/kg power density and 10 Wh/kg energy density for supercapacitors; furthermore, there was a cost target of 10€/kW.

Main objectives of the projects were to:

- develop different types of carbon materials and electrodes (in terms of structures) for supercapacitors in combination with different electrolytes and separating membranes
- select the best supercapacitor cells, also taking into account the cost
- perform a cost and life-cycle analysis of the proposed supercapacitors
- identify supercapacitors and materials technologies for future exploitations
- investigate and develop recycling methodologies.

2.1.2 Driving Cycle Analysis

Driving Cycle Analysis is useful to better understand mechanisms that should be taken into account for the development of the dynamic wireless charging process. With reference to evaluations made in the Firenze city for Urban Bus mission, the number of coils to guarantee expected performance in dynamic

charging scenario is very high. Already developed dynamic charging sites can offer some useful considerations for deeper evaluations. For example, as already mentioned, some tests conducted by KAIST in Korean applications are useful to evaluate the opportunity of using segmented coils with different lengths and only part of the predetermined track is powered. For this reason, it can be useful to define a simple simulator that allows taking into consideration constraints and parameters for wireless dynamic charging:

- Vehicle speed
- Length of primary and secondary coils
- Distances between coils
- Power transfer and efficiency
- Track length and active track
- Vehicle battery energy content
- Vehicle average consumption at constant speed
- …

An example of simulation with following data is shown in Figure 2.1, from the Matlab script simulator.

```
Vehicle_Speed_kmh=30;    %Vehicle Speed (avg) [km/h]
PrimaryCoilLenght=1;     %Primary coil lenght [m]
SecondaryCoilLenght=1;   %Secondary coil lenght [m]
DistanceCoils=0.2;       %Distance between coils   [m]
Efficiency=0.7;          %Power Efficiency (average)
TransferPower=25;        %Transfer Power (max) [kW]
TrackLenghtCoil=3000;    %Track lenght with coils [m]
TrackLenghtTot=10000;    %Track lenght total [m]
InitSOC=50;              %Init SOC Percent
BatteryEnergy=4;         %Battery Energy content [kWh]
VehicleConsumpt=0.16;    %Vehicle Specific Energy Consumption [kWh/km]
```

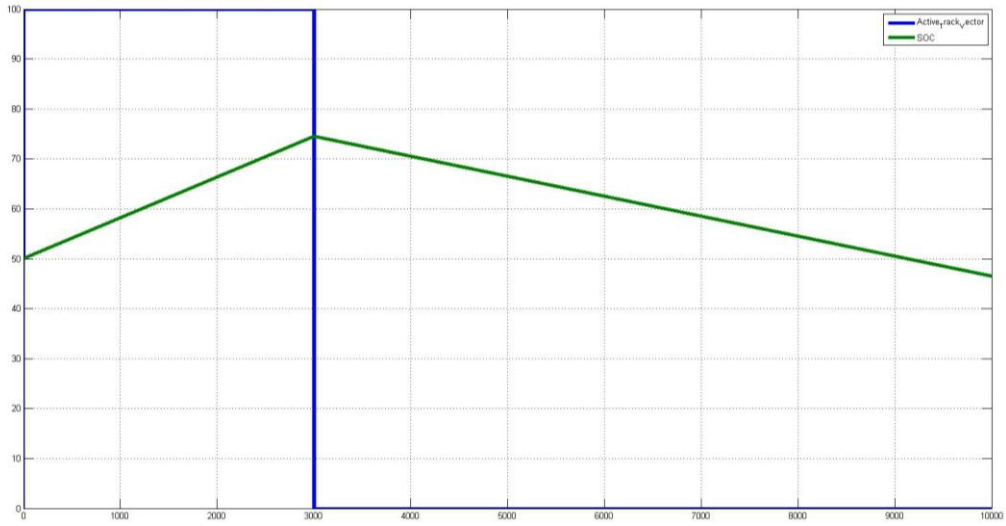

Figure 2.1 – SOC of simulated battery

In the above image, the results of a simulation are shown. Total length of path is 10 km, active track is 3 km (at the beginning of the track, in blue in the image). Image describes battery SOC profile, considering a very small battery (4 kWh, about 20% of a standard battery for small passenger EV). Energy consumption on the entire track is slightly higher than the recharged energy; vehicle consumption is about 1,6 kWh for 10 km, while the recharged energy is about 1,46 kWh (25 kW coils with an average efficiency on the total energy transfer of 70%).

2.2 Impact of recharge device on vehicle layout

From the E/E architecture point of view, dynamic charging should not introduce relevant difference with respect to static or static *en-route* charging, at least for the power components; considerations made in the previous paragraph on energy storage can improve ESS efficiency and enable ESS technology diffu-

sion. However, supplementary components or systems could be necessary to take into account additional problems dynamic charging introduces:

- alignment with respect to lateral displacement
- speed management
- access to charging lane and billing for energy transferred to vehicle
- activation/deactivation of the primary side

2.2.1 Lateral alignment management

While a vehicle is moving on an active track for dynamic charging, the lane alignment (active lane keeping) can be automatically adapted via the driver assist systems. Objective is to optimize the efficiency rate of the energy transfer and to synchronize the energy transfer. For the integration of this function vehicle needs to be equipped with a positioning system and an actuator as control position system, to allow the vehicle to follow a predetermined trajectory. Positions sensors detect vehicle lateral deviation from the trajectory. A control ECU acquires data coming from the sensors to calculate and command steering. The steering actuator is activated according to received commands to maintain vehicle within the maximum allowed deviation. While the steering actuator is generally an electric motor, the automatic control technologies can be distinguished by their method of determining the lateral deviation. Three different technologies can be defined:

Magnetic guidance system: magnetic material (for example magnetic tape or discrete magnets) are used, positioned in the center of the lane (either located on, or embedded in); under the vehicle some magnetometers are mounted to estimate the strength of the magnetic field when the vehicle passes over the magnetic material. On the basis strength and on the characteristics of the magnetic field strength, an ECU calculates the relative deviation. Advantages of this technology are the low sensitivity to environmental factors and the positioning accuracy. Disadvantages are related to possible distortion of magnetic field due to ferrous components inside the vehicle or in the roads and the low maximum lateral range due to low field strength.

Vision based guidance system: one or more cameras are installed on a vehicle to get information; generally, they use specific lane attributes, but last system have been designed to work on unstructured road (without specific lane markers). Advantages are the few modifications needed on the road and the additional data available from the image acquisition (road curvature, slope, traffic signals, obstacles, etc.). Disadvantages are related to sensitivity to environmental and weather factors.

DGPS based guidance system: Global Positioning System (GPS) is an accurate method for the position determination in a global coordinate system. It is quite low cost and accurate, but for precise positioning requirements, the Differential Global Positioning System (DGPS) is needed, to have an accuracy from the roughly 10 meters for standard GPS to centimeter level for DGPS. DGPS uses a fixed network constituted by ground-based reference stations to broadcast the difference signal between the satellite systems information and the known fixed positions. Advantages are the quite low cost infrastructure, the availability in all weather conditions and the unlimited sensor range. Disadvantages are the need for a good GPS signal, possible transient error when the available satellite changes, relatively low update rate (<20 Hz) and significant latency.

2.2.2 Speed management

Outside from the urban environment, for example in highway installation, it could be useful to have a function that keeps the vehicle running at a constant speed with two objectives: managing multiple vehicles access to electrified tracks and facilitate the activation-deactivation mechanism. For the second objective, in any case, it is necessary to enable interaction between vehicle and infrastructure with communication systems or passive technologies for vehicle presence identification and verification. Cruise Control and Adaptive Cruise Control functions, already present in many of new vehicles, could be integrated with dynamic charging control systems.

2.2.3 Additional evaluations on vehicle architecture

For the primary side management, in order to allow activation of energy transfer only when the vehicle is moving on the primary side, specific activation/deactivation mechanism must be defined. Mechanism definition depends on the technology used for the power transfer (both on primary and secondary side)

and for the communication between vehicle and infrastructure. An evaluation of communication gateway used for static or *en-route* charging, developed for this project, must be evaluated for dynamic applications taking into account:

- operative distance
- number of units in primary side
- pairing mechanism and timing
- …

Other possible mechanisms for activation/deactivation can be passive, for example, RFID, but timing constraints are very strict. Communication between primary and secondary side and activation/deactivation mechanism must be guaranteed in particular if the active lane can be freely accessed. To limit these problems, some hypotheses for dynamic charging are being proposed, such as developing specific lanes with limited access to authorized vehicles, where speed can be kept almost constant (e.g. ecoFev demonstration). An hypothesis of authorization mechanism, that allows also defining some billing procedures and options, can be the vehicle identification through its ID plate, using technology already available for highway or traffic restricted area access.

Figure 2.2 – Vehicle ID technology

2.3 Analysis of commercial vehicle ESS for dynamic charge (VTEC)

Rapid recharging is very demanding even for lithium ion batteries, both for WPT and in accepting regenerated braking power. The BMS must aggressively manage the power input (charge) rate to the battery as well as the delivery (discharge) rate, so as to prevent potential damage to the batteries due to overcharge, overheating, and potential fire hazards. As with most other ebus systems, these batteries power the bus traction system as well as auxiliaries (e.g. electric power steering and AC). It is vital that the selected on-board ESS (Energy Storage System) e.g. batteries, ultra-capacitors etc. are appropriately selected (chemistry, capacity, lifecycle thermal properties) and have the energy storage capacity and power recharge/discharge characteristics without physical, electrical or chemical degradation from WPT rapid recharges. However, one should have in mind that we are not necessarily talking about charging. In theory, there is one major use case difference between static and dynamic power transfer: in the static case, you would most likely[1] use the transferred energy to charge the energy storage system for later use for propulsion. In the dynamic case it would be, in an ideal world, not even necessary to have an energy storage system if all roads everywhere was equipped for dynamic power transfer.

When less than 100% of the road being “electrified”, you could use a standard hybrid battery (i.e. small) if using a hybrid vehicle with electrical machine (EM) and ICE. But this is a Catch-22 situation: from the driver point of view it is important to know what is the available charging infrastructure at his arriving place in order to optimize drivetrain, driving attitude, ESS, etc. However, from the infrastructure point of view, it is important to know the number of vehicles and their energy demands in order to optimize the infrastructure dimension.. This implies that the first commercial vehicles intended for dynamic charging will be hybrids (EM and ICE) unless the route and transport mission are very well defined as with e.g. BRT. The hybrid batteries are more power optimized than energy optimized, see Ragone plot in Figure 2.3, and

[1] Even though it is possible to run e.g. HVAC and cooling compressors for refrigerator trucks

should suit the rapid dynamic inductive charging well. Without ICE, you would need larger batteries i.e. more energy optimized if not most of the route used by the vehicle is “electrified”. Full electric vehicles (FEVs) and plugin hybrid electric vehicles (PHEVs) make use of battery cells optimized for high energy rather than for high power. This means that the power abilities of cells in the battery packs are limited. In order to enhance their performance a hybrid Rechargeable Energy Storage System (RESS) architecture can be used combining batteries with electrical-double layer capacitors (EDLCs). Such a hybridized architecture can be accomplished using passive or active systems, see [6] for possible solutions to achieve this.

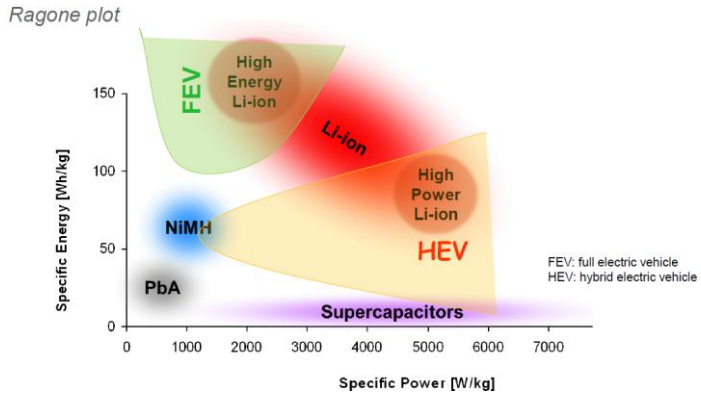

Figure 2.3 - Ragone plot

As a simplified example if you charge 10 minutes @ 125 kW you only need 125 kW x 0.16 h = 20 kWh = 300 to 400 kg batteries. At 90 km/h in a heavy-duty[2] vehicle, this will take you 14 km on battery power. If the electrical road can supply both traction power and charging power at the same time (250 kW), you need 50% of the road electrified to be able to drive 100% electric. Three other examples for a long haul truck, a bus and a distribution truck are shown in below.

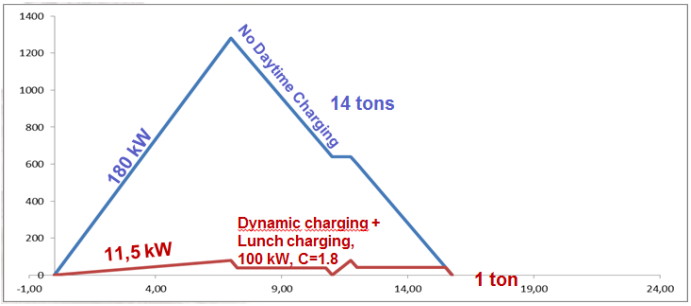

Figure 2.4 Intercity heavy duty truck with and without dynamic charging

In Figure 2.4, an intercity heavy-duty truck is used as an example presenting the difference of battery size with or without dynamic charging. In the blue graph the truck starts with night time charging at 180 kW followed by daytime running when truck is assumed to consume 160kW average at total vehicle and trailer weight of 60 tons. Then you need 14 000 kg of batteries. In the red graph the truck starts with night time charging at 11.5 kW followed by 160 kW dynamic power transfer for propulsion and 100 kW charging at lunch time. Then you need 1000 kg of batteries i.e. a 90 % decrease in battery size! Larger batteries than 1 ton would not be practical since the trailer load capacity would be reduced, and the maximum bogey weight limitation of the truck, would be exceeded. In Figure 2.5, a bus is used as an example presenting the difference of battery size, with or without opportunity charging. In the blue graph the bus starts with night time charging at 46 kW followed by daytime running when bus is assumed to consume 30 kW average at target weight 14 tons. Then you need 3800 kg of batteries. In the red graph the bus starts with night time charging at 1,9 kW followed by 100 kW opportunity charging at end stops. Then you need 250 kg of batteries i.e. a 90 % decrease in battery size! In the green graph, 400 kg of super caps are used instead of batteries and charged at 160 kW at every bus stop. The same amount of energy could be transferred dynamically when route does not have long enough stops, or to far apart. Dynamic charging would also be beneficial when using larger/heavier articulated buses.

[2] 125 kW traction power needed at 90 km/h

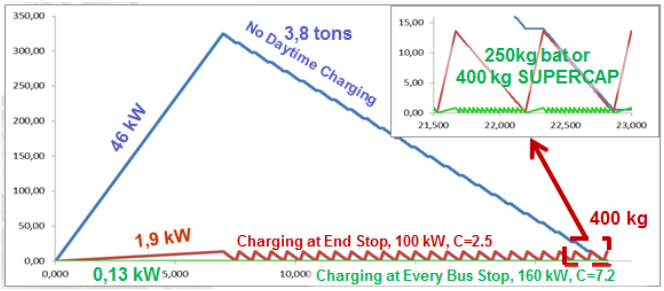

Figure 2.5 - Bus example

The numbers above are theoretical but as have been proven by the KAIST/OLEV system in the city of Gumi, South Korea the rechargeable bus battery can be smaller than usual, only 1/5 the size of a normal electric bus battery when recharging pads cover only 10–15 percent of the bus route. In Figure 2.6, a distribution truck is used as an example presenting the difference of battery size with or without opportunity charging. In the blue graph the truck starts with night time charging at 20 kW followed by daytime running when truck is assumed to consume 18 kW average. Then you need 1 700 kg of batteries. In the red graph the truck starts with night time charging at 1.5 kW followed by driving to loading docks to charge at 40 kW. Then you need 300 kg of batteries i.e. an 80% decrease in battery size! The same amount of energy could be transferred dynamically when route does not have long enough loading/unloading times, or to far apart. Conclusion: Many electric commercial vehicle use cases could be solved with static/stationary charging but for heavy-duty applications like long haul transport you need dynamic charging or the battery weight would be unrealistic.

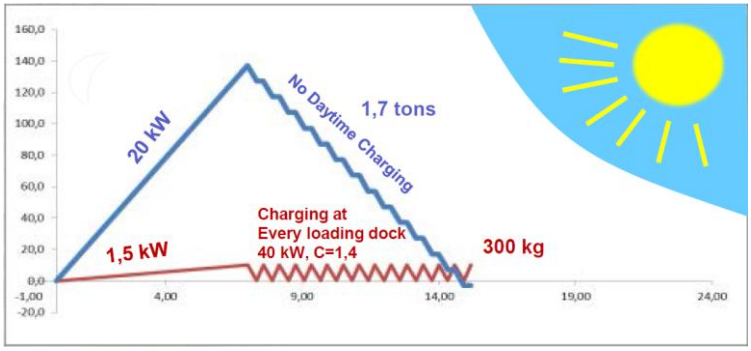

Figure 2.6 - Distribution truck example

2.4 Impact of recharge device on vehicle layout (VTEC)

The same principal electrical architecture used for static charging could also be used for dynamic charging. However, there are some areas beside the electrical properties for the energy storage system that could differ more or less:

- Mechanically
- Alignment requirement
- HMI
- BMS

2.4.1 Mechanically

Coil geometry:

- The longer the length of the coil in the vehicle the more energy could be transferred at the same speed. This advantage may be possible to exploit in some applications e.g. heavy duty buses but impossible in other e.g. short wheel base medium duty trucks.
- Wider coils may be used to be able to tolerate larger misalignment than in the case for static charging. This may be needed especially if the vehicle is not equipped with a lane keeping assistance system.

Shielding:
In a dynamic situation, it may be more difficult to control the exact alignment position where to turn on and off the charging. This implies that a vehicle supposed for dynamic charging may need more magnetic shielding, in front of and after the coil, than a vehicle for static/stationary charging. This is also likely to be the case when longer segments of primary sides are used. To minimize the impact of magnetic fields, shielding needs to be installed underneath and maybe even on the sides of the vehicle. Tests and simulations are needed to optimize the amount, placement and weight of the shielding required.

2.4.2 Alignment requirement and HMI

The positioning system developed within UNPLUGGED makes a rough position estimation using camera based techniques and uses RFID tags for the fine positioning. It determines the actual position and hence calculates the trajectory and displays this information to the driver. This only works at very low speeds (for example in parking maneuvers) and is not applicable for dynamic or even static *en-route* charging. Here a different approach has to be found. Because of the higher speed when approaching a charging segment, the information has to be provided earlier to the driver, maybe using the lane keeping assistance or lane departure warning commonly used in today's vehicles. In addition, since some dynamic charging solutions use long primary side segments, e.g. OLEV and Primove from Bombardier, you need to go within a certain speed range to be able to charge i.e. this makes up for also using commonly used cruise control or adaptive cruise control. So far alignment issue is explained in details only for moving (X – axis) and lateral (Y – axis) directions. However some manufactures e.g. Bombardier suggest that alignment issues might be considered for air gap (Z – axis) direction as well. Alignment in Z direction means to reduce air gap between primary and secondary coil in order to increase mutual inductance and thereby coupling coefficient. As long as obtained power on secondary side and total transfer efficiency are proportional to mutual inductance, any increases on this parameter will directly improve power transfer. Reducing air gap can be achieved by employing a lowering mechanism for the secondary side. Lowering mechanism is generally chained into chassis of vehicle in order to approximate receiver unit into primary unit. This contributes to interoperability by changing mutual inductance value until desired power output level is reached. Lowering mechanisms are actuated only in Z direction and might be equipped either with hydraulic or mechanic tilting system but it will require additional maintenance cost. Even though lowering units improve the power transfer efficiency, they have technical well-known disadvantages, which affects cost and performance of inductive charging system. Since unobstructed underbody structures for vehicles are very limited, integration of lowering mechanism might become difficult. In addition, components of lowering mechanism can collect dirt, snow and dust and thus might affect charger efficiency level. Therefore it can be clearly seen that employing lowering mechanism is totally a trade-off between efficiency and additional weight and should be defined in initial phase of system design whether power transfer range in Z direction is well enough to meet ground clearance of vehicle

2.4.3 BMS

In some vehicles, the battery management system is designed to operate in charge mode or in discharge mode. Therefore, while driving, the vehicle is in discharge mode and does not allow any charging process except for recuperation while braking. If this is the case, there is a potential difference between the BMS in the vehicle charging statically compared to the one dynamically charging. However the energy coming from the dynamic charger may still be used for propulsion directly without taking the longer route via the batteries i.e. it would potentially be more efficient. This in turn implies a fast control loop, perhaps faster than needed for battery charging, between the primary side and the secondary side.

2.5 E/E integration: Wireless communication for dynamic *en-route* charging (CONTI)

For wireless dynamic en-route charging it is evident that communication between the vehicle and the infrastructure has to be wireless, too. Thus a wireless communication system in the EV is required as a communication link between charging management and other vehicle systems on the one side and the infrastructure on the other side.

Today wireless communication is a common technology in almost all fields of everyday life and in vehicles as well. In the near future all new cars and commercial vehicles (particularly EVs) will be equipped with short and long range wireless communication system(s) anyway. These communication systems will be used for different use cases (e.g. navigation, infotainment, communication, and internet) and can obviously be used for wireless charging too.

To enable this use case, the communication system has to be connected (directly or indirectly) with all systems involved in wireless charging of the EV. This can be done by extending existing vehicle buses (e.g. CAN, Flexray, Ethernet, ...) or by implementing new connections. Furthermore the communication system must contain some software modules to support the protocols and all other requirements of wireless charging. Maybe some of these software modules will be placed in other ECU's (e.g. charging management unit) of the vehicle.

Figure 2.7 - Prototype of wireless communication system for UNPLUGGED

For all wireless charging possibilities (static as well as dynamic en-route charging) should be and can be used the same communication system (hardware and procedure). Therefore regarding general requirements we refer to D3.1. But some special requirements for dynamic en-route charging have to be considered.

During driving quick connection establishment between frequently changing communication partners will be of particular importance. For stationary charging there is enough time to exchange data between car and charging station – the car is driving slowly to its parking lot and then it won't move at least for minutes. For dynamic en-route charging the situation differs completely. On a motorway (e.g. at 150 km/h) the use of a specific primary coil by a driving car will be only short term and timing requirements for wireless charging can be more than 10 times higher. To identify and to locate the car exactly a fast, safe and stable communication is needed. Several possibilities to support these requirements are available.

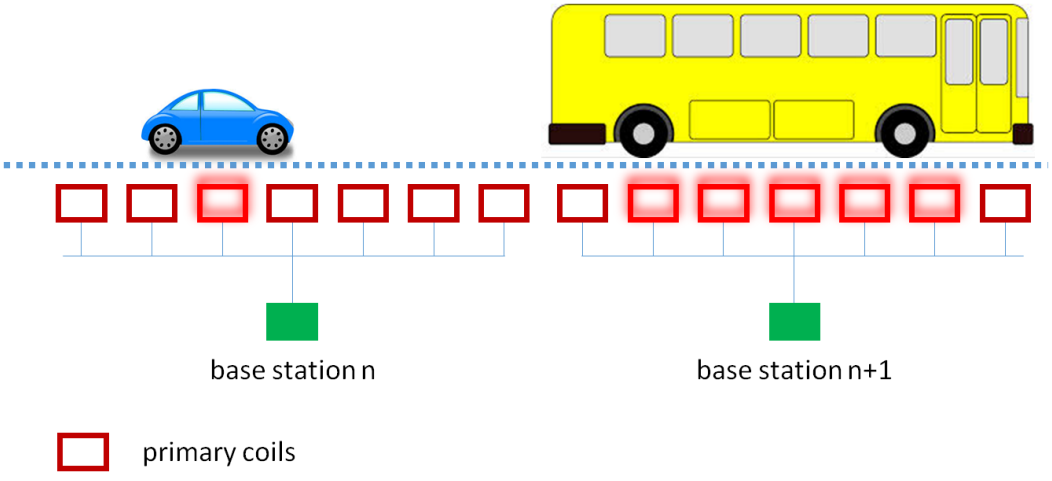

Figure 2.8 - Primary side of wireless charging system for dynamic en-route charging

Basically should be assumed that one base station supports more than one primary coil (see **Fehler! Verweisquelle konnte nicht gefunden werden.**) and possibly more than one vehicle at the same time. In cooperation with the navigation system of the car the planned path should be known and the communication system can connect to the next base station(s) on the vehicle's route. Switching from one to the next base station could be accelerated by using more than one communication channel at the same time.

This provident communication with next base stations should mitigate timing problems to an already today feasible level. For example: A time interval of 500 ms should be enough to log-on the car by a base station. A car driving with a speed of 100 km/h covers a distance of appr. 14 m in 500 ms. Outside of buildings common Wi-Fi systems reach transmit ranges up to 100 m and more. That implies all data exchange needed for charging (identification and authorization of car/driver, status, technical data for charging, …) should be completed before the vehicle reaches the first primary coil of the next section. For lower velocities the situation is even more relaxed.

For wireless communication UNPLUGGED is using a short range communication (2.4 GHz-WLAN). To increase range and data rate upcoming Wi-Fi standards (e.g. long range WLAN, 5 or 60 GHz- WLAN) could be exploited instead. By using more capable antennas and/or repeater transmit range could be extended too. An additional possibility is to use different communication technologies (e.g. long and short range communication) simultaneously. Some general parts of the communication (e.g. general data of the car, identification and authorization of driver, charging schedule,…) could be transmitted via cellular networks precociously too.

Finally to connect the vehicle to a single primary coil we would propose a basic communication direct between primary and secondary coil (near-field magnetic induction communication). By using this method we can be sure to couple the right vehicle with the right coil and the timing to switch on the primary coil can be exactly adjusted.

3 Analysis of dynamic en-route charge: Infrastructure (CIRCE, IDIADA)

3.1 Analysis of technical solutions (CIRCE)

This document covers the energy analysis of an *en-route* dynamic and static charge system for two actual bus route in the city of Florence, one as medium range archetype and one as long range. Moreover, the technical viability of different charge scenarios is assessed, considering static charge, static *en-route* charge, a combination of static *en-route* and dynamic charges, and finally only dynamic charge.

The analyzed cases are:

- Case A: static charge at the beginning and at the end of the route
- Case B: static *en-route* charge at the bus stops
- Case C: static *en-route* charge without time increase
- Case D: dynamic charge only
- Case E: static *en-route* charge without time increment at the bus tops combined with dynamic charge sections
- Case F: static *en-route* and dynamic using discrete primary coils of the same power
- Case G: static *en-route* and dynamic charge using the same coils

3.1.1 Bus data (Firenze line 23)

The bus used is the Volvo 7700

- Vehicle weight: =18900 kg
- Tire-asphalt friction coefficient =0.0056
- Vehicle frontal area =4.288 m^2
- Aerodynamic coefficient =0.65
- Wheel radius =0.452 m

Other Parameters used:

- Gravity =9.81 m/s^2
- Air density=1.25 kg/m^3

In order to assess the energy required during the route, the worst case has been considered, that is, a continuous 6 kW consumption with all the cooling and auxiliary systems connected. A Simulink mathematic model of the vehicle has been developed, whose input is the operation cycle (times and speeds) and provides the required force, instantaneous power and energy consumption.

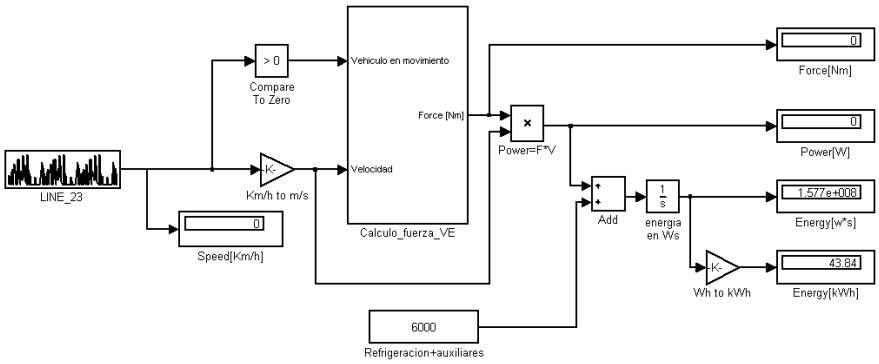

Figure 3.1 - Simulink model of the vehicle

Two cases have been considered for the calculation of the energy consumption: maximum consumption without energy recovery in braking, and consumption considering a 30 % energy recovery during braking.

3.1.2 Data of the studied road

A representative bus route of the city of Florence has been chosen, route number 23, whose time, distance and speed data have been provided by UNIFI.

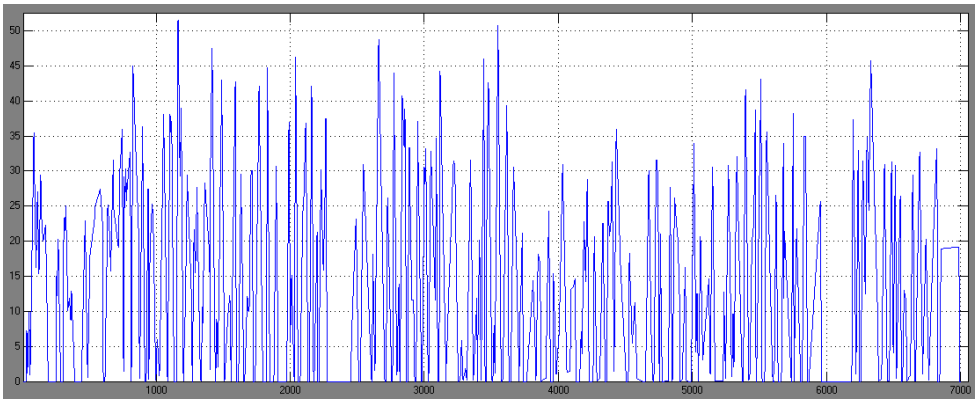

Figure 3.2 - Complete route for Florence bus 23

The route includes 89 stops with a total distance around 27 km (26300 m), and an average route time of **7009 s** (1 h 57 minutes), **1577 s** corresponding to the stops and **5432 s** to the movement. Total maximum consumption according to the calculated cycle is **43.9 kWh**, which divided by the total length of the route gives a result of **1.6 kWh/km**.

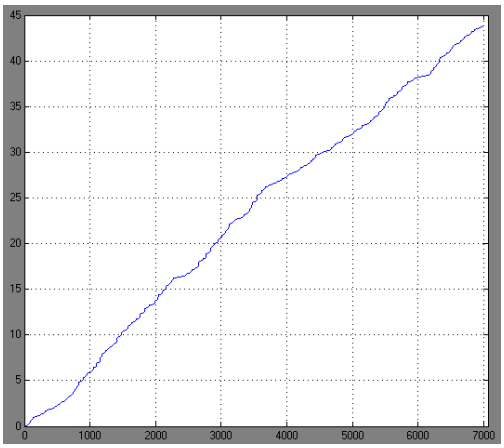

Figure 3.3 - Energy consumption along the route

This average consumption does not consider slopes, that is, it has been obtained considering a completely flat 27 km route. As an example, if a 1% average slope is used, consumption will rise to 66 kWh, or 2.44 kWh/km. For a more accurate energy requirement estimation, each cycle between stops has been individually developed, so as to determine charge requirements at each stop or *en-route*. Each cycle includes the idle time in the first stop and the running time until the bus gest to the next stop. The next figures show two examples. The first one is the cycle between stops 1 and 2, with an initial stop time of 33 s at stop 1.

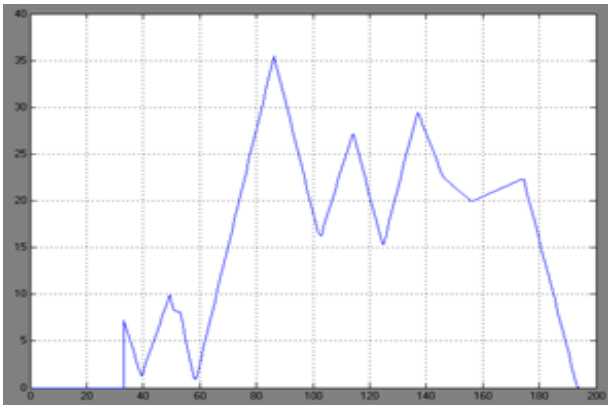

Figure 3.4 - Cycle between stops 1 and 2

Table 3.1 - Cycle between stops 1 and 2

Bus Stop	Number	Time (s)	Total Time (s)	Average speed (km/h)	Distance (m)	Energy [kWh]
Stazione Valfonda	1	33,3	33,3	0	0	
1 to 2		161,2	194,5	17,5	785,6	
Ridolfi - Anche Ind.	2		194,5	0	785,6	1,102

The second one is the cycle composed of stops 48, 49 and 50, where there is no stop at the “Stazione Cellini”, although the vehicle reaches it at zero speed.

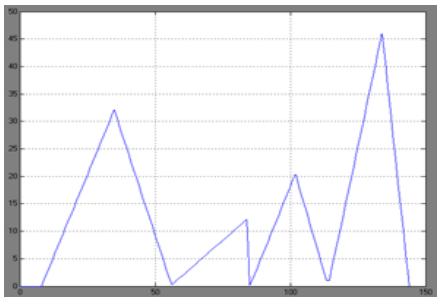

Figure 3.5 - Cycle composed of stops 48, 49 and 50

Table 3.2 - Cycle composed of stops 48, 49 and 50

Bus Stop	Number	Time (s)	Total Time (s)	Average speed (km/h)	Distance (m)	Energy [kWh]
Ricorboli - fm0400	48	8.4	8.4	0	0	
		77.3	85.7	14.2	305.1	
Cellini - fm0541	49	0	85.7	0	0	
		54.7	140.4	33.9	514.5	
Serristori - fm0542	50	6.4	146.8	0	819.6	1.161

The table in “Annex 2 – Energy consumption distribution” shows the whole energy consumption divided into the different stops. It is worth pointing out that there are 14 stations (6, 8, 10, 13, 30, 46, 49, 55, 73, 79, 80, 81, 82 and 86) where the bus does not stop, so the installation of a charge system is not planned.

3.1.3 Consumption between stops

Assuming that consumption during stop time is only due to auxiliary services, which are 6 kW, total idle consumption is 2.63 kWh. The table in “Annex 3 – Idle consumption at the bus stops” shows idle consumption at each stop.

3.1.4 Charge analysis

Assuming that energy requirement for the whole route is approximately 44 kWh, different possibilities to transfer it to the vehicle are studied. Average stop time, route time and speed between stops will be considered. The main idea behind the study is that inductive charge affect as little as possible current times of the route. If a 30 % dynamic braking recovery is considered, total energy consumption is 37 kWh

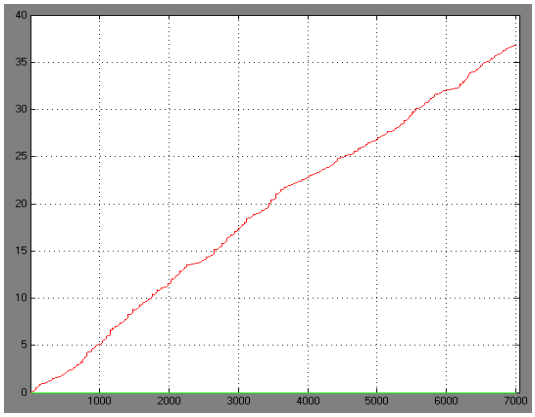

Figure 3.6 - Energy consumption considering braking recovery

3.1.4.1 Case A. Static charge at the beginning and at the end of the route

The first and simplest analyzed solution is static charge at the beginning and at the end of the route. This approach is the one having a lowest infrastructure cost, but implies the drawback of an increase in route time. The cases considered are:

- Using two 37 kW chargers: the bus would have to be one hour at the beginning and end of the route.
- Using two 50 kW chargers: the bus would have to be 44 minutes at the beginning and end of the route.
- Using two 100 kW chargers: the bus would have to be 22 minutes at the beginning and end of the route.

Figure 3.7 - Case A. Static charge at the beginning and at the end of the route

The shorter the desired waiting time at the ends of the route, the higher the power of the chargers and the cost of the infrastructure. As a starting point it is considered that batteries cannot be discharged below 20% SOC, so minimum battery capacity is 55 kWh, which considering a power density between 0,15 kWh/kg and 0,18 kWh/kg for ion-lithium batteries, gives a minimum battery weight between 310 and 370 kg. This capacity should be higher to face eventualities such as traffic jams.

3.1.4.2 Case B. Static *en-route* charge at the bus stops

In this case, there are 1577s (0.438 h) available to perform the charge. Among the 89 stops in the route, only 75 can be used for charging purposes, since there are 14 stations with zero stop time. That means that using for instance 50 kW chargers at every stop, the energy supplied to the vehicle would be 21.9 kWh, 15.1 kWh short of the target.

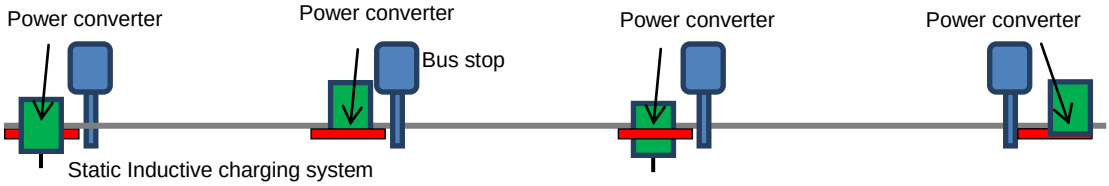

Figure 3.8 - Case B. Static charge at the bus stops

Figure 3.8 shows energy consumption along the route (blue), energy supplied at the stops (green) and their difference (red), which should also be supplied to the bus.

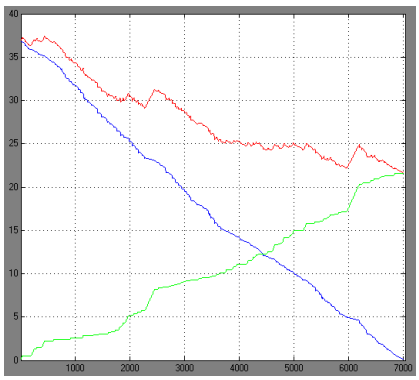

Figure 3.9 - Case B. Battery energy without charging (blue), energy supplied during stops (green) energy in the battery (red)

This extra-required energy (15.1 kWh) could be transferred to the bus in different ways. Two options are proposed:

- B-1: Static+ static *en-route*: charging at the beginning and the end of the route during 19 minutes, using 50 kW chargers.

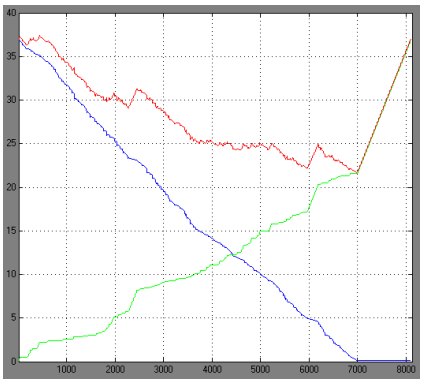

Figure 3.10 - Case B-1. Battery energy without charging (blue), energy supplied during stops (green) energy in the battery (red)

- B-2: Static *en-route* Not performing a long charge at the beginning and the end of the route, but increasing the required 19 minutes at the bus stops.

Both options have the same cost, since the chargers at the beginning and the end of the route are necessary in both cases, and the increase in route time would be the same (19 minutes). The only difference lien in that, in the second case, a 15.2 s average increase in stop time (19*60/75) should be established. Another option would be installing chargers only in those stations with a large stop time, increasing this time enough to transfer the required energy, and then reducing the infrastructure cost. Since route time needs to be increased in order to perform the inductive charge, it seems better to use the first option that is, charging the additional 19 minutes at the beginning and the end of the route, since the vehicle can charge without power consumption. If the extra charge is performed at the stops, instead, the consumption of the auxiliary systems during this additional 19 minutes should be added. If a minimum stop time at each station is considered, the 19 minutes divided among the 89 stations would require an additional 13 stop time, and 89 50 kW chargers. Thus, it is more economical to install chargers only at the stations with a longer stop time

3.1.4.3 **Case C. Static *en- route* charge without time increase**

In order to charge 37 kWh in 0,438 h stop time, rated power of each charger should be 85 kW. That is, 75 85 kW chargers would be required.

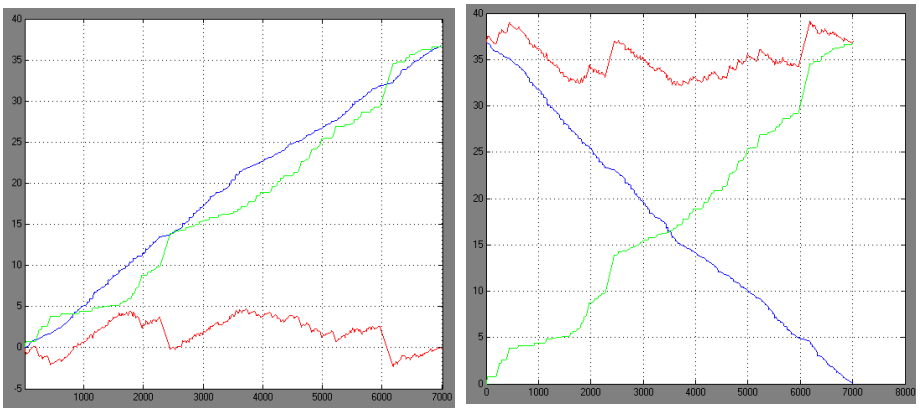

Figure 3.11 - Case C. Battery energy without charging (blue), energy supplied during stops (green) energy in the battery (red)

In this case, the batteries of the vehicle should be able to store 5 kWh at least.

3.1.4.4 Case D. Dynamic charge only

Another possible solution is to take advantage of the moving time of the vehicle (1.5 h) to perform dynamic charge. In order to determine the power required for the continuous charge system, it is necessary to know the distance and average speed of each section. This case does not include static charge at the stops. If the consumed energy for the whole route is 37 kWh, the power required for continuous charge should be 37 kWh/1.5 h ≈ 25 kW. That is, a 27 km line, able to transfer 25 kW all along the route would be required. That implies a very high infrastructure cost and, besides, this line should be composed of consecutive sections that would be energized as the vehicle moves over them, in order to avoid dangerous electromagnetic fields:

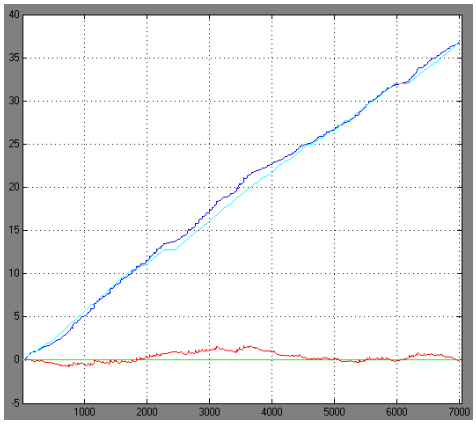

Figure 3.12 - Case B. Energy consumption along the route (dark blue), energy supplied along the route (light blue) and energy in the batteries (red)

In this case, the minimum battery capacity would be around 2 kWh (red line)

3.1.4.5 Number of required coils and chargers

Assuming an emitter coil length three times the size of the vehicle (12 m), the approximate number of coils would be 26300 m/36 m = 730 coils. If a power system is used for every two coils, 365, 25 kW chargers would be needed.

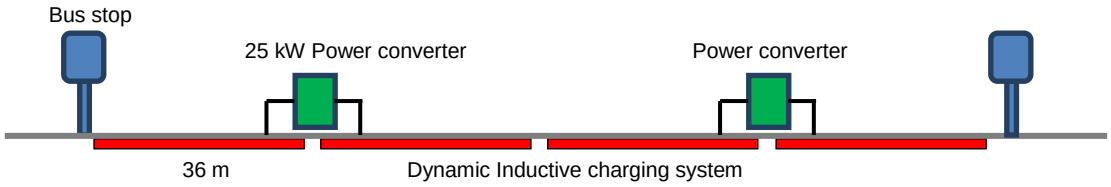

Figure 3.13 - Case D. Example of dynamic charge system between stops, using a charger to feed two coils

It is worth pointing out that the coils cannot be activated if vehicles not prepared for inductive charge are present within a distance shorter than the ground coil length. In the proposed case, the distance between the bus and other vehicles not prepared for inductive charge should be 36 m, if there would be a vehicle closer than 36m, the coil could not be activated and then the charging process will be interrupted. If this distance has to be reduced, the number of coils and chargers should be increased to cover the entire route. For instance, if coils of the same size as the bus are used (12m), the number of coils would be three times larger (2190) and, supposing that a charger can feed 4 coils, 548 chargers would be needed.

3.1.4.6 Case E. Static *en-route* charge without time increment at the bus tops combined with dynamic charge sections

Another possibility, which would not imply an increase on the time required for the bus to cover the route, would be a combination of static *en-route* charge at the stops and dynamic charge. The energy charged at the stops without time increase is, according to case B, 21.9 kWh. The remaining 15.1 kWh required would be transferred continuously while the bus is moving and thus, the required power would be 15.1 kWh/1.5 h = 10 kW.

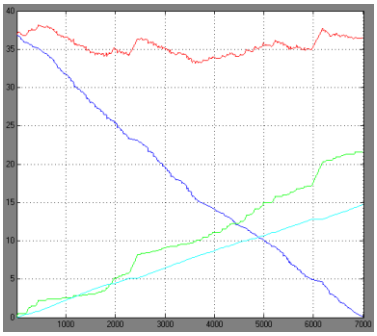

Figure 3.14 - Case E. Battery energy without charging (blue), energy supplied during stops (green) energy in the battery (red)

The minimum storage capacity for this option is around 4 kWh (maximum amplitude of the red line). The power of the dynamic charge system has been reduced from 25 to 10 kW. It should be assessed which has a lower cost, the continuous dynamic charge at 25 kW or the combination dynamic charge at 10 kW plus 50 kW static chargers. In this case, it would be necessary:

- 75, 50 kW chargers at the stops
- 365, 10 kW chargers feeding 730, 36 m coils.

3.1.4.7 Case F. Static *en-route* and dynamic charge using discrete primary coils of the same power

If the power rating of the dynamic charge coils is increases to the same value of the stationary charge ones, 50 kW, charge time would be reduced to 15.1 kWh/50 kW = 0.3 h, which, at the average speed of the route would correspond to a total winding length of 0.3*26300 m/1.5 h =5260 m. These 5260 m divided in sections of 36 m give 146 coils, and one charger per each two coils would lead to 73, 50 kW chargers. In total:

- 75, 50 kW chargers at the stops
- 73, 50 kW chargers along the route, feeding 146 coils of 36 m in length.

3.1.4.8 Case G. Static *en-route* and dynamic charge using the same coils.

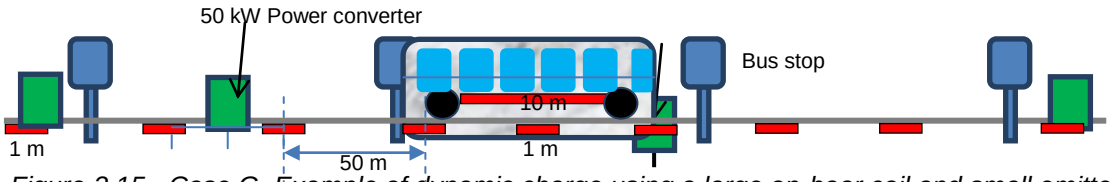

Figure 3.15 - Case G. Example of dynamic charge using a large on-boar coil and small emitter coils

In this case, the coil of the bus is 10m length, and the ground coils are 1 m length. In this case, the time the coils are facing each other at average speed is 2.05 s (10 m*1,5 h/26300 m = 2.05 s). Since the required energy is 15.1 kWh, with 50 kW coils the charge time is 0.3 hours (1080 s) and thus, the number of coils is 1080 s / (2.05 s/coil) = 526 coils. Average distance between coil centers is 26300 m/ 526 coils = 50 m. If each coil is fed by its own charger, 526 of 50 kW chargers are required. If a single charger can feed two coils, 263, 50 kW chargers will be needed.

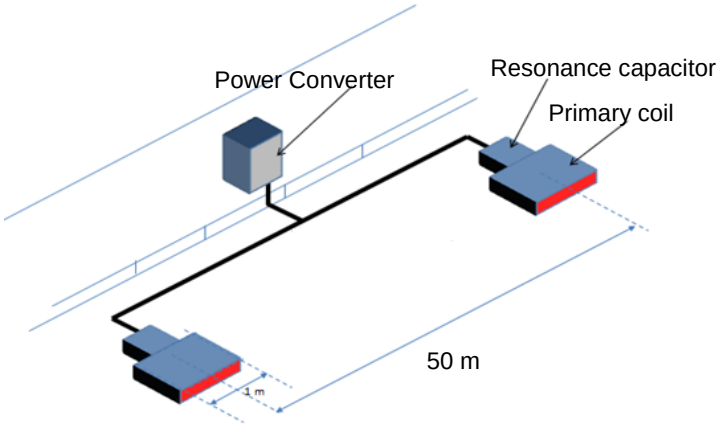

Figure 3.16 - Case G. Coil distribution along the route

That makes a total of 338, 50 kW chargers:

- 75, 50 kW static chargers at the stops
- 263, 50 kW dynamic chargers along the route, feeding 526 coils 1 m in length.

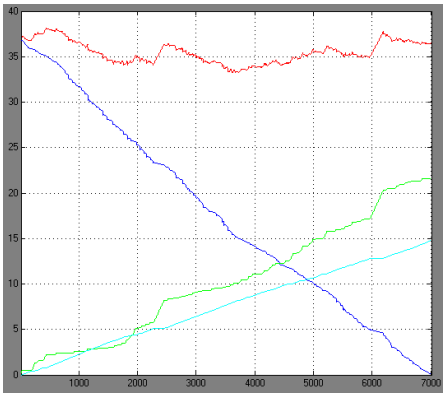

Figure 3.17 - Case G. Energy consumption along the route (dark blue), energy supplied at the stops (static charge, green), energy supplied along the route (dynamic, light blue) and energy in the batteries (red)

This situation presents the following advantages:

- Standardization, since the emitting coils (1 m in length) could be the same for static charge at the stops and for dynamic charge.
- Improved security for the people, since the emitting coil is turned on only when the vehicle is covering it and therefore is fully shielded.
- Reduced civil work, one 11 m coil each 50 m along the route.
- Flexibility: possibility of adding more coils later on if energy transfer has to be increased.
- The longer the length of the coil in the vehicle, the higher the energy transferred for the same speed.
- Interoperability among vehicles of different (smaller) sizes, which can use 1 m emitting coils, such as taxis.
- Mixed use: in case of emergency, dynamic charge coils can be used for stationary *en-route* charge without any danger of electromagnetic emissions, since they are completely shielded by the bus.

3.1.5 Summary

The main parameters of the different cases are summarized in the following table.

Table 3.3 - Case summary

	Time increase line 23	Number of static chargers	Number of dynamic chargers	Number of emitting coils	Battery weight [kg]	Approx. cost [Pike Research] [$]
Case A	44 minutes	2 of 50 kW	0	2 of 1m	305~370	33000
Case B	19 minutes	75 of 50 kW	0	75 of 1 m	-	-
Case C	0	75 of 85 kW	0	75 of 1m	28~33	3000
Case D	0	0	365 of 25 kW	730 of 36 m	11~13	1200
Case E	0	75 of 50 kW	365 of 10 kW	75 of 1m 730 of 36 m	22~27	2400
Case F	0	75 of 50 kW	73 of 50 kW	75 of 1m 146 of 36 m	22~27	2400
Case G	0	75 of 50 kW	263 of 50 kW	338 of 1m	22~27	2400

3.1.6 Bus data (Firenze Line 4)

Line 4 is served by Iveco cityclass 491.10.27 which characteristics are:

- length: 10.79 m
- width: 2.50 m
- height: 2.76
- Vehicle weight: =10600 kg
- Tire-asphalt friction coefficient =0.0056
- Vehicle frontal area =6.9 m^2
- Aerodynamic coefficient =0.65
- Wheel radius =0.45 m

Other Parameters used:

- Gravity =9.81 m/s^2
- Air density=1.25 kg/m^3

In order to assess the energy required during the route, the worst case has been considered, that is, a continuous 6 kW consumption with all the cooling and auxiliary systems connected. A 30 % dynamic braking energy recovery has been considered. A Simulink mathematic model of the vehicle has been developed, whose input is the operation cycle (times and speeds) and provides the required force, instantaneous power and energy consumption.

3.1.7 Data of the studied route

A representative bus route of the city of Florence has been chosen, route number 4, whose time, distance and speed data have been provided by UNIFI (“Annex 4 – Average values for line 4”). In Figure 3.18 is shown the speed-time data along the route.

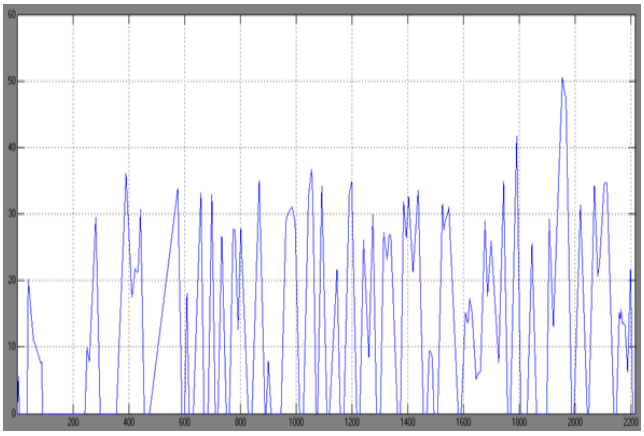

Figure 3.18 - Complete route for Florence bus line 4

The route includes 23 bus stops with a total distance around 9 km (8965 m), and an average route time of 2194 s (36,56 minutes), where 348 s correspond to the bus-stops and 1846 s to the on route movement. The total maximum consumption according to the calculated cycle is **9.2 kWh**, which divided by the total length of the route gives a result of **1.026 kWh/km**.

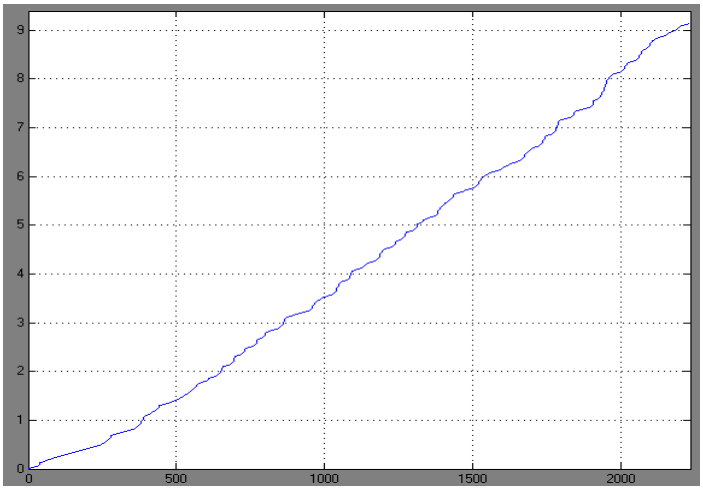

Figure 3.19 - Energy consumption along the route

This average consumption does not consider slopes. It has been obtained considering a completely flat 9 km route. However, if for example a 1% average slope is used, consumption will rise to 13.5 kWh, or 1.5 kWh/km. To determine charging requirements at each stop or *en-route*, each cycle includes the running time until the bus gets to the next stop and the idle time in the station. The next figures show an example of each cycle. The first one is the cycle between stations 23 and 1.

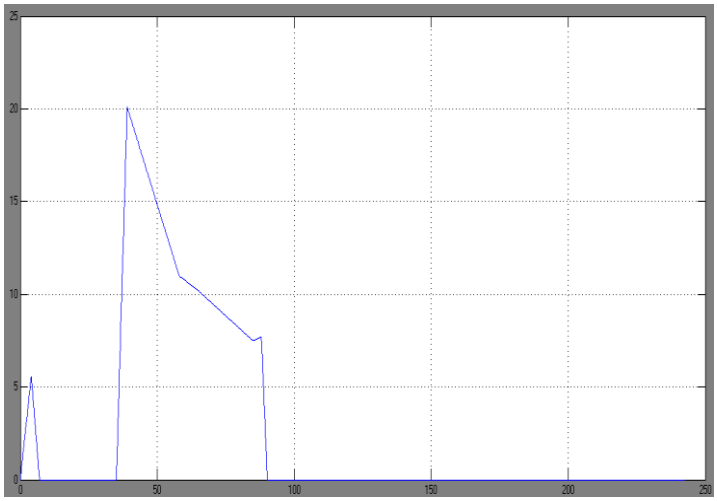

Figure 3.20 - Cycle between stops 1 and 2

Table 3.4 - Cycle between stops 23 and 1

Bus Stop	Number	Time (s)	speed (km/h)	Energy
Stazione Pensilina	23	0	0	
23 to 1		0	0	
		4	5.6	
		7	0	
		35.1	0	
		39	20.1	
		58	11	
		65	10.2	
		85	7.5	
		88	7.7	
		90.2	0	
Mercato centrale	1	152.4	0	
		242.6		0.4851

"Annex 5 – Energy consumption distribution" shows the whole energy consumption divided into the different stations.

3.1.8 Charge analysis

3.1.8.1 Case G. Static *en-route* and dynamic charge using the same coils.

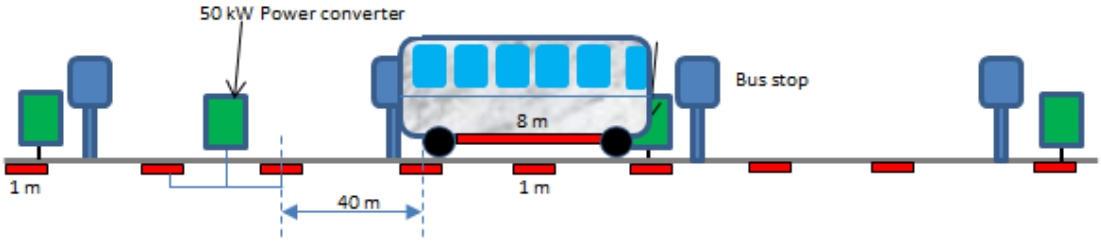

Figure 3.21 - Case G. Example of dynamic charge using a large on-boar coil and small emitter coils

The length of the vehicle is 10.79 m, so the maximum length for the emitter coil, regarding the required shielding distance at the top and rear of the vehicle, is set in 8 m, and the ground coils are set in 1 m length. That means the distance that the two coils are facing is 7 m. Considering an average speed of 19 km/h (according the line 4 data in table 1) the time that the coils are facing and it is possible to charge the batteries is 1.35 s (7 m/ 5.2 m/s).

Calculation of the number of emitter coils

If the power of each charging station is i.e. 50 kW and the energy consumption of the vehicle is 9.2 kWh, a time of 184 h (665 s) is required to recover the energy. Considering a charging time in the stations of 348 s, a time of 317 s is still needed to charge the energy. Thus, the number of coils should be 234 (317 s/1.35 s). The average distance between coils is 8965 m/ 234 coils ≈ 40 m. If a single charger can feed two coils (fig. 6), the number of 50 kW chargers should be 117 placed each 80 m along the route

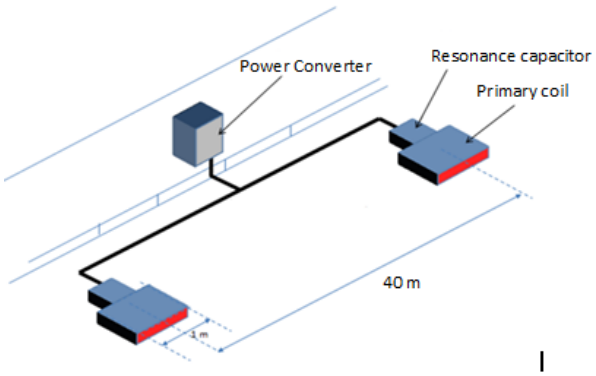

Figure 3.22 - Case G. Coil distribution along the route

That makes a total of 140 units of 50 kW chargers:

- 23 units of 50 kW static chargers at the bus stops
- 117 units of 50 kW dynamic chargers along the route, feeding 234 coils 1 m in length.

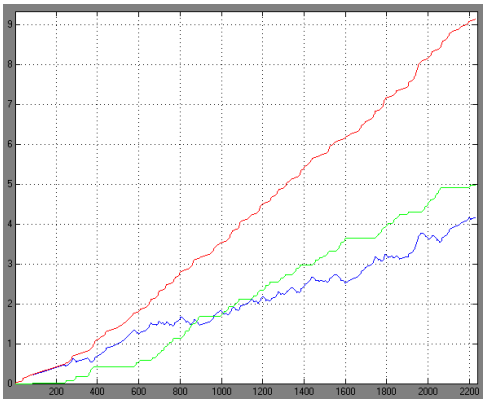

Figure 3.23 - Case G. Energy consumption along the route (red), energy supplied at the stops (static charge, green) and energy supplied along the route (dynamic, blue)

In Figure 3.23 is shown the evolution in the energy consumption for the bus. The energy recovery at the bus stop without time increasing would be 4.83 kWh and the rest is recovery on route.

This situation presents the following advantages:

- Standardization, since the emitting coils (1 m in length) could be the same for static charge at the stops and for dynamic charge.
- Improved security for the people, since the emitting coil is turned on only when the vehicle is covering it and therefore is fully shielded.
- Reduced civil work, one 1 m coil each 40 m along the route.
- Flexibility: possibility of adding more coils later on if energy transfer has to be increased.
- The longer the length of the coil in the vehicle, the higher the energy transferred for the same speed.
- Interoperability among vehicles of different (smaller) sizes, which can use 1 m emitting coils, such as taxis.
- Mixed use: in case of emergency, dynamic charge coils can be used for stationary *en-route* charge without any danger of electromagnetic emissions, since they are completely shielded by the bus.

3.1.8.2 Case E. Static *en-route* charge without time increment at the bus stops combined with continuous dynamic charge.

Another possibility, which would not imply an increase of the time required for the bus to cover the route, would be a combination of static *en-route* charge at the stops and continuous dynamic charge.

The energy charged at the stops with 50 kW charge units and without increased time is 4.83 kWh. The remaining 4.37 kWh required would be transferred continuously while the bus is moving (1846 s) and thus, the required power for the continuous charge process should be 4.37 kWh/ 0.512 h = 8.5 kW.

The numbers of 8.5 kW chargers will depend on the length of each emitter coil covering the whole route. Besides, the length for each emitter coil must be lower than the bus length regarding a suitable shielding.

Thus, considering i.e. 5 m of length, would be required 8965 m/5 m= 1793 emitter coils

If each 8.5 kW charger fed three emitter coils, a number of 597 units would be required

In this case, it would be necessary:

- 23 units of 50 kW chargers at the bus stops

- 597 units of 8.5 kW charger, feeding 1793 emitter coils

This system presents a problem; in order to reduce the number of emitter coils, the length could be increased; but if this length were greater than the bus length, the magnetic field emitted by the coil would not be properly shielded.

3.1.8.3 Case F. Static *en-route* and dynamic charge using discrete primary coils of the same power

If the power rating for the continuous dynamic charge coils is increased to the same value of the stationary chargers (50 kW), charge time would be reduced to 4.37 kWh/50 kW = 0.0874 h, which, at the average speed of the route (19 km/h) would correspond to a total coil length of 19 km/h*0.0874 h =1.66 km

These 1660 m divided in sections of 5 m give 332 units of 50 kW coils, and one charger per each three coils would lead to 110 units of 50 kW chargers.

In total:

- 23 units of 50 kW chargers at the bus stops
- 110 units of 50 kW chargers along the route, feeding 332 coils of 5 m length.

3.1.8.4 Case C. Static *en- route* charge without time increase

In order to charge 9.2 kWh in 0,097 h of stop time (348 s), rated power of each charger should be near 100 kW. That is, 23 units of 100 kW chargers would be required.

In this case, the batteries of the vehicle should be able to store 5 kWh at least.

3.1.8.5 Case A. Static charge at the beginning and at the end of the route

The simplest analyzed solution is to charge at the beginning and at the end of the route. This approach is the one having a lowest infrastructure cost, but implies the drawback of an increase in route time. The cases considered are:

- Using two 50 kW chargers: the bus would have to be 11 minutes at the beginning and 11 minutes at the end of the route.
- Using two 100 kW chargers: the bus would have to be 5.5 minutes at the beginning and end of the route.

Figure 3.24 - Case A. Static charge at the beginning and at the end of the route

3.1.8.6 Case B. Static *en-route* charge at the bus stops

In this case, there are 348 s (0.096 h) available to perform the charge. There are 23 stops, which means that using for instance 50 kW chargers at every stop, the energy supplied to the vehicle would be 4.8 kWh, 4.4 kWh short of the target.

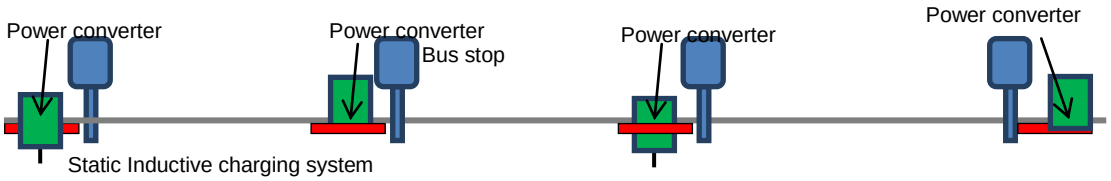

Figure 3.25 - Case B. Static charge at the bus stops

This extra-required energy (4.4 kWh) could be transferred to the bus in different ways. Two options are proposed:

- B-1: extra time Static charge+ static *en-route* charge: charging at the beginning and the end of the route during 5 minutes extra time, using the 50 kW chargers.
- B-2: Static *en-route* Not performing a long charge at the beginning and the end of the route, but increasing the required 19 minutes at the bus stops.

3.1.8.7 Case D. Dynamic charge only

Another possible solution is to take advantage of the moving time of the vehicle (1846 s or 0.513 h) to perform dynamic charge. In order to determine the power required for the continuous charge system, it is necessary to know distance and average speed of each section. This case does not include static charge at the stops. If the consumed energy for the whole route is 9.2 kWh, the power required for continuous charge should be 9.2 kWh/0.513 h ≈ 18 kW. That is, a 9 km line, able to transfer 18 kW all along the route would be required. That implies a very high infrastructure cost and, besides, this line should be composed of consecutive sections that would be energized as the vehicle moves over them, in order to avoid dangerous electromagnetic fields:

3.1.8.8 Number of required coils and chargers

Assuming an emitter coil length three times the size of the vehicle (30 m), the approximate number of coils would be 9000 m/30 m = 300 coils. If a power system were used for every two coils, 150 units of 18 kW chargers would be needed.

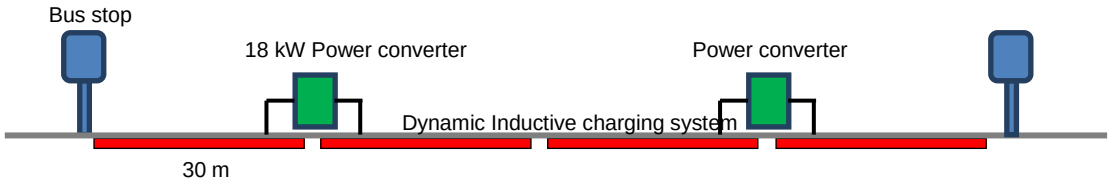

Figure 3.26 - Case D. Example of dynamic charge system between stops, using a charger to feed two coils

It is worth pointing out that the coils cannot be activated if vehicles not prepared for inductive charge are present within a distance shorter than the ground coil length. In the proposed case, the distance between the bus and other vehicles not prepared for inductive charge should be 30 m, if there is a vehicle within 30 m, the coil could not be activated and then the charging process will be interrupted. If this distance has to be reduced, the number of coils and chargers should be increased to cover the entire route. For instance, if coils of the same size as the bus are used (10m), the number of coils would be three times larger (900) and, supposing that a charger can feed four coils, 450 chargers would be needed.

Summary

The main parameters of the different cases are summarized in the following table, assuming the Line4 use case where more than one solution is available.

Table 3.5 - Case summary

	Time increase line 4 [s]	Number of static chargers	Number of dynamic chargers	Number of emitting coils	Battery weight [kg]	Approx. cost [Pike Research] [$]
Case G	0	23 of 50 kW	234 of 50 kW	257 of 1m	22~27	2400
Case E	0	23 of 50 kW	597 of 8.5 kW	23 of 1m 1790 of 5 m	22~27	2400
Case F	0	23 of 50 kW	110 of 50 kW	23 of 1m 332 of 5 m	22~27	2400
Case C	0	23 of 100 kW	0	23 of 1m	28~33	3500
Case A	1200	1 of 50 kW	0	1 of 1m	61~73	6600
Case B	317	23 of 50 kW	0	23 of 1m	11~13	1200
Case D	0	0	450 of 18 kW	900 of 10m	11~13	1200

3.2 Analysis of possible recharge monitoring systems (IDIADA)

Exact metering of the consumed energy by an electric vehicle, when charging at a wireless charging point, is one of the issues to consider for the billing process afterwards. Nowadays lots of charging station providers offer to charge electric vehicles for free, like Hotels or parking areas of shopping centre, but as the number of electric vehicles grows the places where it is possible to charge for free will slowly disappear and a reliable accounting strategy will be necessary each charging station. The power metering system is expected to be a cheap solution, with a small size, accurate and with no billing losses. In order to be able to decide how and where to measure the consumed power, different approaches and technologies will be discussed. A brief introduction of possible alternative technologies for the measurement is reported in ("Annex 1 – "). Then the whole circuit is analysed to decide where to install the metering system. Along the power circuit of a wireless charging system there can be found five possible metering points. The energy type, voltage level and current level are different at each point. For the billing process, it is very important to take into account the power losses along the circuit since the power is converted two times from AC to DC and one time from DC to AC with the corresponding power losses. The induction process is also a non-ideal process, reducing the efficiency of power transfer from the grid to the batteries. In this case, the amount lost depends not only on the induction efficiency of the coils but also on the position of the secondary coil over the primary coil.

3.2.1 Measurements points

Figure 3.27 shows the whole circuit of the power transfer from the grid to the batteries.

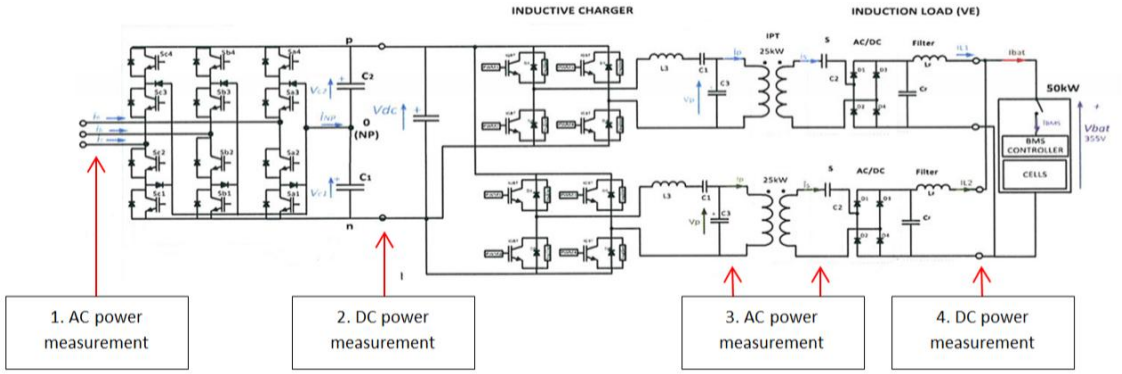

Figure 3.27 - Possible measurement points along the power circuit from the grid to the batteries.

From the left to the right, the possible measurement points are:

1. AC power supply from the grid on the charger side before the AC/DC converter (50Hz and 400V)
2. DC power after the AC/DC converter on the charger side.
3. Left arrow: AC power after the DC/AC converter on the charger side.
   Right arrow: Induced AC power on the vehicle side.
4. DC power after the AC/DC converter on the vehicle side (Battery voltage).

For the analysis of the different measuring points, it is important to be aware of the power losses due to the converters and the induction process from the charger side to the vehicle side as shown in Figure 3.27.

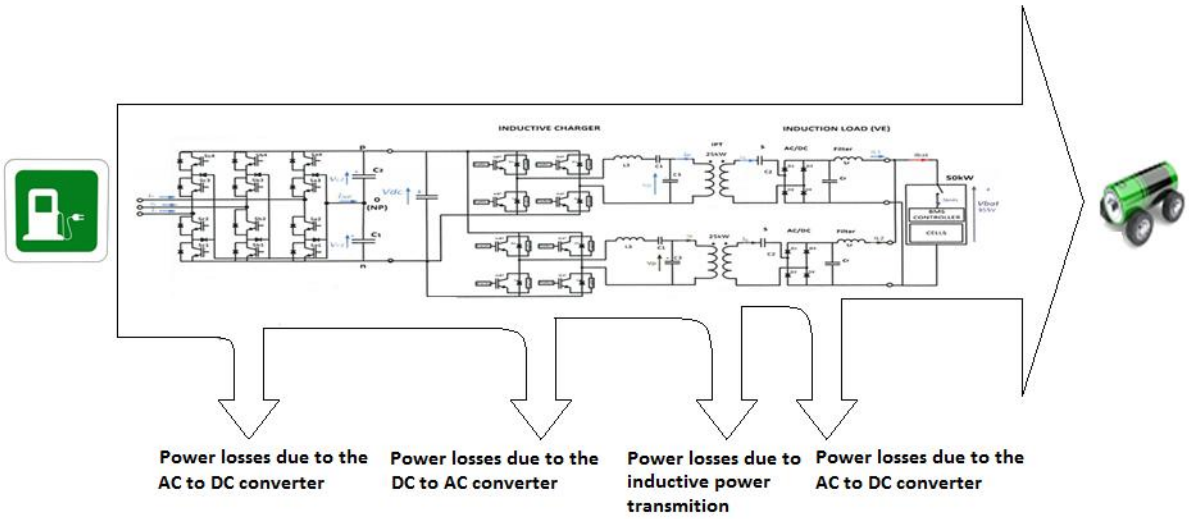

Figure 3.28 - Power losses along the power transfer circuit

In the following, each measuring point is discussed.

3.2.1.1 AC power supply from the grid on the charger side

The first possible measurement point is on the grid side. At this point, the power measured corresponds to the total power consumed by the charging station and it is also the power the owner of the charging station will be billed for. It is important to notice that not all the power measured here, reaches the vehicles batteries, due to the conversion and induction losses of the power along the charging circuit. At this point, the measured power is AC power and has a voltage of around 400V RMS (3 lines with 230V) with a frequency of 50Hz. Since the power is a simple three-phase grid power, most of the commercial monitoring devices for power consumption are suitable to measure at this point. A large number of solid states watt-hour-meters can be found. It is also possible to set up a metering system by the measurement components explained in the previous chapters but, since AC power measurement is very complex, the recommendation is to use a device from the market, which includes the voltage and current measurement, also, taking into account the power factor. At this point, the space available to install the device should not be a problem and the installation of the device is easy when using a power-metering device from the market. In this case, it is only necessary to connect the 3-phases and the neutral to the device. The measurement with this device and at this point is very reliable since these type of commercial devices have passed many quality tests to ensure their reliability and these types of devices currently operate in lots of electrical installations. If the customer is billed taking this measurement value as reference value, the customer will pay not only the charged power into the batteries. In this case, he will pay the whole power consumed from the grid by the charging process, including the power losses along the circuit.

3.2.1.2 DC power after the AC/DC converter on the charger side

At the second possible measurement point, the current has been converted from AC three-phase current to DC one-phase current. The measured power is already less than the power supplied by the grid due to the conversion losses from the AC to DC converter. Owing to the fact that at this point the power is DC power, it is easier to set up a measuring system based on the components discussed in the previous chapters, than for the AC points. To set up a measurement system for this point, the recommended components are:

- Voltage divider to scale down the voltage of the line to the input voltage of the ADC.
- Current transducer based on the Hall effect or shunt resistor to sense DC current.
- Dual-slope ADC since this is the most accurate ADC with a low price. The low sampling rate does not present a problem for DC measurements.
- DSP for the multiplication and filtering processes.

Also for this point, it is possible to find commercial available devices but their usage is not as common as the three phase AC meters and hence the diversity is much lower. A positive aspect of measuring power at this point, against the measurement on the grid side, is that only one power line is necessary to be taken into consideration for the measurements. In the case of 3-phase AC measurements from the grid it is necessary to measure at all three lines enlarging the number of voltage and current transducers and

the ADCs for each transducer. The disadvantage of taking the measurement after the first converter is that at this point the measured power is already less than at the grid side since the converters are not perfect, leading into billing losses for the owner of the charging station when billing the customer. On the other hand, the measured power is closer to the real power flowing into the batteries. The amount of power consumed by the charging station, not covered by the measurement at this point, depends on the efficiency of the AC to DC converter. The space to install a power meter is enough since this point is still on the charger side. Furthermore, the device can be of less size than the devices for 3-phase AC measurements since fewer components are needed.

3.2.1.3 AC power after the DC/AC converter on the charger side

At the third possible measurement point, the power has been converted again from DC power to AC power, but this time the output is AC single-phase power. The frequency of this AC power is much higher than the frequency of the AC power from the grid. The grid in Europe, transports power of a frequency of 50Hz whereas the frequency after the second converter is in the kHz range. Due to this, the power measurement at this point is more difficult, expensive and less accurate. It is also important to be aware of the fact that the voltage is no longer a sinusoidal wave. At this point, the voltage has a quadratic shape. To measure at this point, the following components can be used:

- Voltage divider with low inductive resistors. Resistors have a small inductance in series and a small capacitance in parallel and for measurements at high frequencies this part should be as small as possible. Due to the special manufacturing of these resistors, the price of installation of the voltage divider is higher than at other points.
- Shunt resistor, hall sensor or current converter can be used for the current measurement. It is important to be aware of the frequency limit when choosing a device.
- SAR or a Flash ADC should be used at this point since a high sampling rate is necessary. The Flash ADC has a higher sampling rate but they are more expensive and less accurate.
- DSP for the multiplication and filtering processes.

Power measurements with such high frequencies are not a common application and therefore it would be very difficult or probably impossible to find a commercial device as for the first measuring point. At this point, the measurements obtained are with losses due to the conversion from AC to DC and back from DC to AC. If the customer is billed according to the measurement, the owner has to pay for the power losses of these two conversions. The space to install the metering system should be also in this case enough since this part is still on the charger station side.

3.2.1.4 Induced AC power on the vehicle side

At the fourth possible measurement point, the power is also AC power since an induction process performs the transmission. The induced power has a frequency of the same value as the frequency at the primary coil circuit on the EVSE side but the transfer process is not perfect and the power is less in the secondary coil on the EV side than at the primary coil. The efficiency of the power transfer depends on the efficiency of the coils but also on the position of the secondary coil against the primary coil. The voltage and current waves are sinusoidal in this case. For the power measurement, the same components as for the last measuring point can be used. This measurement point presents the same disadvantage as the last discussed; there are no commercially available devices for this frequency range or at least it is very difficult to find one. Due to all these difficulties, this and the last measuring point are the most expensive ones to install a measuring device. Another problem of this measuring point is that it is placed on the vehicle side and therefore the metering system needs to be installed in the EV. The installation space in the EV is less than in the EVSE side that can be a problem for the vehicle manufacturers. The power loss depends not only on the efficiency of the converters but also on the position of the EV over the primary coil. If the customer is billed, taking this measurement as reference value, the owner has to pay for the conversion losses and the mismatching of the secondary coil over the primary coil due to customers alignment faults. Another disadvantage is that additional communication is needed to transmit the measured power value at this point to the charger. It should be also taken into consideration the possibility that the vehicles owner can manipulate measuring systems, installed on the vehicles side, in order to pay less for the charged power.

3.2.1.5 DC power after the AC/DC converter on the vehicle side

The last measuring point is at the terminals of the battery and therefore the voltage is the battery voltage. The power has been converted another time from AC power to DC power. The power measured at this point is the power that reaches the batteries. Since the power to measure is DC power, it is much simpler

to set up a device than for the last two points. The advantage is that the vehicles already has a preinstalled measuring device at this point to control the current which goes in and out of the batteries and also to control the voltage value of the batteries, therefore it is not necessary to install an additional device. The voltage and current values, measured by the EV, are transmitted during charging to the EVSE through the communication messages according to the ISO15118 thus the EVSE receive this data. If this measurement is taken as reference for the billing process the customer pays for the real power charged into the batteries. In this case, the owner of the charging station is billed for all the power losses along the circuit and the mismatching losses of the vehicle over the charging point. Similar to the previous measuring point, an disadvantage of measuring at this point is that the metering systems is installed on the vehicle side and it exist the possibility of manipulating the measured values by the vehicles owner in order to pay less for the charged energy.

3.2.1.6 Summarize of the advantages and disadvantages of different measuring points

The following table summarize the advantages and disadvantages of each measurement point:

Table 3.6 - Comparison of the different measuring points. Very bad (--), bad (-), average (0), good (+) and very good (++)

Measurement point	AC power from the grid	DC power after the first converter	AC power after the DC/AC converter (EVSE side)	Induced AC power (EV side)	DC power to the batteries
Device complexity	-	++	-	-	++
Reliability	++	++	-	-	++
Space for installation	++	++	++	-	-
Power losses	++	+	0	-	--
Billing losses	++	+	0	-	--
Commercially available device	++	0	--	--	0

4 Analysis of dynamic *en-route* charge: Driver behavior (UNIFI)

Within this paragraph, results about the drivers' ability to center the vehicle over the electrified path will be given. A drive simulator has been used to collect data over a large number of drivers and, subsequently, an analysis on a real car has been conducted in order to validate the data acquired by simulator.

4.1 The simulator

LaSIS (Laboratorio per la Sicurezza e l'Infortunistica Stradale, [9]) is a laboratory of the Università degli Studi di Firenze and it is equipped with a drive simulator constituted by a car body mounted over six electric operated pistons that give the driver the acceleration sensation and a large curved screen. A set of computers and projectors simulate and make the driver interact with a driving scenario (with traffic, traffic lights, queues, etc.) in order to quickly and safely test infrastructures and new technologies. In addition, the greatest possible adherence to the real-world conditions is guaranteed by an engine sound emulator, small screens over the rear mirrors and fully functional gearshift, steering wheel, etc. (Figure 4.1).

Figure 4.1 - Driving simulator

For the developed tests, a town scenario has been built. To simulate the dynamic recharge infrastructure a blue line was positioned over the road surface. The simulator control software automatically calculates the lateral shift of the car center of gravity from the blue lines inside the town at 10 Hz. In Figure 4.2, a conceptual map is reported.

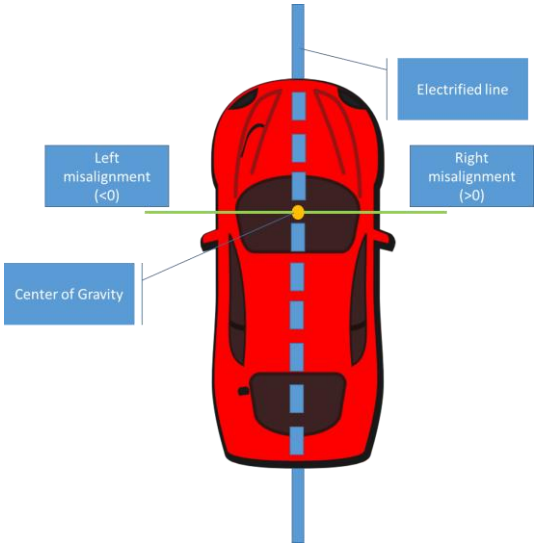

Figure 4.2 - Vehicle conceptual map

The data logger creates a .txt file where negative data is referred to left lateral misalignment and positive data referred to right lateral misalignment. In order to statistically process data, it is mandatory to consider only positive values and so the left/right information has been removed (and used only for one of the

analysis provided) by using the absolute values of the records instead of raw data. This information has been used to stratify the sample.

In Figure 4.3 it is represented an example of the scenario view.

Figure 4.3 – Screenshot of the drive simulator cabin view

The built scenario is represented in Figure 4.4:

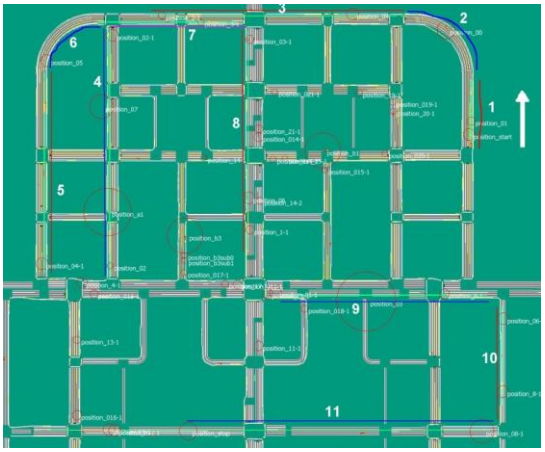

Figure 4.4 - Plan of the proposed scenario

11 electrified segments have been positioned within scenario and each of the drivers has to follow the path from segment 1 to segment 11. To help the navigation, where more than one way were possible, a green arrow overlapped to the screen indicates the right way to choose. Nine segments were straight and two segments were curved, one to the left and one to the right. Within the city, in addition to a random decided traffic, also a pedestrian crossing and a double-parked car have been introduced to study their interaction with the infrastructure functionality. It has been asked to the tested drivers to behave as normal as possible and to center the blue line, when present, with the car front.

4.2 Test and sample design

Before starting the data acquisition campaign, a set of possible stratification variables have been designed in order to understand possible interaction with drive precision:

- Gender
- Age
- Years of the drive license
- Average speed
- A self-assigned score about their driving frequency (1 = very rarely, 5 = very often).

It is interesting to notice that last variable is defined with a non-objective value. The first idea was to ask for average year mileage driven, however all of the answer were between 10.000 and 15.000 km per year and so without an appreciable difference. Final decision has been to switch to a non-objective variable instead of eliminate this information from the study.

In “Annex 6 – Sample characteristics” is reported the sample characteristic. It is possible to notice (highlighted in blue, pink and green) that some of the drivers repeated the test more than once: it is to understand if the practice on the simulator could reflect better results on the lateral misalignment. Finally, the variable “Age” has been removed because it was coincident with the variable Yrs. driving: all of the tested drivers obtained their license when 18 years old. Within the test, two response variables have been considered: precision and accuracy of each driver for each of the path segments. More in details, an accurate driver has an average misalignment close to 0, the target and a precise driver has a low deviation from his average. The best possible, is an accurate and precise driver (Figure 4.5).

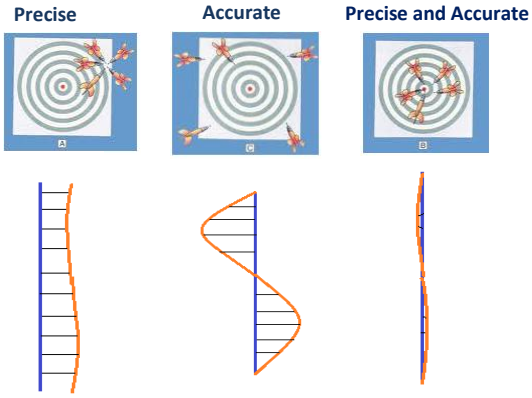

Figure 4.5 - Accuracy and precision disambiguation

In more detail, each of the tests gave 11 vectors with lateral misalignment of the driver. The length of each vector is directly proportional to the average speed. This set of data has been considered as a normal distributed set of data with an average and a standard deviation value. The average has been considered as the driver accuracy and the standard deviation as the driver precision (Figure 4.6). In this way, each of the drivers will have two response variables values, one for precision and one for accuracy, for each of the eleven path segments.

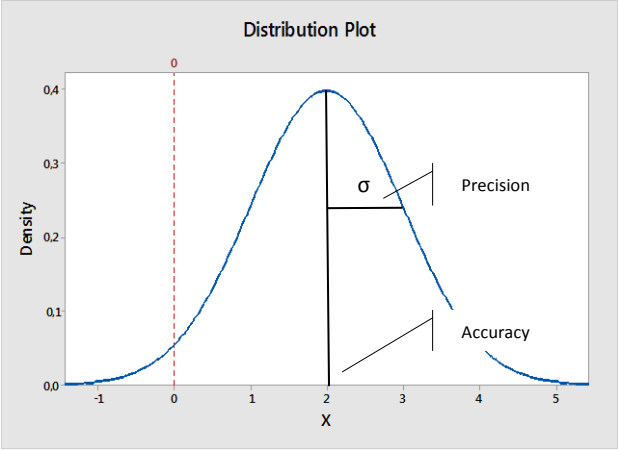

Figure 4.6 - Accuracy and precision disambiguation

A study over the power of sample size has been carried out, to understand if the number of tested drivers could be enough. Initially, a pre-test has been carried out: the first ten drivers of the table in “Annex 6 – Sample characteristics”, in fact, have been firstly measured and analyzed to have information about the population. The recursive process has evaluated the standard deviation of the pre test sample and assumed that it is the same of the population, and then it defined the minimum sample size to achieve a satisfying precision. At the end of this procedure, the precision achievable with the new standard deviation and the higher number of samples has been calculated in order to understand if it is satisfactory. If it is, the procedure stops, hence a new set of samples has to be tested and precision calculated again. For the case here reported, only the first step has been made. The results are:

Accuracy:

- σ population = σ pre test sample =0.133 m
- α level chosen = 95%
- Acceptable margin of error = 0.02 m

With this data, the minimum set of elements are 173. Whereas that each test has eight straight segments without obstacles, the total number of persons that have to be involved in the study is 22 (10 in the pre-test + 12 in the second data collection campaign). After the second data collection campaign, the total number of person involved has been 28. Three persons, in fact, has been tested three time as said before to understand the "learning effect" (22 single test + 6 repetition of three persons). Finally, the margin of error has been calculated on the new data:

- σ population = σ final test sample =0.151 m
- α level chosen = 95%
- # of samples 219 (the total should be 224, but the drive simulator caused nausea drawbacks to three people, and so the test necessarily have been stopped before the end).

The calculated margin of error with these data in 0.02 m, and so it is acceptable.

Precision:

Same has been made for the precision.

- σ population = σ pre test sample =0.104 m
- α level chosen = 95%
- Acceptable margin of error = 0.02 m

Therefore, the 219 tests that have to be carried out for the accuracy analysis are enough. Margin of error and new data coming from the complete data collection campaign are:

- σ population = σ final test sample =0.172 m
- α level chosen = 95%
- # of samples 219.

The calculated margin of error with these data in 0.023 m, that is still acceptable.

4.3 Data analysis

The study took into account four different aspects:

1. Correlation between response variables (precision and accuracy) and the dependent variables (Gender, Yrs. driving, Drive frequency, Average speed) to understand if a repetitive pattern could be hypothesized.
2. Drive behavior in straight road segments, with a pedestrian cross, a two rows parked car and a light random traffic.
3. Drive behavior in curved road segments, with a light random traffic.
4. Electrified segment entry and behavior after an overtaking, in order to understand what could happened after a forced detour.

The final data are available in "Annex 7 – Complete final results". Here below is possible to find stratified and plotted data. This is useful to visually determine possible interactions.

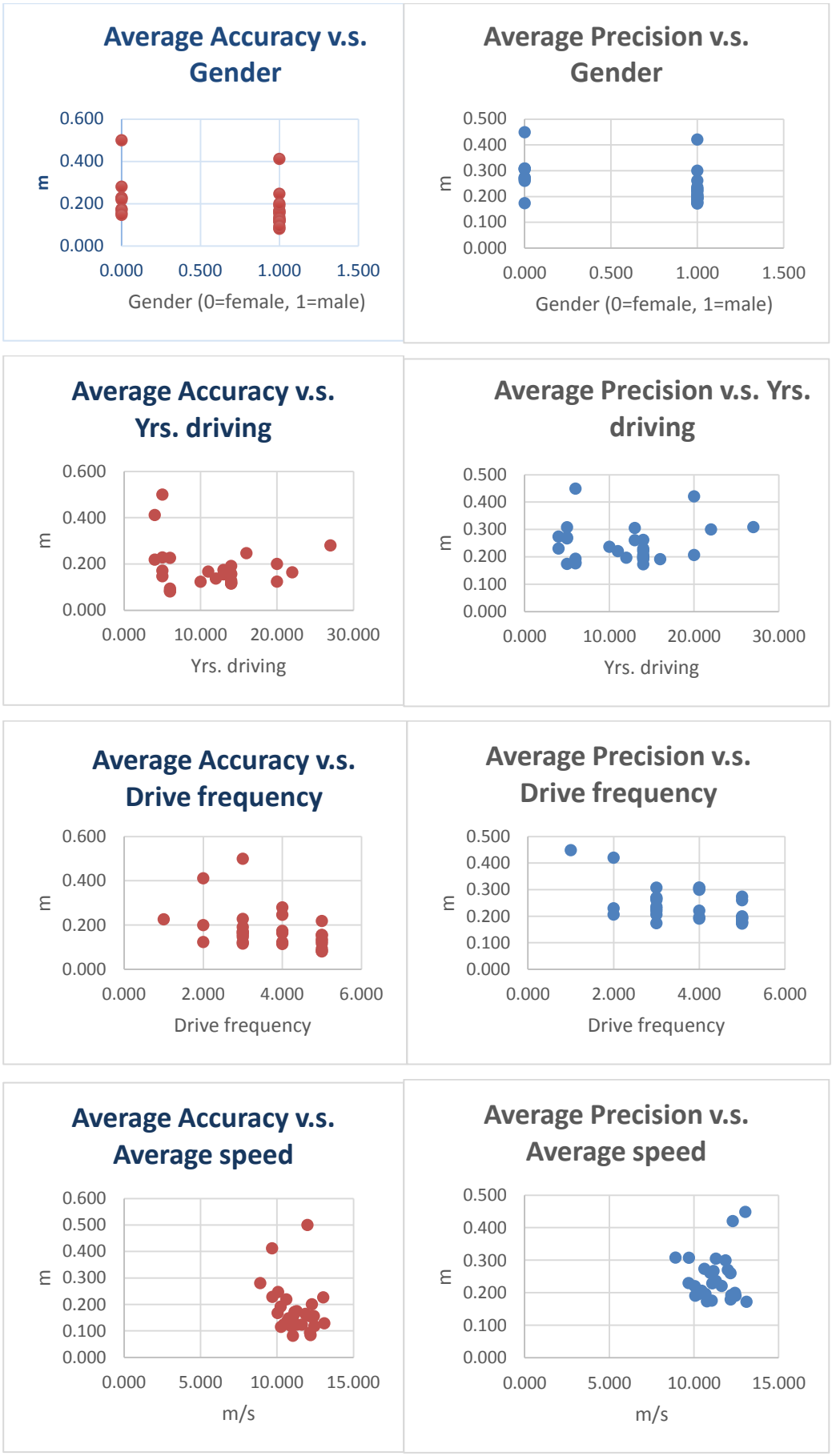

Figure 4.7 – Analysis of test accuracy and precision

Reading the above graphics, the only possible interaction could be with the first variable, the gender. Visually, in fact, seems that the male behavior is better for both accuracy and precision. A regression analysis of these data is reported in "
Annex 8 – Regression analysis for accuracy and precision".

4.3.1 Training effects

To assess if training affects positively the drive accuracy and precision, it has been asked to three of the drivers to repeat the test three times. As above mentioned, the drivers that repeated the test more than once are Driver5 (in different days), Driver18 (with one hour stop between tests) and Driver21 (without no pauses between tests). The complete table of results are shown in "Annex 9 – Repeated tests final results".

One paired t-test has been provided for each of the driver between test number one vs. test number three. The null hypothesis is that difference "Accuracy ride 1 – Accuracy ride 3" = 0 vs. alternative hypothesis that difference is ≠ 0. Results are summarized in Table 4.1:

Table 4.1 - Paired t test results for accuracy

Driver	**T-Value**	**p-Value**
Driver18	6.11	0.000
Driver21	-0.39	0.705
Driver5	0.82	0.434

Same analysis has been provided also for the precision. Results are reported in Table 4.2:

Table 4.2 - Paired t test results for precision

Driver	**T-Value**	**p-Value**
Driver18	3.51	0.006
Driver21	1.00	0.340
Driver5	-0.24	0.815

As it is possible to obtain from data, the only driver that experienced a statistically significant improvement is Driver18. This because she experienced in her first ride a very important parallax issue and she has been warned about at the end of first test. Therefore, the initial training is important to reach better alignment with the electrified path especially to avoid parallax issues. The training does not influence the other two drivers, Driver5 and Driver21: their performance are the same across the three tests provided. In conclusion, training can positively affect the driving performance if the driver is experiencing a completely wrong utilization of the vehicle (high parallax issues). In the short time, instead, it seems that the training could not affect the driving performance: the two drivers that did not experienced macro errors did not improve their performance along the three tests.

4.3.2 Curved strokes

In the proposed scenario there are two curved strokes, segment number 4 (curve to the left) and segment number 6 (curve to the right). Please refer to Figure 4.4. In *Figure* 4.8 and Figure 4.9 is reported the behavior of each of the drivers. Red lines refer to 0 = target, 20 cm left and 20 cm right.

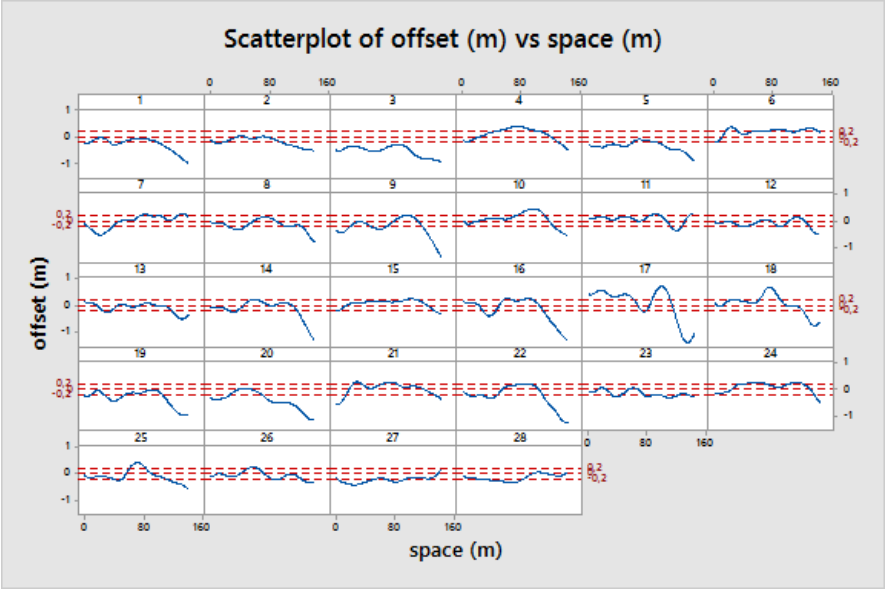

Figure 4.8 - Drivers' behavior in segment number 4

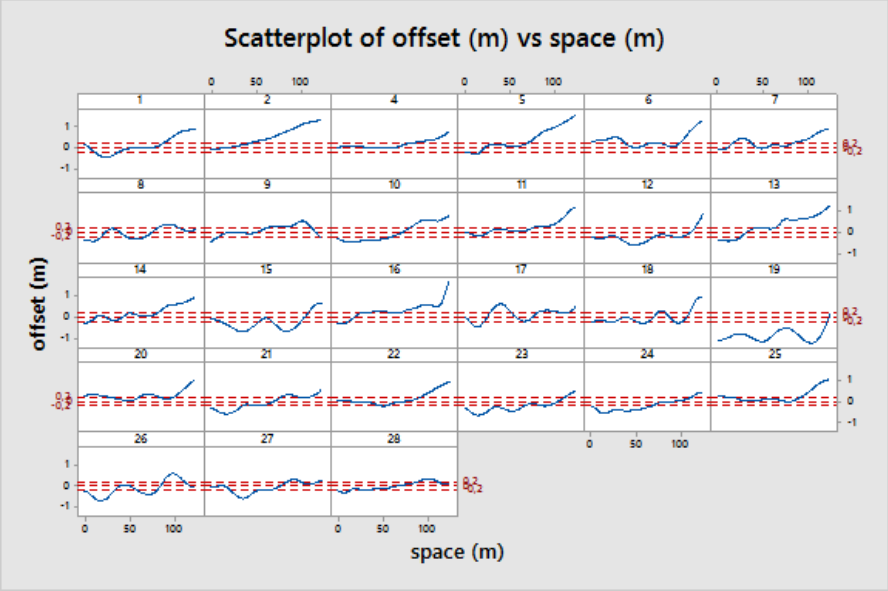

Figure 4.9 - Drivers' behavior in segment number 6

The two segments have been divided in three parts and analyzed. Results are reported in Table 4.3.

Table 4.3 - Drivers' behavior in curved strokes

Segment	Part	Accuracy (m)	Precision (m)	Avg. Speed (Km/h)
4	1	-0,118	0,215	11,508
4	2	0,014	0,229	12,245
4	3	-0,296	0,412	12,620
6	1	-0,152	0,303	13,112
6	2	-0,024	0,279	13,461
6	3	0,393	0,431	12,911

The general trend of the drivers is to close the curve inwards. This conclusion is evident both from visual analysis of the scatterplots and of the accuracy and precision values. The last part, in fact, is always the one with worst results.

4.3.3 Straight sections

From the data reported in “

Annex 10 – Straight segments results”, the average accuracy is 0.158m and the precision is 0.169m. Considering a normal distribution for the data coming from this test and using average accuracy as mean and average precision as standard deviation of a normal distribution, it is possible to find the time percentage a vehicle should be within specific (+0.2~-0.2 meters), in this case 58.1%.

4.3.4 Initial part of the segment

Figure 4.10 reports the drivers’ behavior in the initial part of a straight segment:

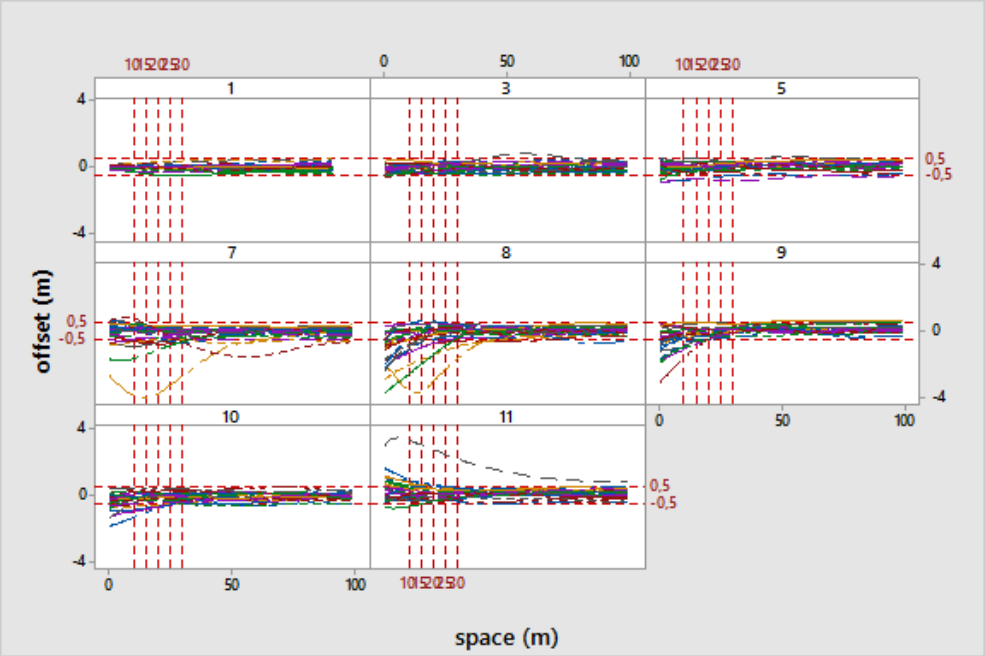

Figure 4.10 - Drivers' behavior in initial part of a straight segment

From the graphs, it is possible to notice that issues in the initial part are in segments 7, 8, 9, 10, 11. This because the electrified path starts after a crossroad and so the vehicle is misaligned after the curve. Data of the first 15m of segments 7, 8, 9, 10, 11 has been eliminated and analysis has been repeated. Avg. accuracy is 0.151m and avg. precision now is 0.122m. The percentage between specific limits is 65.4%.

4.3.5 Double row vehicle behavior

Within the segment 4, a vehicle was parked in double row (Figure 4.11).

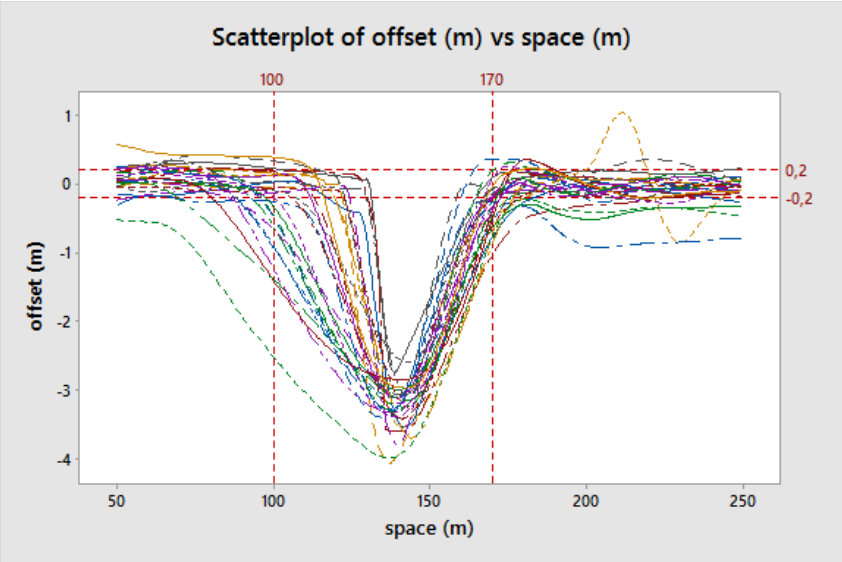

Figure 4.11 - Drivers' behavior with a double row parked car

On average, the electrified path that is missed when an obstacle occurs is ~70m.

4.4 Simulator analysis conclusion

The conclusion of this analysis is a list of preferred characteristics of the road to be electrified:

- A straight segment.
- Position about 15m after the initial point of a straight segment after a crossroad.
- Central part of a curved road.
- Initial part of a curved road.
- Final part of a curved road.

For what concern the presence of an obstacle over an electrified path the solution is to develop the dynamic charge only in preferential track.

4.5 Test on real vehicle

Analysis on the drive simulator is very useful to quickly investigate drivers' behavior over a large number of cases and with a large number of tested drivers. However, it is necessary to analyze how close the simulator results are to the real world ones. To evaluate this issue, a second data collection campaign has been carried out using a real car equipped with optical sensors to measure continuously the car position respect to a line painted on the road.

4.5.1 The instrumented vehicle and the test field

Within a private area of the Università degli Studi di Firenze an archetype of an electrified road has been created. It is a line painted over the ground within a road (Figure 4.12). The chosen road has all the characteristics of a normal road and during the test some cars were also parked left and right. The "A" segment is about 50 meters long and the curved one is about 20 meters long. The crosscut segments at each start and end are necessary for the post-processing phase.

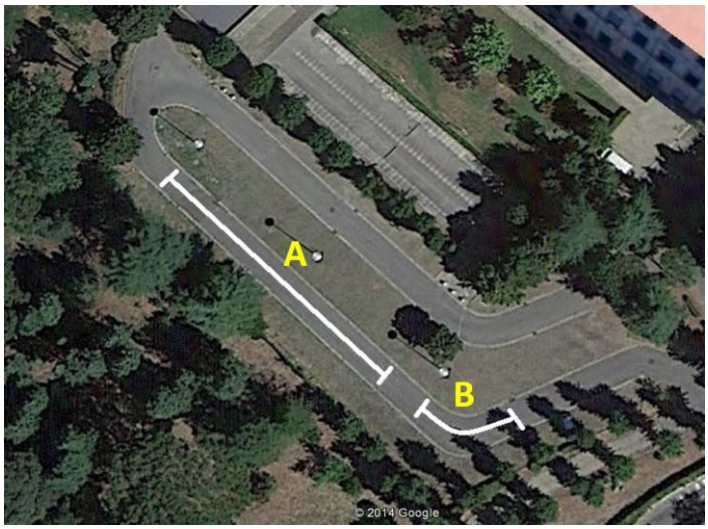

Figure 4.12 - Private road within University of Firenze

The field tests have yielded similar results to in the research study. Some more drivers have been involved in order to increase the sample size. For this test, each driver was asked to repeat the path three times: during the first lap, no advice has been given to the driver, before the second lap only an indication of the misalignment side has been given and during the third lap a continuous indication has been given to the driver. This to prove if training and a driver's aid could improve drivers' behavior. During the drive, a camera mounted in front of the vehicle recorded the performance (Figure 4.13) and then a blob analysis on each frame has been provided to calculate the lateral misalignment. Tested person list and results are reported in "

Annex 11 – Real car results". By using this sample, the obtained margin of error calculated has been 0.012m, which has been considered acceptable. Tested drivers have achieved better performance on the real vehicle. Regression analysis of these data are reported in "
Annex 8 – Regression analysis for accuracy and precision".

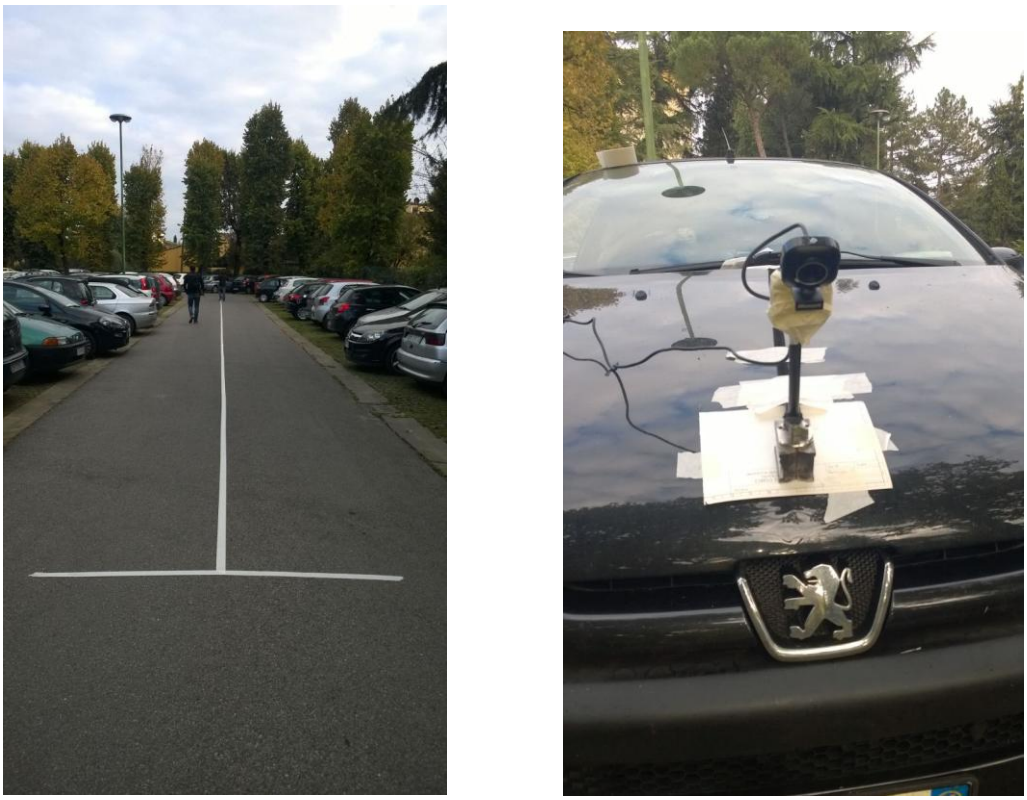

Figure 4.13 – Instrumented road and vehicle

To understand if training could affect the drivers' performances, a paired t-test has been carried out. The tested equation is performance 1st lap vs. performance 3rd lap where null hypothesis is that the difference is equal to zero and the alternative is different from zero. Performance means that the test has been repeated once for the accuracy and once for the precision. Results are reported in Table 4.4:

Table 4.4 - Paired t-test results for training

Performance	**T-value [m]**	**p-value**
Accuracy	0.026	0.043
Precision	0.003	0.351

From these results, it is possible to conclude that, on the issue of accuracy. An improvement is statistically significant and so training and support driving devices could provide very good results, where the precision is something that could not be improved with simple solutions.

Lastly, two 2-sample t-test, one for accuracy and one for precision, have been carried out in order to evaluate the different behavior between simulation and real world data. From these data, it is evident that the real-world tests provided improved accuracy and precision when compared to the simulator ones. So the simulator could be used as a worst case scenario to define the driver accuracy.

Result of the t-test for accuracy is:

Two-sample T for accuracy simulator vs accuracy real

```
                          N  Mean  StDev  SE Mean
accuracy simulator      199  15,3   15,0      1,1
accuracy real            39  6,76   4,12     0,66

Difference = μ (accuracy simulator) - μ (accuracy real)
Estimate for difference:  8,54
T-Test of difference = 0 (vs ≠): T-Value = 6,83  P-Value = 0,000  DF = 214
```

And for the precision

Two-sample T for precision simulator vs precision real

	N	Mean	StDev	SE Mean
precision simulator	192	16,7	16,7	1,2
precision real	39	4,00	1,72	0,28

Difference = μ (precision simulator) - μ (precision real)
Estimate for difference: 12,69
T-Test of difference = 0 (vs ≠): T-Value = 10,27 P-Value = 0,000 DF = 208

5 Business model for *en-route* dynamic charging (UNIFI)

Within this chapter, a possible future mobility system based on dynamic wireless charging for the city of Firenze will be presented. The analysis is based on the data elaborated by CIRCE in paragraph Analysis of technical solutions (CIRCE) for public and private mobility. The assumption made in this paragraph are the same of Deliverable 3.3, chapter 4. The three bus lines chosen as archetype of the service are the same: for long-range buses the line 23 has been chosen where for medium range buses line 4 has been chosen. Up to this point, the conceptual map of the analysis is the same of the one in deliverable 3.3. Given that for dynamic charging the occupation of the same electrified track is more critical than for static wireless charging, for the short range bus scenario the whole number of buses that operate in the city center area has been simulated.

5.1 Bus and private mobility scenario analysis for the city of Firenze

5.1.1 Bus analysis

5.1.1.1 Short range bus case – Line C1, C2 and C3

Differently from deliverable 3.3 chapter 4, the short-range bus analysis has been carried out by taking into account three bus lines (C1, C2 and C3) to evaluate possible interactions between lines. Data and model used are the one already presented in deliverable 3.2, Annex III – Analysis of power consumption in Firenze, with one exception: the balance equation to determine the battery state of charge in this case has to take into account also the possibility of *en-route* dynamic recharge. In deliverable 3.2 (page 98 of 144) the equation was:

$$SOC_{out} = SOC_{in} + PI_{capacity} * TIME_{stop} - DISCHARGE$$

Where now is

$$SOC_{out} = SOC_{in} + PI_{dinamic} * TIME_{over\ dinamic\ segment} + PI_{static} * TIME_{stop} - DISCHARGE$$

To assess how much time a vehicle spend over a recharging segment, it is necessary to use average speed of the vehicle within the road segment between two stops. From this, it is possible to assess:

$$TIME_{\ over\ dinamic\ segment} = \frac{Electrified\ road\ segment\ lenght}{Average\ vehicle\ speed}$$

That became:

$$TIME_{\ over\ dinamic\ segment} = \frac{Electrified\ road\ segment\ lenght}{\frac{Entire\ road\ segment\ lenght}{Entire\ road\ segment\ crossing\ time}}$$

It is important to notice that the dynamic power inverter capacity could be also different from the static one. For the analysis, both static and dynamic power inverters are set at 50kW power. It is also important to notice that the static charge at terminal and normal bus stops are always available: this scenario complies with Case E (Paragraph 3.1.4.6 of this document) where dynamic charge is used to maintain same service level provided by internal combustion engine vehicles. To choose which road segment has to be electrified it has been selected firstly the common ones, in order to keep the costs as low as possible, and then the road segment with lower average speed to maximize the time in which the vehicles are over the coil. The proposed scenarios are two, one with the batteries actually equipped on board of the Tecnobus Gulliver vehicles supplied to the Firenze public transport provider and another one where the minimum possible battery capacity to assure a good service level is provided to the final user. Stops, vehicles and other characteristics of the C1, C2 and C3 bus lines are reported in Deliverable 3.2, Annex III – Analysis of power consumption in Firenze. For the first scenario, 57kWh batteries has been considered and 0.2 * Complete charge has been chosen as protection limit from deep discharge. Results after the simulation are:

- Line C1: 560 meters have to be electrified in 8 road segments – segments 5-6-17-19-24 with 80 electrified meters each. Segment 7 needs 100 electrified meters. Segments 13-15 instead need 30 electrified meters.

- Line C2: 490 meters have to be electrified in 8 road segments – segments 7-8-9-11-12-13-14-28 with 70 electrified meters each. Segment 7 needs 100 electrified meters.
- Line C3: 970 meters have to be electrified in 13 road segments – segments 10-27 with 100 electrified meters each. Segments 4-5-18-25-26 with 80 electrified meters each. Segment 16 with 10 electrified meters. It is important to notice that segment 9 is already electrified with 80 meters and segments 11-12-13-14 are already electrified with 70 meters each.

By extending this data to all the city vehicles, the electrified meters in common between different bus lines are 18%.

Second proposed scenario, the one with the lowest possible battery capacity, is characterized with a battery of 12kWh capacity, with lower limit set at 2.4kWh to prevent deep discharge issues. In other words, battery is only a device used to reach next stop point. Results after simulation are:

- Line C1: 1340 meters have to be electrified in 20 road segments – segments 1-2-5-6-7-8-10-11-12-13-15-16-17-18-19-20-21-22-23-24 with 67 electrified meters each.
- Line C2: 790 meters have to be electrified in 10 road segments – segments 4-8-9-12-13-14-20-21-28 with 80 electrified meters each. Segment 11 with 70 electrified meters.
- Line C3: 1550 meters have to be electrified in 20 road segments – segments 4-5-6-10-16-18-19-20-22-23-25-26-27 with 80 electrified meters each. Segments 1-9-11-12-13-14-15 are already electrified.

By extend this data to all the city vehicles, the electrified meters in common between different bus lines are 14%. Thus Tecnobus Gulliver used in C1, C2 and C3 are half length of the normal bus (only 6 m so a coil could be 5 m long) used in other line (such as line 23 and line 4), it is possible to scale results CIRCE provided in chapter 3 also for short range buses. Solution described in “Case G” of line 4 and line 23 example is the most cost effective and so for C1, C2 and C3 lines the two scenario proposed are:

1. Actual battery size:
    a. C1: 560/5=112 dynamic coils + 25 static coils thus 81 50kW charger
    b. C2: 490/5=98 dynamic coils + 28 static coils thus 77 50kW charger
    c. C3: 970/5=194 dynamic coils + 27 static coils thus 124 50kW charger

Therefore, on average and considering 18% traits in common, 111 dynamic coils + 27 static coils thus 82 50kW chargers.

2. Minimum possible battery size:
    a. C1: 1340/5=268 dynamic coils + 25 static coils thus 159 50kW charger
    b. C2: 790/5= 158 dynamic coils + 28 static coils thus 107 50kW charger
    c. C3: 1550/5= 310 dynamic coils + 27 static coils thus 182 50kW charger

Therefore, on average and considering 14% traits in common, 245 dynamic coils + 27 static coils thus 129 50kW chargers.

5.1.1.2 Medium and long range bus cases – Line 4 and Line 23

These analyses are reported in Chapter 3 of this document.

5.1.1.3 Scaling the entire city of Firenze

By using the bus line classification reported in Deliverable 3.3 Table 5 page 22 of 64, it is possible to scale the results provided above to the entire city of Firenze. It has also assumed a common road electrified segment percentage of 20% to consider that including the whole city there could be greater opportunity to use electrified road segment for more than one bus line (considering only short-range buses this percentage is 18%)

Table 5.1 - Number of power electronics (Solution A of bus line classification D3.3)

Bus range	**Static charger**	**Dynamic charger**	**Emitting coils**
Short range – solution 1	367	748	1863

Short range – solution 2	748	1387	3699
Medium range	368	3744	4122
Long range	1080	3787	4867

Table 5.2 - Number of power electronics (Solution B of bus line classification D3.3)

Bus range	**Static charger**	**Dynamic charger**	**Emitting coils**
Short range – solution 1	453	924	2301
Short range – solution 2	924	1714	4570
Medium range	460	4680	5140
Long range	540	1893	2433

5.1.2 Private Mobility analysis

To assess the needs of private mobility within the city of Firenze, some data were taken from previous deliverable and some assumptions have been made. The data taken from previous deliverable are the forecasted number of electric vehicle that will circulate in Firenze (Deliverable 3.3, Chapter 4, Table 21 page 30), average consumption of private cars (Deliverable 3.2, Chapter 2, Table 4 page 27). The assumption made are the average kilometers travelled per year in Tuscany [10], the average speed in high frequented streets in Firenze, the number of vehicles circulating in high frequented streets of Firenze (data provided by the mobility office of the Firenze municipality). The average vehicles circulating in the high-frequented streets of Firenze and the related frequency percentage are reported in Table 5.3:

Table 5.3 - Average number of circulating vehicles in Firenze

Street name	**Avg # vehicles**	**Frequency percentage[%]**
Via Aretina	10430	8
Via Bolognese	5697	4
Via Sestese	15108	12
Via Pistoiese	14258	11
Via Guidoni	42247	33
Via Europa	13027	10
Via Nenni	8294	7
Via Pratese	18181	14

The electric vehicles running in Firenze of the Deliverable 3.2, Chapter 2, Table 4 page 27 are multiplied with the Table 5.3 Frequency percentages and with the energy absorbed by the EVs in one day of Deliverable 3.2, Chapter 2, Table 4 page 27 in order to evaluate the average absorption of the vehicles within the proposed streets. The proposed scenarios refer to 1%, 5% and 10% of automotive market penetration of Electric Vehicles (Table 5.4).

Table 5.4 - Energy to be provided [kWh]

Street name	**1% market penetration energy**	**5% m.p.**	**10% m.p.**
Via Aretina	183,03	915,17	1830,34
Via Bolognese	99,97	499,85	999,71
Via Sestese	265,14	1325,70	2651,40
Via Pistoiese	250,21	1251,07	2502,14
Via Guidoni	741,42	3707,10	7414,20
Via Europa	228,61	1143,05	2286,10
Via Nenni	145,54	727,74	1455,48

Via Pratese	319,06	1595,30	3190,61

From the data of Table 5.4, it has been calculated the total time per street the electric infrastructure has to give energy. The total time [h] that each street segment will operate is reported in Table 5.5:

Table 5.5 - Total operating time of one charging devices within each street [h]

Street name	1% m.p. opearting time	5% m.p.	10% m.p.
Via Aretina	3,66	18,30	36,61
Via Bolognese	2,00	10,00	19,99
Via Sestese	5,30	26,51	53,03
Via Pistoiese	5,00	25,02	50,04
Via Guidoni	14,83	74,14	148,28
Via Europa	4,57	22,86	45,72
Via Nenni	2,91	14,55	29,11
Via Pratese	6,38	31,91	63,81

It means that some of the streets will need some parallelization (more than one electrified lane) to reach maximum 20 hours per day of working time. Finally, by assuming 40km/h of average driving speed, the kilometers that will have to be electrified are reported in Table 5.6:

Table 5.6 - Kilometers to be electrified

Street name	Km to be electrified
Via Aretina	0,50
Via Bolognese	0,28
Via Sestese	0,73
Via Pistoiese	0,69
Via Guidoni	2,05
Via Europa	0,63
Via Nenni	0,40
Via Pratese	0,88

That are all within the streets' length.
By assuming the Case G of Chapter 3 as the most cost effective solutions, it is possible to calculate the number of chargers and of emitting coils. The length of secondary coil equipped on board of vehicles is assumed 1.5 meters (Table 5.7).

Table 5.7 – Number of emitting coils and dynamic chargers

Street name	Emitting coils	Dynamic chargers
Via Aretina	336	168
Via Bolognese	183	91
Via Sestese	487	243
Via Pistoiese	460	230
Via Guidoni	1363	681
Via Europa	420	210
Via Nenni	267	133
Via Pratese	586	293

5.1.3 Predicted cost of the technical solution

For what concern the total cost of ownership of the possible Firenze wireless charge technology within public and private scenarios, the assumptions made and the forecasted components costs are the ones reported in Deliverable 3.3 chapter 4. It is also important to notice that, as in Deliverable 3.3, due to the public nature of the deliverables, costs are expressed in percentages (the object of the percentage is

reported in each case) in order to keep the privacy. Total costs of infrastructure are reported in Table 5.8 and Table 5.9:

Table 5.8 – Cost of short-range buses with 57kWh battery equipped on board:

Bus range	Static chargers	Dynamic chargers	Emitting coils
Short range – solution 1	3%	6%	36%
Short range – solution 2	6%	12%	72%
Medium range	3%	32%	80%
Long range	9%	32%	95%

Table 5.9 – Cost of short-range buses with 12kWh battery equipped on board:

Bus range	Static chargers	Dynamic chargers	Emitting coils
Short range – solution 1	4%	8%	45%
Short range – solution 2	8%	15%	89%
Medium range	4%	40%	100%
Long range	5%	16%	47%

Higher infrastructure costs of the solution with lower batteries will be recovered with battery downsizing.

For what concerns the private mobility scenario, percentage costs are reported in Table 5.10.

Table 5.10 – Percentage costs for private mobility integration in Firenze

Street name	Emitting coils	Dynamic chargers
Via Aretina	25%	5%
Via Bolognese	13%	3%
Via Sestese	36%	8%
Via Pistoiese	34%	7%
Via Guidoni	100%	22%
Via Europa	31%	7%
Via Nenni	20%	4%
Via Pratese	43%	9%

5.2 Business models

The business model for the dynamic charging service provider is not significantly different in respect to the ones developed for static charging, presented in D3.3 chapter 5.1. For the other agents, it has been assumed that there will be only a single grid manager (generally called Charging System Provider) because the technology is so complex and interconnected that it is not possible to split its management among different partners (public or private). For the static charging it has been assumed that private companies could be able to provide the charging spot service as a primary or secondary business (i.e. shopping mall that provide this service to increase the number of potential customers installing the devices in their private parking). In case of dynamic charging, the infrastructure will be installed on the public access road and it is not probable that the city government could assign to different subjects the management of just a part of the electrified segments within the city. Therefore, in this case the DSO will be only one organization. We can assume that this could be a public controlled company for the first test case implementation but then move to a private company for a larger implementation within the city. The business model could be so represented as in Figure 5.1. This DSO will receive both public economical

support for the service provided and the revenues from energy billing to the users. For what concern the "Public Area with Public Access", it has been assumed that business could be made both with static and with dynamic *en-route* charge.

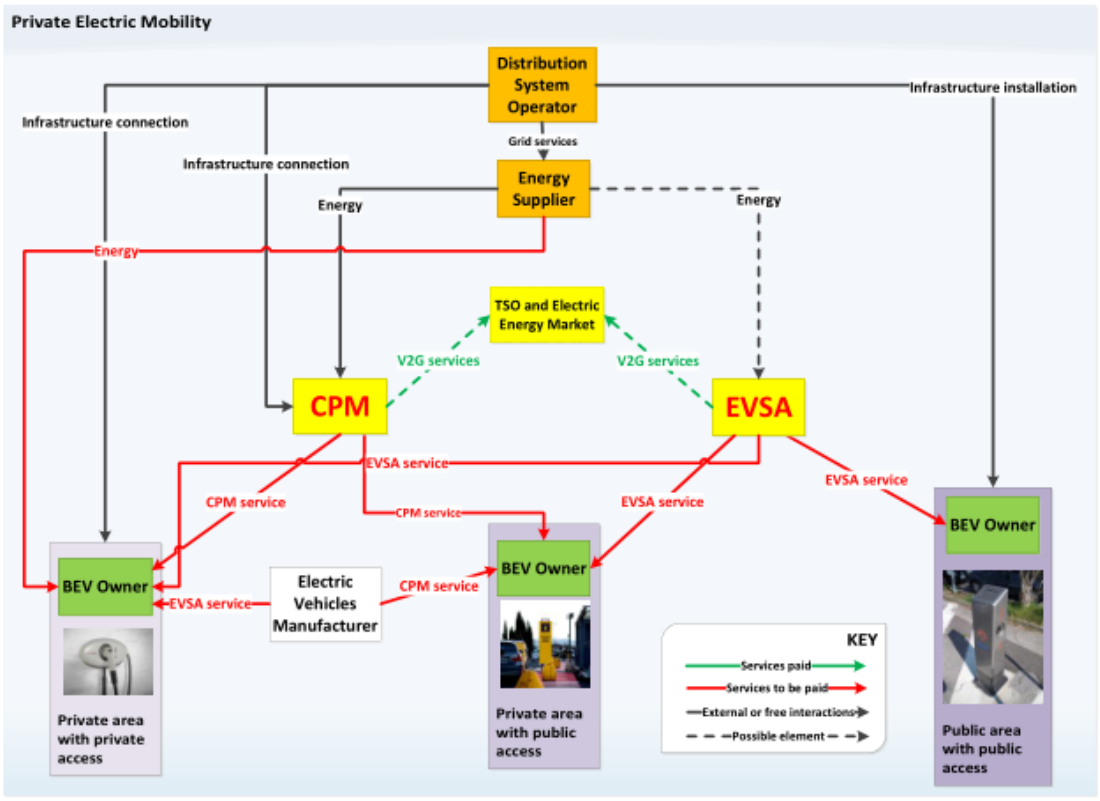

Figure 5.1 – Private electric mobility Agent Interaction Diagram

The business opportunities for the CPM are reported in Figure 5.2, where two possibilities are described. On the left, the CPM acts as retailer, buys energy and resells it to its customers through the charging services. As mentioned before, in the first period this agent will be surely public, but nothing prevents that it will be a private subject when the technology will be widespread. On the right hand, instead, the CPM acts as the owner of the accessible street. In the example, the highway service is reported as a possible future scenario where a street owner could provide to its customers also recharge services.

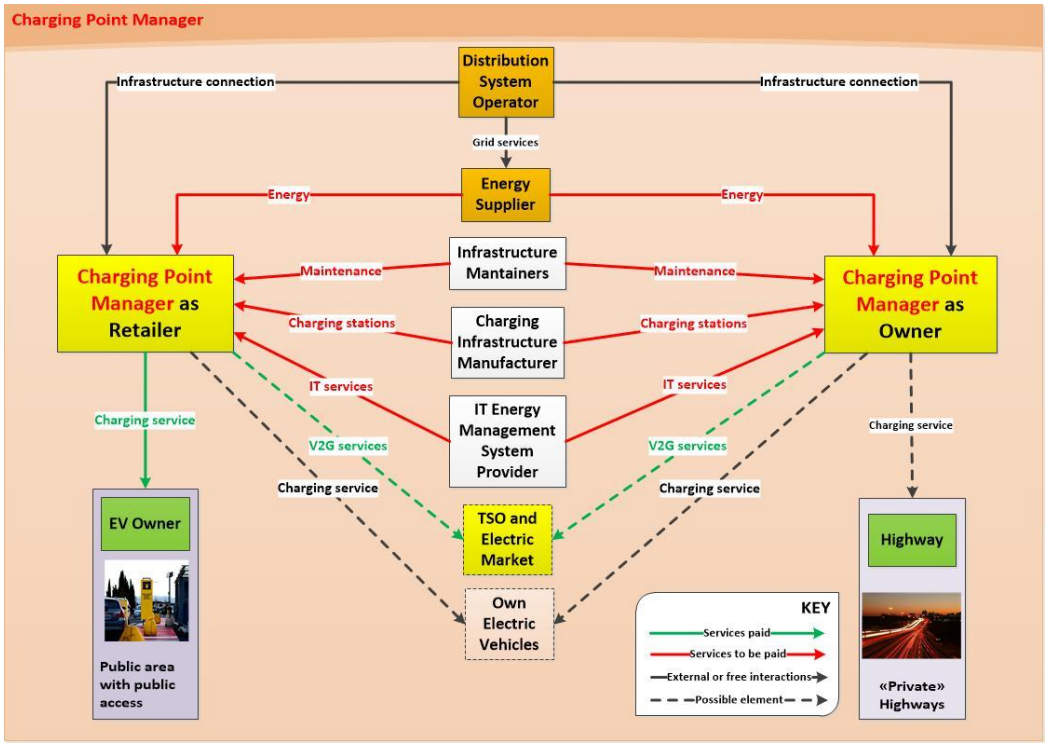

Figure 5.2 – Charging System Provider Agent Interaction Diagram

The business model canvas for the two possibilities presented above is reported in " Annex 12 – Municipality/Highway society business model canvas". The business model presented in Deliverable 3.3 chapter 5 perfectly fits the business opportunities of the dynamic recharge; the model presented in the annex of this document highlights the new possibilities given by the dynamic.

6 Conclusions

Within this document a complete feasibility analysis on *en-route* charging technology is provided. First chapter reports a comparative analysis of alternative energy storage systems: the dynamic charging strategy introduces a different energy management of the system: current and power peaks could occur while the vehicle is crossing the electrified path and the storage system have a faster and high frequency charge-discharge cycle. The energy storage system could be downsized due to nearly continuous charge of the vehicle but this have some implications on the energy cycle. In particular, the storage system must be able to support fast charge and discharge and last for a high number of cycle. One positive feature is that the SOC of the system will remain usually high. The analysed storage systems are:

- Carbon nanotube electrode lithium
- Copper nanowire cathode lithium
- Lithium air carbon
- Lithium silicon
- Carbon foam capacitor hybrid (very promising, combines energy density of the lithium-based batteries with the power peak management of supercapacitors. They could be recharged thousands without showing performance degradation).
- Lithium silicon polymer
- Lithium sulphur carbon nanofiber
- Lithium manganese composite/silicon carbon nanocomposite.
- Ultra capacitors

Due to very high currents, short charging intervals and market readiness, the ultra capacitors solution is the most promising one for the vehicles' dynamic *en-route* charge. To mitigate the total cost of the system a compromise could be to couple the ultra capacitors with a tradition, smaller, lithium battery pack.

The energy storage system is not the only feature that could be changed introducing a dynamic *en-route* recharge, also some additional devices could be adapted/introduced to fit specific technology needs. They are the lateral alignment management systems, the speed management and pairing mechanism. The functionality of some of them have been tested and results will be presented later in this paragraph. It is important to notice that the wireless communication system is very similar to the static charging one; the only difference is the increased working range necessary to ensure enough time to share information between vehicle and infrastructure. To obtain the needed performance for the dynamic en-route charging process, the solution proposed for static configuration - a WLAN solution working at 2.4GHz - has been modified in a long range Wi-Fi standard that work at 60GHz.

Dynamic charging also present problems of energy consumption measurement and cost accounting, and so also metering technologies have been taken into account. To monitor the power consumption during the charging process, digital devices are the best option since they have better accuracy, are more flexible and they already have an analogue to digital signal converter that allows to share it over internet to control the charging process remotely. Digital DC power measurement devices are less complex than AC power measurement devices thus the measuring point after the first AC/DC converter on the charger side and the last measuring point at the terminals of the energy storage system selected the best option when it is desired to set up the measuring device by parts. In addition, a good choice is to perform the measurement at the AC 3-phase grid side because it is possible to find many accurate, very reliable and specialised devices for this measurement on the market. To bill the customer for the charged power it is very important to be aware of the power losses throughout the circuit. If the customer is billed at the grid side, he pays the energy charged to the vehicles batteries but also the losses of the AC/DC converters, DC/AC converters and the induction losses. Otherwise, if the customer is billed for the real energy going into the batteries the owner of the charging station needs to take in the power losses through the circuit. Considering this, measurement points closer to the grid are better for the billing process because that is the energy the owner of the charging station needs to pay. The best measuring points are therefore the 3-phase AC grid side or the first DC point after the first AC to DC converter since it is easy to find a suitable device, for the AC case, or set up the device by parts, for the DC case.

In the third chapter, the drivers' behaviour has been studied both with a drive simulator and with a real vehicle to understand the impact of the lateral misalignment. The scope of this test activity has been to understand if a lateral misalignment device is necessary to provide energy to the vehicle with an acceptable efficiency or the natural accuracy of the average driver is fit to run the system with enough efficiency.

Also the effect of visual aid painted on the pavement has been considered. The first comparison has been between the visually aided and unaided visualization of the electrified track and the effect of driver training and experience. The initial tests have been carried out using a realistic simulator and they showed how, on average, a 20cm lateral misalignment is achievable by the tested drivers. The study of the trend of misalignment provided also some directions for the choice of the path to electrify (e.g. misalignment become higher during and after a turn). The tests on real vehicle, carried out with a vehicle with a real time position tracking system, proved that the simulator could be used as “worst case” analysis: in fact, simulation overestimates the misalignment of 40% respect to the real world results.

This analysis makes difference between the results carried out by unaided drivers and results with trained drivers. The analysis carried out using the drive simulator indicates that, and a set of suggestion for the segments to be electrified is given.

State of art analysis and solutions presented in this deliverable have been tested for a real urban case study, provided by the city of Firenze, Italy, member of the advisory board. In this case also an in-depth feasibility analysis has been carried out. First step of the analysis has been the definition of possible infrastructure layouts for the bus scenario in order to define all the possibilities enabled by dynamic en-route wireless charging technology.

Two bus routes of Firenze, line 23 and line 4 archetypes of long and medium range respectively, have been measured for 10 times and the driving cycles have been analyzed to understand the consumption and driving behavior characteristics: the route 23 includes 89 stops and 26300m distance travelled. On average, 5432s are the time effectively on movement and 1577s the stop time. Maximum consumption has been calculated in 43.9kWh per route that results a maximum average consumption of 1.6kWh/km. Route 4 includes 23 stops and 8965m distance travelled. On average, 1846s are the time effectively on movement and 348s the stop time. Maximum consumption has been calculated in 9.2kWh per route that results a maximum average consumption of 1.026kWh/km.

Starting from these data, a set of possible solutions has been considered:

- Case A: static charge at the beginning and at the end of the route
- Case B: static *en-route* charge at the bus stop
- Case C: static *en-route* charge without time increase
- Case D: dynamic charge only
- Case E: static *en-route* charge without time increment at the bus stop combined with dynamic charge sections
- Case F: static *en-route* and dynamic charge using discrete primary coils of the same power
- Case G: static *en-route* and dynamic charge using discrete primary coils of the same power

Table 3.3 and Table 3.5 report the numeric results of the seven possibilities respectively for line 23 and for line 4. Here are reported the costs and the service level indicators with an idea of civil works needed to build the infrastructure itself. From an economic point of view only, best solution is the Case B for both line 23 and line 4.

In the last chapter, an analysis on the cost to implement a wireless charging technology within an urban environment is given. For this analysis, the city of Firenze has been used as case study considering both the public transport service and the private mobility. A business structure to assess the wireless recharge economic possibility is given for the possible future owner of the infrastructure. In this scenario, the CPM has been thought as a public agent, but the economic flows let imagine that, when the technology will widespread, it will be opened to private subjects such as energy retailers and/or tolled streets owner as highways are.

7 References

1. Suh I.S. “Application of shaped magnetic field in resonance (SMFIR) technology to future urban transportation” (2011), CIRP Design Conference 2011.
2. *http://www.popularmechanics.com/cars/news/fuel-economy/8-potential-ev-and-hybrid-battery-breakthroughs#slide-1*
3. *http://www.dailykos.com/story/2011/08/12/1005272/-New-battery-approaches-gasoline-energy-density*
4. *http://www.graphene-battery.net/graphene-battery.htm*
5. *http://pubs.acs.org/doi/abs/10.1021/nl800957b*
6. Electrical Double-Layer Capacitors in Hybrid Topologies—Assessment and Evaluation of Their Performance, Noshin Omar et al, 2012
7. http://es.rs-online.com/web/
8. www.mouser.es/
9. http://www.lasis.unifi.it/mdswitch.html
10. http://www.lanazione.it/siena/foto/toscani-guida-auto-1.332687#1
11. http://electrical-engineering-portal.com
12. Antony Collins, "Solid state solutions for electricity Metology"
13. Bill Drafts, "Methods of current measurement"
14. www.nde-ed.org
15. Von Nicola O'Byrne, "Strom- und Spannungsmessung in der Signalkette
16. www.soyouwana.com
17. techybeams.blogspot.com
18. www.maximintegrated.com
19. Vaccumschmelze, "Current transformers and power line transformers
20. S.Wolf, R.F.M. Smith, "Electronic Instrumentation Laboratories
21. http://materias.fi.uba.ar
22. A. Van Putten, "Electronic measurement systems"
23. http://www.inti.gov.ar
24. http://circutor.es/es
25. http://www.gavazzi-automation.com/es/index.asp
26. http://www.web-books.com/eLibrary/ON/B1/B1397/108MB1397.html

8 Annex 1 – Power measurements techniques and devices

Before starting to analyse where and how to measure the power consumed by the customer, at first a brief introduction to the existing measurement methods is given in order to provide the necessary background for the following chapters. For power measurements, analogue and digital devices can be found. Analogue meters present lots of disadvantages compared to the digital ones like less flexibility, less accuracy and, which is the most important of all disadvantages, they cannot be connected to the Ethernet or a computer for data transmission and further analysis. Due to these disadvantages, the analogue devices are presented but the focus of this document is more towards the digital methods. Before starting with the analyses of the different devices, it is important to understand the differences between Direct Current (DC) power and Alternating Current (AC) power. DC power can be obtained by multiplying the voltage at the terminals of the load by the current through the load, since the current and voltage are of a constant value over time. In the case of AC power, the voltage and current periodically change the direction that leads to a more complex calculation of the power consumption. In this case, it is necessary to calculate the root mean square (RMS) of the voltage and current, and the power factor must be also taken into account.

The power factor (PF) is the ratio between the real power, also called useful power, and the apparent power, also called total power, of the circuit and has a value between -1 and 1.

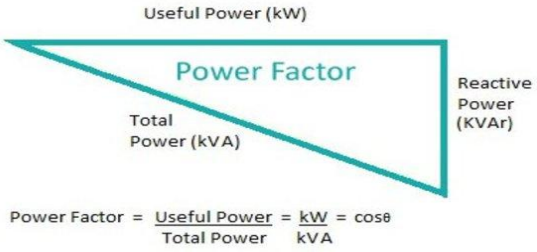

Figure Annex1.1 - The power factor is the ratio between the real power (Useful Power) and the apparent power (Total Power).

The apparent power can be calculated with the following equation:

$$P_{apparent} = V_{RMS} \cdot I_{RMS}$$

The equation to calculate the real power is shown next:

$$P_{real} = V_{RMS} \cdot I_{RMS} \cdot PF$$

For both, AC and DC power measurements, it is necessary to measure the voltage and the current of the circuit. The measurement devices for sensing voltage are set in parallel with the load whereas the current sensing devices are placed in series with the load as shown in Figure.

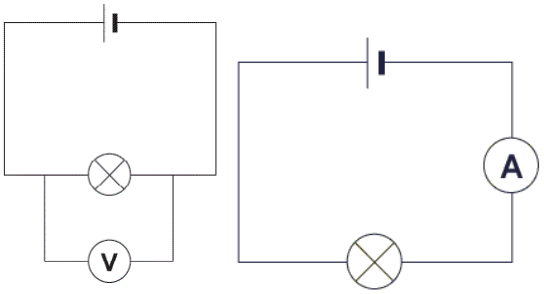

Figure Annex1.2 - Left: Voltage measurement. Right: Current measurement

At first, the analogue devices for power measurement will be discussed and after that the focus will be placed on the digital devices.

This section shows price ranges for different components and devices to have an estimation of the implementation costs. The prices for the components used to set up a power metering device by parts are obtained only from two distributors of electric components [7, 8] in order to have the same reference. The price of the components and devices for power metering are only a reference value since the price can reduce significantly when the amount of order of components or devices grows.

8.1 Analogue measurement methods

Analogue measurement methods are based on sensing the magnetic field generated by the current flux through coils. In these devices, the power consumption is obtained mechanically without the help of a microprocessor for the calculations. The most common devices based on analogue measurement methods are the electromechanical induction watt-hour meters and the analogue watt-meter. The first method can only be used for AC power monitoring whereas the second method can be used to measure AC and DC power.

8.1.1 Electromechanical induction watt-hour meter:

This device is still the most used device for power consumption metering. Nowadays, these types of power meters are slowly becoming obsolete, being replaced by the digital devices since they are cheaper, with more functionalities and new possibilities (like monitoring power consumption with an internet connection). The electromechanical induction watt-hour meter counts the revolutions of a non-magnetic metal disc that rotates at a speed proportional to the power passing through the meter. The number of revolutions is thus proportional to the power consumption. The disc spins due to the magnetic field generated by two coils (or sets of coils), one coil is connected in series with the load, producing a magnetic flux in proportion to the current, and the other is placed in parallel to the load, producing a magnetic flux in proportion to the voltage. The field of the voltage coil is delayed by 90 degrees, producing eddy currents in the disc. The effect of the eddy currents is a force exerted on the disc in proportion to the instantaneous current, voltage and phase angle (power factor) between them. A permanent magnet exerts an opposing force. The action of this two opposite forces results in a disc rotation at a speed proportional to the power consumption. Figure Annex1.3 shows the schematic and a photo of an electromechanical induction watt-hour meter.

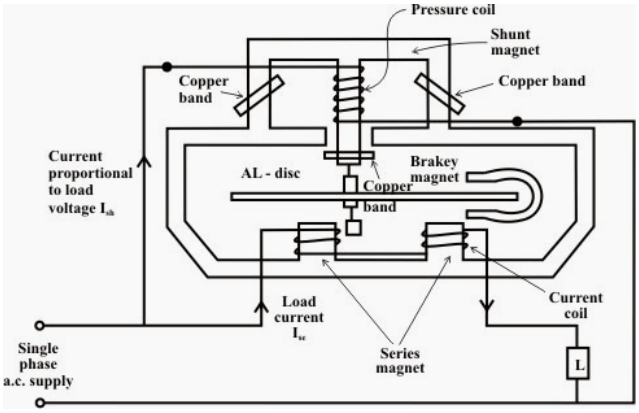

Figure Annex1.3 - Electromechanical induction watt-hour meter [11]

8.1.2 Analogue Watt meter:

The analogue watt meter is an electrodynamics instrument, used to measure energy from AC or DC sources. This method uses the reaction between the magnetic fields of two current carrying coils, one fixed, known as current coils, and other one movable, called potential coil. The current coils, connected in series with the circuit, while the potential coil is connected in parallel as Figure Annex1.4 shows. The potential coil carries a needle that moves over a scale to indicate the measurement. A current flowing through the current coils generates an electromagnetic field around the coils. The strength of this field is proportional to the line current and in phase with it. The potential coil has, as a general rule, a high-value resistor connected in series with it to reduce the current that flows through it.

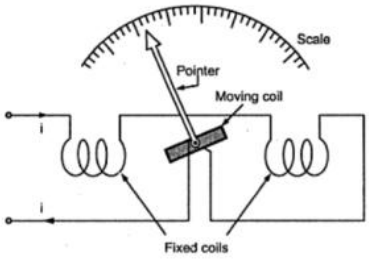

Figure Annex1.4 - Analogue watt meter

The result of this arrangement is that on a DC circuit, the deflection of the needle is proportional to both, the current and the voltage, thus conforming to the equation P=VI.

For AC power, current and voltage may not be in phase, owing to the delaying effects of circuit inductance or capacitance. On an AC circuit the deflection is proportional to the average instantaneous product of voltage and current, thus measuring true power, P=VI cos φ. The two circuits of a wattmeter can be damaged by excessive current. The ammeter and voltmeter are both vulnerable to overheating — in case of an overload, their pointers will be driven off scale — but in the wattmeter, either or even both the current and potential circuits can overheat without the pointer approaching the end of the scale. This is because the position of the pointer depends on the power factor, voltage and current. Thus, a circuit with a low power factor will give a low reading on the wattmeter, even when both of its circuits are loaded to the maximum safety limit. Therefore, a wattmeter is rated not only in watts, but also in volts and amperes. The problem of this device is that it shows the instantaneous power but without metering the consumption over time.

8.2 Digital measurement methods

All digital metering devices count with an Analog to Digital Converter (ADC), converting the voltage signal from the input into a digital value proportional to the magnitude of the analogue input signal. These devices count also with a voltage and current sensing part, a signal conditioning circuit and a microprocessor for the data analysis. At first, the voltage and current transducer will be explained. These components are necessary to adapt or transform the voltage and current signals into a voltage signal with a range suitable for the ADC. After that, the ADCs will be introduced since they are the heart of the digital devices. ADCs are necessary for the conversion of the analogue input signals from the transducers to a digital output code readable by Microprocessors. Finally, the processing of the digital output of the ADC is discussed.

A device that includes all these parts is called solid state energy meter and the schematic of such a device is shown in Figure Annex1.5.

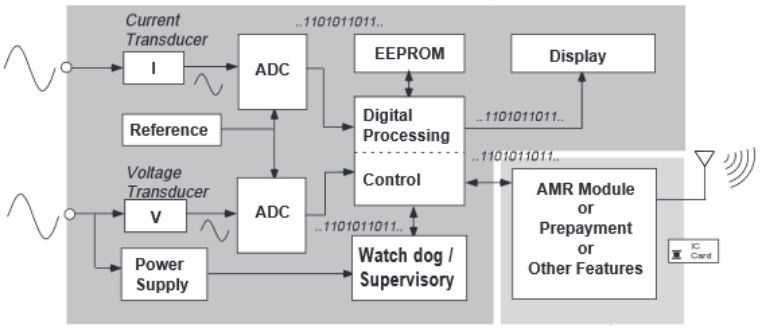

FigureAnnex1.5 - Schematic block of a Solid State Energy Meter [12]

Commercially available solid state energy meters will be introduced at the end of this chapter.

8.2.1 Voltage transducer:

In order not to saturate and probably damage the ADC, it is necessary to scale down the input voltage to the input voltage range of the ADC when measuring high voltages. To scale down the voltage a voltage divider or a voltage transformer can be use. In most of the applications, a voltage divider is preferred due to their simplicity, less power consumption, higher accuracy and better price.

Voltage divider: A simple voltage divider is set up by two resistors in series, producing the necessary voltage drop in the first resistor and leaving a suitable voltage at the point between the two resistors as input for the ADC. The schematic of such a component is shown in Annex1.6.

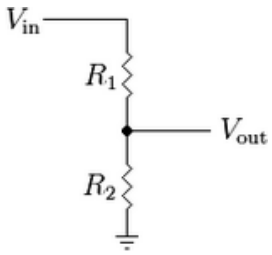

Figure Annex1.6 - Voltage divider

Next equation shows the relation between the input voltage and the output voltage of the voltage divider based on the schematic of Figure Annex1.6.

$$V_{out} = V_{in} \cdot \frac{R_2}{R_1 + R_2}$$

In order to get a high precision it is important to choose a voltage divider that produces, at Full Scale (FS), a voltage output adjusted to the maximum input range of the ADC.

To achieve a good accuracy it is also important to be aware of the temperature coefficient of the resistances and the tolerances percentage of them.

- Accuracy: The accuracy of those devices depends on the linearity, temperature coefficient and the tolerance of the resistors.
- Precision: The precision is very good and in order not to lose sensitivity it is important that the output range of the divider is the same as the input of the ADC at FS.
- Reliability: Since voltage dividers are set up by resistors, the reliability is very good.
- Power limit, voltage limit and current limit: The limit of power is around 2W. Most of the resistors for those applications have values in the MΩ range; therefore, the power limit does not present a problem for applications under 1000V.
- Frequency limit: Resistors have a small value of serial inductance and parallel capacitance thus it is important to use resistors with low inductances value when working at high frequencies.
- Price: The price starts at around 3 Euros for a resistor tolerance of 1% and temperature coefficient over 100ppm/ºC up to 25 Euros for resistors with a tolerance of 0,01% and temperature coefficient of less than 1ppm/ºC.
- Size: Typical sizes are 20mm x 8mm x 7mm.
- Power consumption: Since the resistors can be chosen in the MΩ range, the power consumption is very low. For a voltage of 1000V and a total resistance of 1 MΩ, the consumption is about 1mW.

Voltage transformer: A transformer is a device that transfers AC energy from the primary circuit to the secondary circuit. The working principle of these devices is that the winding of the primary circuit, around a high magnetic permeable material, induces a magnetic flux in the material that induces a current and voltage in the secondary wiring as it can be seen in Figure Annex1.7.

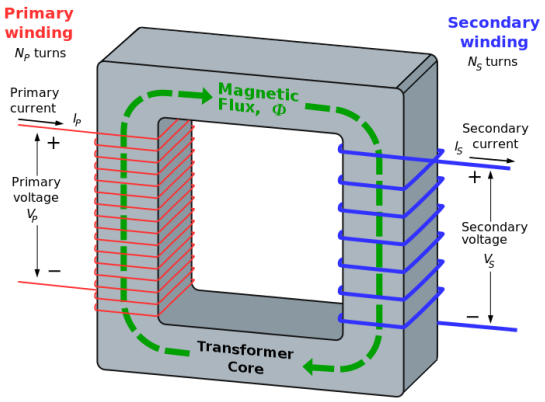

Figure Annex1.7: Transformer [13]

The relation between the current and voltage in the primary circuit and the voltage and current induced in the secondary circuit depends on the number of turns of the wire in each winding. The next equation shows the relation for an ideal transformer:

$$\frac{N_p}{N_s} = \frac{I_s}{I_p} = \frac{V_p}{V_s}$$

In a real transformer, it is necessary to take into account the energy losses due to the non-ideality of the wirings and the magnetic permeable material. Transformers can be used to change high voltage values of the primary circuit into a voltage suitable for the ADC or converting a high current into a smaller current in the secondary device for the current measurement. When the transformer is used as a voltage transformer the wiring of the primary circuit is connected in parallel to the load and the number of turns is much higher than in the secondary circuit. Measuring the voltage of the secondary circuit and knowing the ratio of turns of the primary circuit and the secondary circuit, it is simple to determine the voltage of the primary circuit.

- Accuracy: The accuracy of a voltage transformer depends on many factors like the external temperature, external electromagnetic fields, losses in the magnetic permeable core, ratio between the primary and secondary wiring and induced phase shift.
- Precision: The precision of the device depends on the output range since an ADC does the conversion.
- Reliability: The reliability of those devices is good since the mechanism is very simple.
- Power limit: The power limit depends on the dimensions of the wiring and the core. For power measurements, the power limit should not be a problem since in this application there is very high load inserted in the secondary circuit and hence the power consumption of the device is minimized.
- Voltage limit: The voltage limit of most of the commercial available devices is 230AC since they are designed for applications where the primary circuit is the mains grid.
- Current limit: The current limit does not concern in this application since the current through the primary circuit is minimized.
- Frequency limit: Commercially voltage transformers are normally designed for 50Hz-60Hz mains applications. The limit is given by the core and wiring used.
- Price: Voltage transformers can be found, starting from 4 Euros.
- Size: Normal dimensions of such a device are 20mm x 30 mm x 25mm.
- Power consumption: The power consumption of those devices, even in non-load applications, is much higher than the voltage divider circuits. The consumption can easily be around 1W.

Normally, voltage dividers are used to drop the voltage to a usable level for the ADC since they present many advantages compared to the voltage transformers. The accuracy is better, the size is smaller and the weight is less but probably the most important issue is that the power consumption of the voltage transformer is much higher than from the voltage divider. Table Annex1.1 shows the advantages and disadvantages of each voltage sensing component.

Table Annex1.1 - Comparison of the different voltage sensing component. Bad (-), Average (0), Good (+)

	Voltage divider	**Voltage transformer**
Voltage to measure	AC and DC	AC
Accuracy	+	0
Output voltage range	+	+
Reliability	+	0
Temperature stability	0	+
Frequency limits	+	+
Price	+	-
Size	+	-
Galvanic Isolation	-	+
Power consumption	+	-

8.2.2 Current measurement methods:

Since the current sensing devices presented in this part produce a voltage proportional to the current flowing through the circuit at their output, it is necessary to count on an ADC to obtain a binary value proportional to the measurement. To reach higher precision during the conversion it can be convenient to use an amplifying circuit to adapt the output of the current sensing device to the input range of the ADC.

The most common devices to sense current are:

- Shunt resistor
- Hall sensors
- Current transformers

Shunt resistor: This method of current measurement consists of inserting a resistance of a very small value in series with the load. The value of the resistance should be in the range of 300μΩ to 1mΩ for 100A. The resistance causes a voltage drop that is proportional to the current flowing through the shunt. For example, for a current of 100A and a 300μΩ shunt resistor the voltage drop is 30mV at FS and the power consumption is 3W.

Normally, shunt resistors are used together with an amplifying circuit since the output voltage is very small at FS. With an integrating ADC this voltage can be measured, converting the voltage value into a binary value and by applying the Ohms law the current can be obtained from the voltage measurement. The precision of the measurement depends on the value of the resistor since a higher resistor causes a higher voltage drop that leads to a higher range of input voltage for the ADC, increasing the precision. The disadvantage is that higher resistor values also increase the power consumption of the component. Shunt resistors can be inserted in the high voltage line or in the ground or neutral line. In the case the resistor is inserted in the high voltage path, it is necessary to isolate the rest of the metering system from the high voltage.

- Accuracy: The accuracy of the current lecture of a shunt resistance depends on the accuracy of the resistance and is normally around 5% to 0,5%. The temperature of the resistor is also an important factor since the resistor value changes with the temperature. The variation for 1ºC can be between 30ppm/ºC up to 100ppm/ºC depending on the quality of the component.
- Precision: Components with higher resistor values give better precision since an ADC measures the voltage drop and higher resistors give a higher voltage range at the output. The disadvantage of this is that resistors with higher resistance consume more power and therefore are more invasive.
- Reliability: The reliability is good when working within the working temperature and power limit of the shunt resistor. At temperatures outside of the normal temperature range, the thermal drift gets more and more important, causes important changes in the measurement, and can even damage the device. It is also important not to use the resistor for higher current than allowed in order not to damage the device.
- Power limit, voltage limit and current limit: Since the shunt resistor has a fixed value and the voltage drop through the resistor is small it is only necessary to define the current limit or the power limit, since both depend on each other. Typical limits are 3W to 10W.
- Frequency limit: These components do not have a frequency limit. The ADC that transforms the voltage value of the shunt resistor into a binary value imposes the limit. However, when the application is an AC measurement it is important that the inductive part of the resistor is low. The special manufacturing process of this kind of resistors leads to raise the price.
- Price: Shunt resistance can be found from 2 Euros up to 170 Euros.
- Size: The size of these devices is related to the maximum power they are rated for. It is possible to find devices with a size of 10mm x 30mm x 1,5mm.

Figure Annex1.8 - Shunt resistor (Ohmite)

Current transducer based on Hall effect: These devices measure the electric current in the conductor, without making a physical contact with it. Current transducer based on Hall effect can be used to measure AC current and DC current.

The Hall effect consists of measuring the magnetic field produced by moving charges along a conductor. When a semiconductor is placed near a current carrying cable and a current supplied by the measuring device is passed through it, the charges in the semiconductor redistribute producing a charge difference on both sides of the semiconductor due to the magnetic field. The voltage generated by this difference of charge on both sides of the semiconductor can be measured and depends on the value of the magnetic field of the current carrying conductor. Figure Annex1.9 shows the measurement setup of a Hall effect component where the Primary Current is the current coming from the power supply of the component and the Magnetic Field, B, is generated by the current flux through the conductor under test. The measured voltage, V_h, is thus proportional to the magnetic flux through the component.

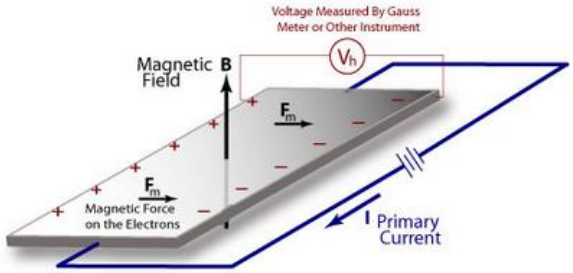

Figure Annex1.9 Hall effect measurement setup [14]

Since the voltage output of the Hall sensor is very small it is normally necessary to use an amplifying circuit to adjust the output value to the range of the ADC. Devices based on the Hall effect can be part of the circuit or be clamped around the current carrying cable as Figure shows.

Figure Annex1.10 - Left: Current sensing device to install in series with the circuit (Tamura). Right: Current sensing device to clamp around the current carrying cable (LEM).

The disadvantage of these devices is that they need to be powered externally.

- Accuracy: The cheap devices can be found with an accuracy of 13% for a full scale of 100A and for devices that are more expensive the accuracy can be around 1,5%. In these devices, it is also necessary to take into account the linearity of the output voltage that can add an error up to 1%. The thermal drift of these devices is normally less than of the shunt resistor devices and is around 0.1% of the Full Scale (FS).
- Precision: The precision depends on the voltage output range of the device since the ADC measures this vale. Typical output values are 1,5V up to 10V for better devices.
- Reliability: The reliability is good when working within the specification of the manufacturer.
- Power limit: Since the device is not directly in contact with the circuit or only has a part where the current flow through, without power losses it is not necessary to speak about power limits.
- Voltage limit: Since the sensor is galvanically isolated from the voltage of the circuit, it is only necessary to be aware of the isolation voltage limit. This limit is high enough for the applications in this project.
- Current limit: It is possible to find these devices for a huge range of different current limits starting from mA up to more than 1000A.
- Frequency limit: There are Hall sensors especially for DC current measurements but most of them are also suitable for AC current measurements. The frequency limit depends on the re-

sponds delay of the charges in the Hall Element when the magnetic field changes. The response time can be high like 100ms for a change of 100A or low like 10µs/100A. The first would be not suitable for AC current measurement whereas the second on can be perfectly used for AC current measurements.

- Price: It is possible to find devices starting at 8 Euros up to 1500 Euros. The difference between a more expensive and a cheaper device is the range of generated output voltage and the accuracy.
- Size: This component can be found with a size from 13mm x 15mm x 7mm for devices, which need to be included in the circuit or 30mm x 57mm x 77mm for devices that need to be placed around the cable.

Current transformer: The current transformer is based on the same method explained at the section of voltage transformer. In this case, the desired behaviour is that in the secondary wiring appears current proportional to the current in the primary wiring producing a negligible voltage drop in the primary circuit. To obtain the current from the first wiring, a resistor is introduced between the terminals of the secondary circuit of the current transformer as Figure Annex1.11 shows.

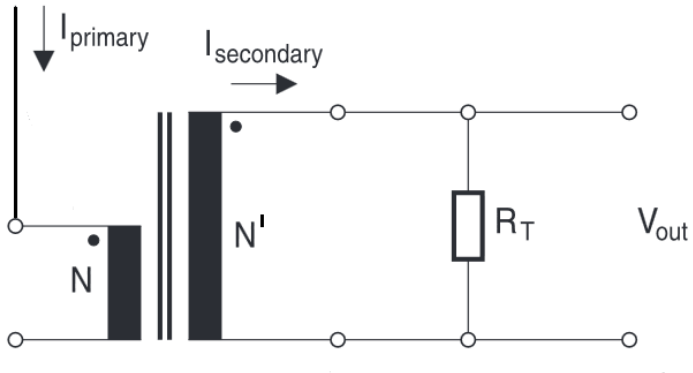

Figure Annex1.11 - Measuring circuit with the current transformer

The relation between the primary and the secondary current is the following:

$$R_T = \frac{V_{out}}{I_{secondary}} = \frac{V_{out} \cdot N'}{I_{primary} \cdot N} => I_{primary} = \frac{V_{out} \cdot N'}{R_T \cdot N}$$

Where N is the number of winding turns on the primary coil and N' is the number of winding turns on the secondary coil. A simple current transformer can be achieved by placing the magnetic permeable core with the secondary wiring around the cable under test as shown in Figure Annex1.12. This is the most used current transformer for current measurement devices.

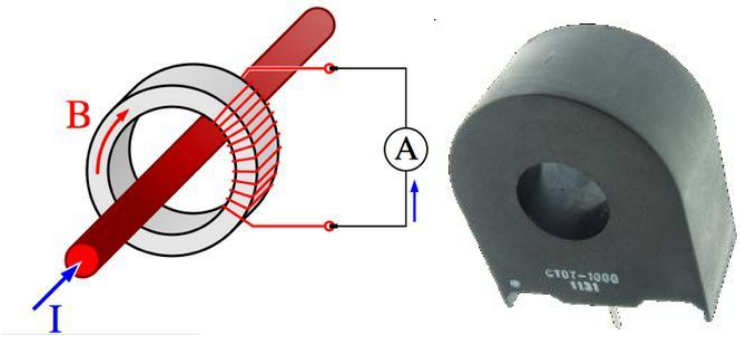

Figure Annex1.12 -: Left: Current transformer for current measurements [16]; Right: Current transformers (ICE components)

The permeable magnetic core can be opened in some devices for easier placing of the device around the cable. Another method is using the Rogowski coil. The Rogowski coil is a coiled wire without magnetic permeable core that can be placed around the cable under test. Due to the magnetic field, a voltage is induced in the Rogowski coil that can be measured.

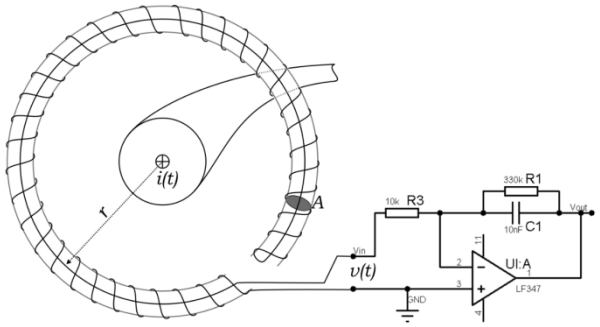

Figure Annex1.13 - Rogowski coil [13]

The disadvantage of the Rogowski coil is the high sensitivity to external magnetic fields.

The following characteristics are referred to the normal current transformers.

- Accuracy: The accuracy of a current transformer depends on many factors as the external temperature, external electromagnetic fields, losses in the magnetic permeable core, ratio between the primary and secondary wiring and phase shift. Depending on the temperature the phase angle error can varies up to 6º at high temperatures and the current error of the full scale is around -0,5% approximately. A higher phase shift, when the PF is close to 1 is not so important but as the PF decrease the error induced in the measured power gets more and more important since PF = cos(θ + phase shift). It is also very important to take into consideration the accuracy of the resistor, inserted at the terminals of the second wiring for the current measurement, and add this value to the errors already defined.
- Precision: The precision of these components is good but it is important to note that the output range of the component should be the same as the input range of the ADC to maximise the precision of the digital lecture.
- Reliability: The reliability of these devices is good since the mechanism is very simple.
- Power limit: There is no power limit. The important parameters are the current through the cable and the frequency of this current.
- Voltage limit: Since there is no direct contact between the primary circuit and the secondary circuit and the voltage drop in the wiring of the primary circuit is negligible it is not necessary to be aware about the voltage limits. For measurements with very high voltages, the isolation limit of the component should be taken into account.
- Current limit: Typical values are current limits of 35A up to 200A.
- Frequency limit: Current transformer can be found for a huge range of frequency limits, starting at 40Hz up to 500kHz approximately.
- Price: Current transformers are much cheaper than hall sensors. They can easily found between 2 Euros and 8 Euros.
- Size: Typical dimensions of such a component are 23mm x 12 mm x 26mm.

The following table shows the advantages and disadvantages of the different current transducers discussed in this section.

Table Annex1.2 - Comparison of the different current sensing devices. Very bad (--), Bad (-), Average (0), Good (+) and Very good (++)

	Shunt resistor	**Hall sensor**	**Current transformer**
Current to measure	AC and DC	AC and DC	AC
Accuracy	++	+	0
Output voltage range	-	+	++
Reliability	++	0	+
Temperature stability	+	++	++
Current limits	-	++	+
Frequency limits	++	++	++
Price	++	-	+
Size	++	0	0
Galvanic Isolation	--	++	++

External power supply	++	--	++

8.2.3 Analog to digital converter:

An analog to digital converter (ADC) is a device which takes samples of an analogue signal at discrete instances of time, converting the measured values into a binary number. The resolution of the conversion of an ADC depends on the number of output bits and the Full Scale range of the input of the ADC. To guarantee that the input voltage of the ADC is constant during the conversion time it is used a sample and hold device (S/H) that captures the voltage of a continuously varying signal and hold its value until the end of the conversion. In the following section, the five most used types of ADCs are introduced since the ADC is the heart of all digital metering devices. The most used conversion methods are:

- Dual slop integration ADC
- Voltage to frequency ADC
- Sigma delta ADC
- Successive Approximation ADC (SAR)
- Flash ADC

Dual slope integrating ADC: This type of ADC is the most used ADC for measurement devices. The conversion method is based on switching the input of an integrator amplifier between a reference voltage and the voltage to be measured. During a fixed time the integrator is connected to the voltage to be measured, charging the capacitor, and after this time the integrator is connected to the reference value (of opposite sign than the voltage to be measured). The discharge timer of the capacitor, reaching the zero cross, is counted and this time is proportional to the voltage input. Figure Annex1.14 shows on the left side the schematic of a dual-slop integrator and on the right side the voltage at the point Vx during one conversion, showing the charge and discharge of the capacitor.

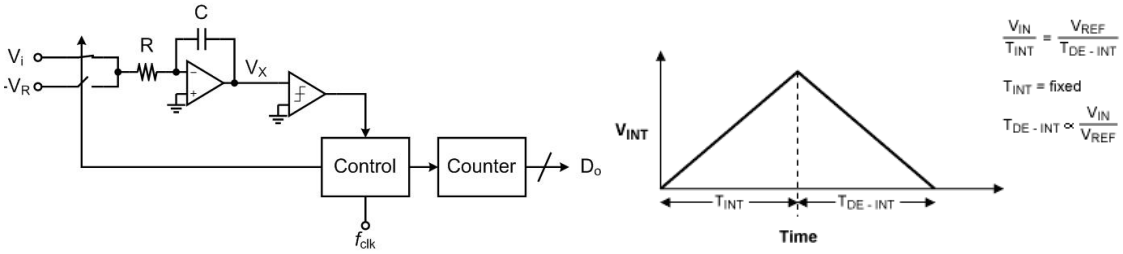

Figure Annex1.14 -: Left: Block diagram of a dual-slope integrating ADC [17]; Right: Voltage at the point Vx after the integrator [18];

In this kind of ADCs, longer integration times, allow higher resolutions. The noise rejection is good and they are ideal for digitalizing low bandwidth signals. Therefore, the advantages of dual slop integrating ADC are their very good accuracy, linearity, immunity to noise and their cheap price. A disadvantage is the low conversion rate. An increase of the accuracy leads to a reduction of the conversion rate.

Voltage to frequency ADC: In this type of ADCs, the input voltage is converted into pulses with a frequency proportional to the input voltage. Like in the dual slop ADCs, these ADCs use an integrating amplifier circuit with the difference that in this case the capacitor of the integrating amplifier is charged until reaching a reference voltage level. When this happens, the capacitor is discharged, one pulse is counted and the process starts again. The advantages of these ADCs are the very good noise reaction and good accuracy. These devices have the same disadvantage as the dual slop ADCs, the low conversion rate.

Sigma Delta ADCs: This ADC also uses an integrating amplifier. This method consists of switching between two reference voltages of opposite sign. The idea is to keep the capacitor uncharged. A comparator is used to determine if the input should be switched from one reference value to the other one or if the input should be kept at the same reference value in order to discharge the capacitor. Figure Annex1.15 shows the block diagram of a Sigma Delta ADC.

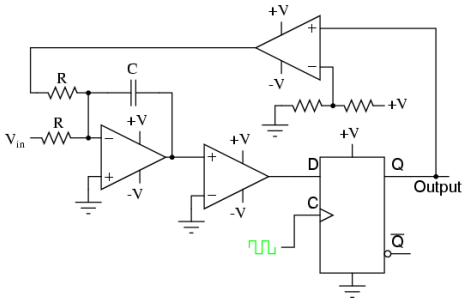

Figure Annex1.15 - Block diagram of a Sigma Delta ADC [25]

The change of the switch is performed, if necessary, with a specific frequency. The times the switch is connected to the positive reference voltage and the time the switch is connected to the negative reference voltage, during a fixed period of time, is recorded. The input voltage is hence proportional to:

$$V_{in} = \frac{V_{ref}(n_{up} - n_{down})}{n_{up} + n_{down}}$$

Where n_{up} and n_{down} are the times the capacitor is connected to the positive reference voltage and the negative reference voltage respectively. The advantages of these ADCs are their high accuracy and resolution keeping a good conversion rate but the power consumption is higher than the power consumption of the two ADC already discussed [12].

Successive Approximation (SAR) ADC: In these ADCs, the input voltage is compared to a reference voltage that can adopt all the possible voltage values. At first, the input is compared to the half scale that corresponds to the most significant bit. If the input voltage is above this vale, the Most Significant Bit (MSB) = 1 and the next reference voltage takes the value of ¾ of full scale. If the input voltage is below the first reference voltage the MSB = 0 and the next reference voltage is ¼ of the full scale. With each comparison, the resolution of the ADC grows by 1 bit, therefore it is possible to get high resolution and high conversion speed but they are more expensive than the ADCs already shown [19]. Figure Annex1.16 shows the voltage reference value along a 4-Bit conversion. The comparator decides if the input voltage is higher or lower than the reference value, adding a 1 or 0 to the binary number.

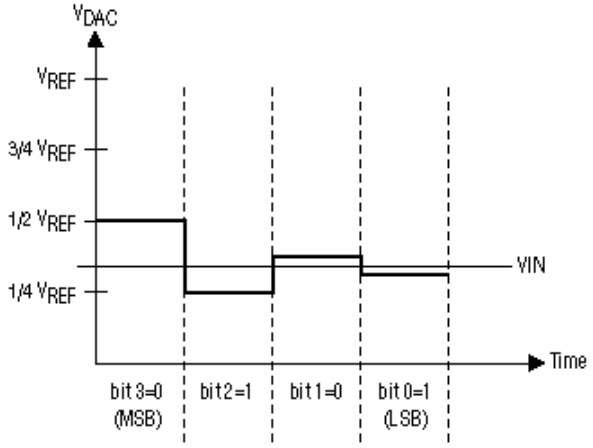

Figure Annex1.16 - Output bit generation of an SAR ADC [21].

Flash ADC: This converter is also called parallel converter since for an n-Bit ADC the input voltage feds 2^n-1 comparators. All the comparators compares the input voltage to a reference voltage, different for all the comparators, getting as result a code of 1..10..0. To interpret this code it is necessary to count also with an Encoder to convert this code to a binary value. The reference voltages are obtained by using n^2 resistors of the same value in series and each terminal of the resistors is used as reference input voltage of one comparator as shown in FigureAnnex1.17.

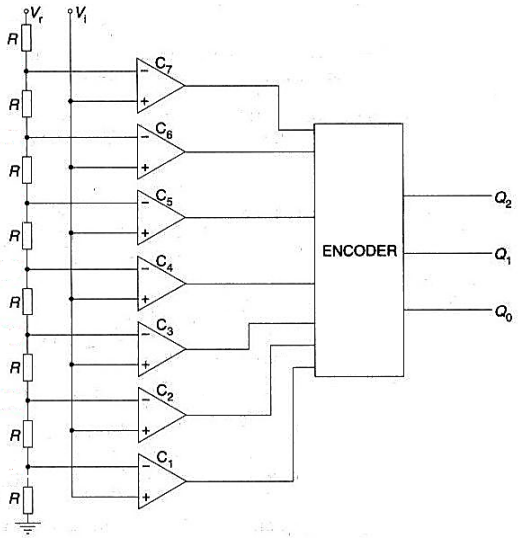

Figure Annex1.17 - Flash 3Bit ADC converter

The advantage of these ADCs is their very high speed but they are the most expensive due to the large number of components needed [22]. The large number of components is also responsible for the lower accuracy. The following table shows the advantages and disadvantages of the ADCs discussed in this section.

Table Annex1.3 - Comparison of the different types of ADC. Disadvantage (-), Average (0), Good (+) and Very good (++)

	Dual slop	Voltage to frequency	Sigma delta	SAR	Flash
Conversion Speed	-	-	0	+	++
Accuracy	++	+	+	0	-
Price	+	+	0	0	-

8.2.4 Processing the data:

After converting the analogue current and voltage signals into digital signals, a Microprocessor is used to analyse the data. The Microprocessor normally used is a Digital Signal Processor (DSP), which is a microprocessor specialized for the execution of mathematic algorithms, performing mathematical calculations very rapidly and carrying out a fast analysis of a large number of samples per second. The DSP is used to extract from the measurements all the necessary information like the power factor, apparent power and real power in a very short time. This device is also responsible of the communication with other parts of the EVSE like the screen to show the power consumed and the internet for the billing process.

8.2.5 Solid-state watt-hour meters:

Solid-state watt-hour meters are devices for AC power consumption monitoring which include all the parts already discussed in the above sections. These devices include a current sensing part, a voltage drop circuit, ADCs for the conversion from analogue to digital and a microprocessor to analyse the data. Actually, the solid-state watt-hour meters, shown in Figure Annex1.18, are replacing the old electromechanical induction watt-hour meters to measure AC power. This type of meters has many advantages against the electromechanical induction watt-hour meter since they transform the measured value in a digital value which can be send for example through an internet connection. With the system a power consumption control can be performed, different types of billing can be applied, etc.

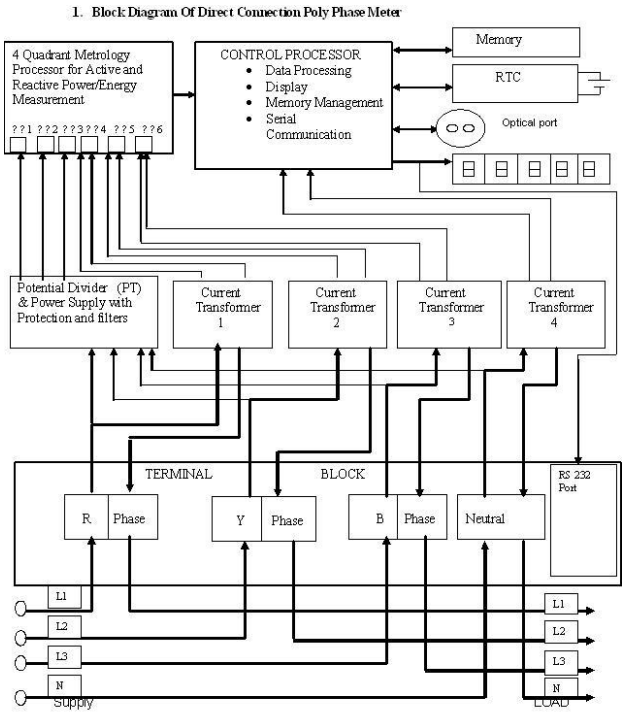

Figure Annex1.18 - Solid-state block diagram

- Accuracy: The accuracy for this type of devices is standardized into accuracy classes. The energy meters have to be into classes 1 and 2. This means that the percentage of error is 1% in class 1 and 2% in class 2, and, of course, a class 1 meter is more expensive than a class 2 meter.
- Precision: The precision of a solid-state watt-hour meter is usually 0.1 kWh. The precision of the device can vary with the temperature.
- Reliability: Solid-state watt-hour meters are as reliable as current transformers. Like other power meters, it is necessary to review the device every 6 months.
- Voltage limit: The voltage limit of a solid-state watt-hour meter is related to the electronic components and is important for the voltage reference. This voltage reference is the voltage value against which some features are set in the meter [23].
- Current limit: The current limits for this type of meters are related to the current transducers used in its construction.
- Frequency limit: The frequency limits of a solid-state watt-hour meter are related to the current transducer integrated in the meter.
- Price: The price of a solid-state watt-hour meter varies in order of its precision, accuracy, frequency, etc… It is possible to find a three-phase meter starting at a price of 90€, for low quality devices, up to more than 2000€.
- Size: The size of a solid-state watt-hour meter is more or less a 127 mm box.

Figure Annex1.19 shows a DC power monitoring device on the left side and a 3-phase AC power monitoring device on the right side.

Figure Annex1.19 - DC power monitoring device [24] (left) and AC power monitoring device [25] (right)

9 Annex 2 – Energy consumption distribution

Bus Stop		Time [s]	Time [s]	Average speed [km/h]	Distance [m]	Energy [kWh]
Stazione Valfonda	1	33,3	33,3	0	0	
1 to 2		161,2	194,5	17,5	785,6	1,102
Ridolfi - Anche Indipendenza	2	57,8	252,3	0	0	
2 to 3		37,5	289,7	21,9	228	0,2922
Santa Reparata	3	15,5	305,2	0	0	
3 to 4		86,2	391,4	10,7	257,1	0,4428
San marco	4	50,4	441,7	0	0	
4 to 5		27,6	469,3	23,8	182,2	0,3193
Santissima annunziata	5	17,8	487,1	0	0	
5 to 6		74,3	561,4	13,1	270,3	
Pergola	6	0,0	561,4	0	0	
6 to 7		31,9	593,3	18,3	162,1	0,5923
Colonna 01	7	15,9	609,2	0	0	
7 to 8		65,7	674,9	18,8	342,1	
D'Azeglio 01 - Anche Niccolini	8	0,0	674,9	0	0	
8 to 9		71,3	746,1	11,6	228,7	0,969
Leopardi	9	9,7	755,8	0	0	
9 to 10		22,9	778,7	30,9	196,7	
Beccaria - porta alla croce	10	0,0	778,7	0	0	
10 to 11		26,2	804,9	29,8	216,9	0,575
Giovine Italia	11	8,3	813,2	0	0	
11 to 12		53,3	866,4	25,8	382	0,695
Zecca Vecchia	12	9,5	875,9	0	0	
12 to 13		69,3	945,2	20	385,1	
Zecca Vecchia 02	13	0,0	945,2	0	0	
13 to 14		53,5	998,7	16,3	242,9	0,947
Tintori	14	10,2	1008,9	0	0	
14 to 15		77,4	1086,3	14,7	315,9	0,5937
Ponte Alle Grazie	15	9,7	1096,0	0	0	
15 to 16		39,6	1135,5	27,8	305,6	0,5819
Piazza Poggi - fm0573	16	12,0	1147,5	0	0	
16 to 17		64,1	1211,6	34,1	607,6	0,968
Fornace - fm07696	17	10,2	1221,8	0	0	
17 to 18		47,6	1269,3	19,5	257,8	0,4063
Orsini	18	9,3	1278,6	0	0	
18 to 19		53,8	1332,4	15,7	234,5	0,3986
Salutati	19	3,2	1335,5	0	0	
19 to 20		63,1	1398,6	23,6	413,2	0,3913
Ripoli	20	2,9	1401,5	0	0	
20 to 21		36,9	1438,3	16,1	165,2	0,6283
Gavinana - fm0433	21	2,7	1441,0	0	0	

21 to 22		59,2	1500,2	21,7	355,8	0,5533
Gualfredotto	22	9,2	1509,4	0	0	
22 to 23		42,5	1551,8	29,8	351,3	0,156
Datini	23	10,0	1561,8	0	0	
23 to 24		29,0	1590,8	21,2	170,6	0,54
Traversari - fm0222	24	15,5	1606,3	0	0	
24 to 25		64,7	1671,0	17	305,3	0,3217
Gran Bretagna	25	5,8	1676,8	0	0	
25 to 26		45,9	1722,6	26,4	336,6	0,3938
Edimburgo	26	16,0	1738,6	0	0	
26 to 27		56,4	1795,0	16,3	255,3	0,5932
Kiev - fm0077	27	26,7	1821,6	0	0	
27 to 28		28,3	1849,9	24,7	193,6	0,55
Portogallo	28	7,5	1857,3	0	0	
28 to 29		53,1	1910,4	14,2	209,9	0,363
Francia	29	63,6	1974,0	0	0	
20 to 30		62,4	2036,3	25	433,6	1,12
Marco Polo	30	0,0	2036,3	0	0	
30 to 31		21,8	2058,1	37,8	228,2	
Park Pino	31	16,1	2074,2	0	0	
31 to 32		67,9	2142,1	18,9	36,6	0,51
Olmi	32	4,5	2146,5	0	0	
32 to 33		28,6	2175,1	26,3	208,6	0,488
Sorgane Via Roma	33	5,4	2180,4	0	0	
33 to 34		25,3	2205,7	21,3	149,7	0,1674
Croce	34	10,1	2215,8	0	0	
34 to 35		49,3	2265,1	19,7	269,9	0,655
Sorgane	35	192,0	2457,0	0	0	
35 to 36		53,3	2510,3	21,6	319,7	0,56
rodolico - fm0774	36	13,4	2523,7	0	0	
36 to 37		84,3	2608,0	8,8	205,2	1,379
Cimitero Del Pino	37	2,9	2610,9	0	0	
37 to 38		93,8	2704,6	23	58,3	
Olanda - fm0777	38	8,6	2713,2	0	0	
38 to 39		43,2	2756,4	32,9	395,3	0,2714
Kassel	39	6,5	2762,9	0	0	
39 to 40		54,3	2817,1	19,9	300,1	1,23
Kyoto	40	3,3	2820,4	0	0	
40 to 41		39,7	2860,1	30,5	335,7	
Carlo D'Angio'	41	8,6	2868,6	0	0	
41 to 42		57,4	2926,0	17,5	278,1	0,41
Federico D'Antiochia	42	11,1	2937,1	0	0	
42 to 43		42,6	2979,6	22,9	271	0,425
Ser Lapo Mazzei	43	6,4	2986,0	0	0	
43 to 44		42,6	3028,6	15,9	187,6	0,416
Bocchi	44	4,5	3033,1	0	0	

44 to 45		54,5	3087,6	20,6	311,9	0,69
G. Dalle Bande Nere	45	9,5	3097,0	0	0	
45 to 46		62,3	3159,3	20,2	311,9	1,096
Leonardo Bruni	46	0,0	3159,3	0	0	
46 to 47		67,8	3227,0	18,7	352,5	
Baldovini	47	36,7	3263,7	0	0	
47 to 48		45,6	3309,2	15,2	192,9	0,1118
Ricorboli - fm0400	48	8,4	3317,6	0	0	
48 to 49		77,3	3394,9	14,2	305,1	1,16
Cellini - fm0541	49	0,0	3394,9	0	0	
49 to 50		54,7	3449,5	33,9	514,5	
Serristori - fm0542	50	6,4	3455,9	0	0	
50 to 51		49,8	3505,7	27,8	385,1	0,56
Demidoff - fm0543	51	12,2	3517,9	0	0	
52 to 52		59,6	3577,5	14,9	246,5	0,7858
Benci	52	16,3	3593,7	0	0	
52 to 53		61,7	3655,4	19,5	334,3	0,4934
Verdi	53	14,0	3669,4	0	0	
53 to 54		66,8	3736,2	10	185,5	0,58
Salvemini	54	26,4	3762,6	0	0	
54 to 55		70,0	3832,6	10,9	211,8	0,4086
Sant'Egidio	55	0,0	3832,6	0	0	
55 to 56		36,0	3868,6	16,3	163,2	
Bufalini anche ospedale sant	56	5,6	3874,2	0	0	
56 to 57		67,3	3941,4	14,3	267,8	0,2784
Pucci	57	17,4	3958,8	0	0	
57 to 58		150,2	4108,9	12,4	515,9	0,7582
Museo Di San Marco	58	42,7	4151,6	0	0	
58 to 59		81,0	4232,5	12,5	282,2	0,4861
San Zanobi	59	24,2	4256,7	0	0	
59 to 60		112,3	4369,0	6,9	215,8	0,4612
Ridolfi	60	10,3	4379,3	0	0	
60 to 61		130,3	4509,6	24,8	898,9	1
Stazione Pensilina	61	25,9	4535,5	0	0	
61 to 62		87,8	4623,3	8,7	212,1	0,3468
Stazione Scalette - fm1455	62	38,6	4661,9	0	0	
62 to 63		52,4	4714,2	20,4	296,9	0,37
Scala	63	6,8	4721,0	0	0	
63 to 64		53,7	4774,7	23,7	353,5	0,4963
Fratelli Rosselli	64	22,5	4797,1	0	0	
64 to 65		74,5	4871,6	9,1	187,4	0,6479
Pier Luigi da Palest. - fm0560	65	11,6	4883,2	0	0	
65 to 66		93,5	4976,7	15	388,8	0,173
Scarlatti	66	22,9	4999,6	0	0	
66 to 67		187,3	5186,9	7,3	377,9	1,109
Ponte All'Asse	67	88,0	5274,8	0	0	

67 to 68		115,0	5389,8	10,3	330,5	0,968
Circondaria - fm0782	68	4,1	5393,9	0	0	
68 to 69		76,0	5469,8	19,9	420,3	0,9882
Massaio	69	5,6	5475,4	0	0	
69 to 70		46,0	5521,4	18,8	239,8	0,5485
Ponte Di Mezzo	70	29,9	5551,3	0	0	
70 to 71		56,0	5607,3	20,1	313,4	0,4931
Terzolle - fm0785	71	11,5	5618,8	0	0	
71 to 72		31,5	5650,3	26,5	232	0,4826
Del Prete - fm0786	72	20,1	5670,4	0	0	
72 to 73		70,7	5741,1	22,2	435,1	
Magellano	73	0,0	5741,1	0	0	
73 to 74		11,6	5752,7	37,6	121,1	
Caboto - fm0292	74	4,5	5757,1	0	0	
74 to 75		51,3	5808,4	21,5	305,8	1,118
Panciatichi 01 - fm0293	75	10,2	5818,5	0	0	
75 to 76		42,2	5860,7	25,7	301,6	0,42
Tre pietre - fm0788	76	10,7	5871,4	0	0	
76 to 77		93,2	5964,6	15,1	391,6	0,2427
Nuovo Pignone	77	225,9	6190,4	0	0	
77 to 78		43,9	6234,3	24,8	302,3	1,09
Perfetti Ricasoli	78	13,0	6247,3	0	0	
78 to 79		42,7	6290,0	21,3	252,4	
fiorentinagas - fm0296	79	0,0	6290,0	0	0	
79 to 80		43,4	6333,4	19,3	233,1	
Panciatichi - fm0297	80	0,0	6333,4	0	0	
80 to 81		22,9	6356,2	21,8	138,5	
Campo Sportivo Rifredi	81	0,0	6356,2	0	0	
81 t0 82		21,2	6377,4	42,3	248,5	
Caciolle	82	0,0	6377,4	0	0	
82 t0 83		59,4	6436,7	18,2	300,9	1,65
Maddalena	83	14,3	6451,0	0	0	
83 to 84		35,0	6486,0	24,2	235,5	0,6
Pionieri Dell'Aviazione	84	12,7	6498,7	0	0	
84 to 85		59,9	6558,6	24,4	406,1	0,2376
Giovanni Dei Marignolli	85	11,5	6570,1	0	0	
85 to 86		32,9	6603,0	13,5	123	
Via del Massaio - fm0794	86	0,0	6603,0	0	0	
86 to 87		58,9	6661,9	27,5	449,6	0,4516
Corsica	87	6,0	6667,8	0	0	
87 to 88		164,6	6832,4	9,8	447,6	1,038
san Iacopino - fm3016	88	14,4	6846,7	0	0	
88 to 89		150,6	6997,3	13	546	0,5972
Guido Monaco	89	11,8	7009,1	0	0	
Total		7009,1			26322,6	43,9435

10 Annex 3 – Idle consumption at the bus stops

Stop		stop time (s)	energy (6 kW*tstop/3600)
Stazione Valfonda	1	33,3	0,0555
Ridolfi - Anche Indipendenza	2	57,8	0,0963
Santa Reparata	3	15,5	0,0258
San marco	4	50,4	0,0839
Santissima annunziata	5	17,8	0,0297
Pergola	6	0,0	0,0000
Colonna 01	7	15,9	0,0265
D'Azeglio 01 - Anche Niccolini	8	0,0	0,0000
Leopardi	9	9,7	0,0161
Beccaria - porta alla croce	10	0,0	0,0000
Giovine Italia	11	8,3	0,0138
Zecca Vecchia	12	9,5	0,0158
Zecca Vecchia 02	13	0,0	0,0000
Tintori	14	10,2	0,0170
Ponte Alle Grazie	15	9,7	0,0162
Piazza Poggi - fm0573	16	12,0	0,0200
Fornace - fm07696	17	10,2	0,0169
Orsini	18	9,3	0,0154
Salutati	19	3,2	0,0053
Ripoli	20	2,9	0,0048
Gavinana - fm0433	21	2,7	0,0045
Gualfredotto	22	9,2	0,0153
Datini	23	10,0	0,0167
Traversari - fm0222	24	15,5	0,0258
Gran Bretagna	25	5,8	0,0097
Edimburgo	26	16,0	0,0266
Kiev - fm0077	27	26,7	0,0444
Portogallo	28	7,5	0,0124
Francia	29	63,6	0,1060
Marco Polo	30	0,0	0,0000
Park Pino	31	16,1	0,0268
Olmi	32	4,5	0,0074
Sorgane Via Roma	33	5,4	0,0089
Croce	34	10,1	0,0168
Sorgane	35	192,0	0,3199
rodolico - fm0774	36	13,4	0,0223
Cimitero Del Pino	37	2,9	0,0048
Olanda - fm0777	38	8,6	0,0143
Kassel	39	6,5	0,0108
Kyoto	40	3,3	0,0055
Carlo D'Angio'	41	8,6	0,0143
Federico D'Antiochia	42	11,1	0,0185
Ser Lapo Mazzei	43	6,4	0,0107
Bocchi	44	4,5	0,0075

G. Dalle Bande Nere	45	9,5	0,0158
Leonardo Bruni	46	0,0	0,0000
Baldovini	47	36,7	0,0611
Ricorboli - fm0400	48	8,4	0,0140
Cellini - fm0541	49	0,0	0,0000
Serristori - fm0542	50	6,4	0,0107
Demidoff - fm0543	51	12,2	0,0203
Benci	52	16,3	0,0271
Verdi	53	14,0	0,0233
Salvemini	54	26,4	0,0440
Sant'Egidio	55	0,0	0,0000
Bufalini anche ospedale s.ta maria nuova	56	5,6	0,0093
Pucci	57	17,4	0,0289
Museo Di San Marco	58	42,7	0,0711
San Zanobi	59	24,2	0,0403
Ridolfi	60	10,3	0,0172
Stazione Pensilina	61	25,9	0,0432
Stazione Scalette - fm1455	62	38,6	0,0643
Scala	63	6,8	0,0113
Fratelli Rosselli	64	22,5	0,0374
Pier Luigi da Palestrina - fm0560	65	11,6	0,0193
Scarlatti	66	22,9	0,0382
Ponte All'Asse	67	88,0	0,1466
Circondaria - fm0782	68	4,1	0,0068
Massaio	69	5,6	0,0093
Ponte Di Mezzo	70	29,9	0,0498
Terzolle - fm0785	71	11,5	0,0192
Del Prete - fm0786	72	20,1	0,0335
Magellano	73	0,0	0,0000
Caboto - fm0292	74	4,5	0,0074
Panciatichi 01 - fm0293	75	10,2	0,0169
Tre pietre - fm0788	76	10,7	0,0178
Nuovo Pignone	77	225,9	0,3764
Perfetti Ricasoli	78	13,0	0,0216
fiorentinagas - fm0296	79	0,0	0,0000
Panciatichi - fm0297	80	0,0	0,0000
Campo Sportivo Rifredi	81	0,0	0,0000
Caciolle	82	0,0	0,0000
Maddalena	83	14,3	0,0238
Pionieri Dell'Aviazione	84	12,7	0,0212
Giovanni Dei Marignolli	85	11,5	0,0192
Via del Massaio - fm0794	86	0,0	0,0000
Corsica	87	6,0	0,0099
san Iacopino - fm3016	88	14,4	0,0239
Guido Monaco	89	11,8	0,0196
TOTAL		**1577,1**	**2,6285**

11 Annex 4 – Average values for line 4

station name	station	avg time [s]	Time (s)	Avg distance[m]	Avg speed [km/h]
	23 to 1	111,9	0,0	281,9	9,1
Stazione mercato centrale	1	120,0	111,9	0,0	0,0
	1 to 2	94,1	232,0	244,9	9,4
Stazione Largo Alinari	2	41,9	326,0	0,0	0,0
	2 to 3	211,2	367,9	971,2	16,6
Lorenzo Il Magnifico	3	12,4	579,1	0,0	0,0
	3 to 4	43,9	591,5	226,7	18,6
Cernaia - fm0119	4	9,0	635,4	0,0	0,0
	4 to 5	25,8	644,4	197,9	27,6
Statuto 01	5	5,4	670,2	0,0	0,0
	5 to 6	28,4	675,6	159,3	20,2
Statuto Fs	6	6,5	704,0	0,0	0,0
	6 to 7	68,4	710,5	381,3	20,1
Fabroni	7	6,7	778,9	0,0	0,0
	7 to 8	58,4	785,5	254,3	15,7
Gioia	8	9,8	843,9	0,0	0,0
	8 to 9	80,8	853,7	499,9	22,3
Giorgini - fm0256	9	9,8	934,4	0,0	0,0
	9 to 10	46,2	944,2	301,4	23,5
Montelatici	10	2,3	990,4	0,0	0,0
	10 to 11	73,0	992,7	343,2	16,9
Celso	11	8,6	1065,7	0,0	0,0
	11 to 12	49,4	1074,4	274,2	20,0
Mercati	12	8,8	1123,8	0,0	0,0
	12 to 13	54,6	1132,5	273,8	18,1
Cappuccini	13	3,7	1187,1	0,0	0,0
	13 to 14	60,4	1190,8	332,2	19,8
Massaia	14	6,9	1251,2	0,0	0,0
	14 to 15	39,4	1258,1	290,2	26,5
Massaia 02	15	1,7	1297,5	0,0	0,0
	15 to 16	97,7	1299,1	348,2	12,8
Vittorio Emanuele	16	14,4	1396,8	0,0	0,0
	16 to 17	86,7	1411,1	503,1	20,9
Bigozzi	17	5,1	1497,8	0,0	0,0
	17 to 18	38,5	1502,9	181,7	17,0
Paoletti - fm0265	18	1,7	1541,4	0,0	0,0
	18 to 19	130,7	1543,0	581,2	16,0
Guasti -fm0266	19	12,4	1673,7	0,0	0,0
	19 to 20	49,6	1686,1	244,4	17,8
Statuto 04 - fm0267	20	16,4	1735,7	0,0	0,0
	20 to 21	40,7	1752,1	197,3	17,5
Statuto	21	16,9	1792,7	0,0	0,0
	21 to 22	198,3	1809,6	964,2	17,5
G. Monaco	22	5,6	2007,8	0,0	0,0
	22 to 23	158,9	2013,4	912,2	20,7
Stazione Pensilina	23	21,8	2172,3	0,0	0,0
Total			2194,0	8964,5	

12 Annex 5 – Energy consumption distribution

station name	station	Avg distance[m]	Avg speed [km/h]	Energy [kWh]
Starting point	23 to 1	281,9	9,1	
Stazione mercato centrale	1	0,0	0,0	0.4851
	1 to 2	244,9	9,4	
Stazione Largo Alinari	2	0,0	0,0	0.331
	2 to 3	971,2	16,6	
Lorenzo Il Magnifico	3	0,0	0,0	0.5372
	3 to 4	226,7	18,6	
Cernaia - fm0119	4	0,0	0,0	0.5429
	4 to 5	197,9	27,6	
Statuto 01	5	0,0	0,0	0.2053
	5 to 6	159,3	20,2	
Statuto Fs	6	0,0	0,0	0.1691
	6 to 7	381,3	20,1	
Fabroni	7	0,0	0,0	0.3546
	7 to 8	254,3	15,7	
Gioia	8	0,0	0,0	0.3689
	8 to 9	499,9	22,3	
Giorgini - fm0256	9	0,0	0,0	0.3303
	9 to 10	301,4	23,5	
Montelatici	10	0,0	0,0	0.302
	10 to 11	343,2	16,9	
Celso	11	0,0	0,0	0.395
	11 to 12	274,2	20,0	
Mercati	12	0,0	0,0	0.2877
	12 to 13	273,8	18,1	
Cappuccini	13	0,0	0,0	0,3453
	13 to 14	332,2	19,8	
Massaia	14	0,0	0,0	0.2876
	14 to 15	290,2	26,5	
Massaia 02	15	0,0	0,0	0.5052
	15 to 16	348,2	12,8	
Vittorio Emanuele	16	0,0	0,0	0.0827
	16 to 17	503,1	20,9	
Bigozzi	17	0,0	0,0	0.3587
	17 to 18	181,7	17,0	
Paoletti - fm0265	18	0,0	0,0	0.1603
	18 to 19	581,2	16,0	
Guasti -fm0266	19	0,0	0,0	0.574
	19 to 20	244,4	17,8	
Statuto 04 - fm0267	20	0,0	0,0	0.3457
	20 to 21	197,3	17,5	
Statuto	21	0,0	0,0	0.2127
	21 to 22	964,2	17,5	
G. Monaco	22	0,0	0,0	0.9527
	22 to 23	912,2	20,7	
Stazione Pensilina	23	0,0	0,0	0.7605
Total		8964,5		9.2

13 Annex 6 – Sample characteristics

	Name	Yrs driving	Gender	Age	Drive frequency
Test1	Driver 1	11	m	29	3
Test2	Driver 2	12	m	30	5
Test3	Driver 3	4	m	22	2
Test4	Driver 4	20	m	38	2
Test5	Driver 5	14	m	32	3
Test6	Driver 6	16	m	34	4
Test7	Driver 7	10	m	28	3
Test8	Driver 8	14	m	33	5
Test9	Driver 9	22	m	40	4
Test10	Driver 10	14	m	32	4
Test11	Driver 11	14	m	32	4
Test12	Driver 12	14	m	33	5
Test13	Driver 13	13	f	32	5
Test14	Driver 14	5	f	23	3
Test15	Driver 12	14	m	33	5
Test16	Driver 15	13	f	31	4
Test17	Driver 16	6	f	24	1
Test18	Driver 17	4	f	22	5
Test19	Driver 18	5	f	23	3
Test20	Driver 5	14	m	32	3
Test21	Driver 18	5	f	23	3
Test22	Driver 19	27	f	45	4
Test23	Driver 18	5	f	23	3
Test24	Driver 20	20	m	38	2
Test25	Driver 5	14	m	32	3
Test26	Driver 21	6	m	24	5
Test27	Driver 21	6	m	24	5
Test28	Driver 21	6	m	24	5

14 Annex 7 – Complete final results

Accuracy	Precision	Gender	Yrs. Driving	Drive frequency	Avg. Speed [km/h]
0,167	0,221	m	11	3	10,043
0,137	0,197	m	12	5	10,674
0,368	0,230	m	4	2	9,679
0,136	0,207	m	20	2	10,445
0,135	0,229	m	14	3	11,077
0,245	0,191	m	16	4	10,073
0,144	0,237	m	10	3	11,291
0,148	0,200	m	14	5	12,416
0,161	0,300	m	22	4	11,861
0,166	0,221	m	14	4	11,629
0,115	0,196	m	14	4	10,264
0,155	0,191	m	14	5	12,450
0,168	0,261	f	13	5	12,153
0,256	0,308	f	5	3	9,699
0,180	0,173	m	14	5	13,097
0,225	0,305	f	13	4	11,291
0,392	0,449	f	6	1	13,028
0,227	0,274	f	4	5	10,612
0,515	0,271	f	5	3	11,994
0,195	0,207	m	14	3	10,241
0,185	0,267	f	5	3	11,151
0,172	0,308	f	27	4	8,905
0,150	0,174	f	5	3	10,762
0,281	0,421	m	20	2	12,285
0,134	0,262	m	14	3	10,954
0,073	0,193	m	6	5	12,199
0,084	0,176	m	6	5	11,043
0,097	0,180	m	6	5	12,162

15 Annex 8 – Regression analysis for accuracy and precision

To better describe the influence of the variables, a regression analysis has been made both for accuracy and for precision. The regression equation after the p-value analysis is:

```
Accuracy[m] = 0,3924 + 0,0 Female - 0,0819 Male + 0,0 Drive_frequency_1
                     - 0,0490 Drive_frequency_2 - 0,1378 Drive_frequency_3
                     - 0,1571 Drive_frequency_4 - 0,1878 Drive_frequency_5
```

With a R^2adjusted = 32.55%.

Within the data, two measurements are outlier. One of them in particular, 19th measure, is referred to a driver that have experienced a high parallax issue. If the test is repeated without 19th measure, the equation became:

```
Accuracy[m] = 0,3924 + 0,0 Female - 0,0477 Male + 0,0 Drive_frequency_1
                     - 0,0832 Drive_frequency_2 - 0,1918 Drive_frequency_3
                     - 0,1799 Drive_frequency_4 - 0,2145 Drive_frequency_5
```

With a R^2adjusted = 50.41%. There is still a problem within the analysis, because drive frequency is not behaving as expected because its effect on the accuracy is not linear. This could be because one of the tested person is coming from a foreign country where vehicles are driven opposite than the simulator. If this value is removed from the analysis, this issue is overcome and the regression equation is:

```
Accuracy[m] = 0,3924 + 0,0 Female - 0,0546 Male + 0,0 Drive_frequency_1
                     - 0,0763 Drive_frequency_2 - 0,1875 Drive_frequency_3
                     - 0,1918 Drive_frequency_4 - 0,2091 Drive_frequency_5
```

With an R^2adjusted = 55.88%. It is possible to conclude that a good accuracy is reachable for mid-experienced drivers and experienced drivers. A training period has to be established for drivers with less experience (training results are shown in 4.3.1). Same analysis has been made also for the precision. The regression equation is a more complex because the statistically significant variables are more than before and because they are discrete:

```
       Drive
Gender Frequency
Female      1          Precision [m] = 0,4276 + 0,00354 Yrs. driving

Female      2          Precision [m] = 0,2998 + 0,00354 Yrs. driving

Female      3          Precision [m] = 0,2456 + 0,00354 Yrs. driving

Female      4          Precision [m] = 0,2351 + 0,00354 Yrs. driving

Female      5          Precision [m] = 0,2211 + 0,00354 Yrs. driving

Male        1          Precision [m] = 0,3616 + 0,00354 Yrs. driving

Male        2          Precision [m] = 0,2338 + 0,00354 Yrs. driving

Male        3          Precision [m] = 0,1796 + 0,00354 Yrs. driving

Male        4          Precision [m] = 0,1691 + 0,00354 Yrs. driving

Male        5          Precision [m] = 0,1551 + 0,00354 Yrs. driving
```

With a R^2adjusted = 55.97%.

It is possible to conclude that also the drive precision is highly affected by the drive frequency and by the gender. Drivers training is responsible for a positive effect on precision. The regression analysis for real data acquisition are reported here below:

The regression equation is for accuracy

```
Accuracy = 0.127+ 0 drv. frequency_2- 0.047 drv. frequency_3- 0.025 drv. frequency_4 -
 0.015 drv. frequency_5+ 0 lap_1- 0.030 lap_2- 0.031 lap_3+ 0 female- 0.031 male
```

And for precision

```
Precision = 0.057+ 0 drv. frequency_2- 0.017 drv. frequency_3- 0.014 drv. frequency_4
- 0.006 drv. frequency_5+ 0 female- 0.013 male
```

The R2adj values have been 39.90% for accuracy and 34.13% for precision; it means that results are encouraging also if the variability is not well described by the regression fit equation.

16 Annex 9 – Repeated tests final results

Final results of Driver 18

Accuracy test 1	Accuracy test 2	Accuracy test 3	Precision test 1	Precision test 2	Precision test 3
0,127	0,378	0,001	0,042	0,103	0,027
0,321	0,026	0,155	0,294	0,225	0,116
0,451	0,336	0,149	0,189	0,102	0,102
0,761	0,552	0,272	0,636	0,729	0,608
0,668	0,079	0,060	0,212	0,067	0,078
0,898	0,081	0,243	0,272	0,317	0,278
0,312	0,016	0,076	0,212	0,222	0,125
0,523	0,178	0,199	0,316	0,625	0,281
0,365	0,067	0,132	0,208	0,130	0,156
0,672	0,030	0,109	0,352	0,194	0,117
0,399	0,140	0,220	0,104	0,201	0,075

Final results of driver Driver21

Accuracy test 1	Accuracy test 2	Accuracy test 3	Precision test 1	Precision test 2	Precision test 3
0,032	0,114	0,148	0,036	0,070	0,154
0,059	0,228	0,153	0,153	0,119	0,125
0,093	0,006	0,004	0,125	0,069	0,138
0,235	0,222	0,244	0,782	0,839	0,775
0,158	0,057	0,029	0,132	0,133	0,061
0,080	0,011	0,003	0,356	0,253	0,193
0,079	0,042	0,107	0,281	0,096	0,065
0,037	0,012	0,053	0,080	0,060	0,155
0,054	0,086	0,147	0,093	0,082	0,089
0,082	0,075	0,051	0,132	0,066	0,081
0,012	0,042	0,088	0,090	0,074	0,105

Finale results of driver Driver5

Accuracy test 1	Accuracy test 2	Accuracy test 3	Precision test 1	Precision test 2	Precision test 3
0,099	0,100	0,031	0,021	0,072	0,047
0,364	0,407	0,089	0,167	0,327	0,236
0,190	0,062	0,001	0,132	0,100	0,065
0,124	0,301	0,259	0,670	0,798	0,707
0,026	0,130	0,218	0,127	0,137	0,117
0,347	0,278	0,239	0,521	0,211	0,295
0,076	0,164	0,008	0,104	0,085	0,136
0,162	0,151	0,015	0,370	0,082	0,341
0,096	0,176	0,049	0,155	0,189	0,163
0,231	0,248	0,098	0,153	0,141	0,231
0,019	0,087	0,277	0,095	0,103	0,254

17 Annex 10 – Straight segments results

Accuracy	1	3	5	7	8	9	10	11
1	0,131	0,151	0,271	0,026	0,012	0,031	0,393	0,026
2	0,090	0,020	0,059	0,034	0,216	0,020	0,297	0,017
3	0,253	0,453	0,297	0,405	0,327	0,327	0,553	0,177
4	0,034	0,045	0,141	0,018	0,159	0,116	0,266	0,052
5	0,099	0,190	0,026	0,076	0,162	0,096	0,231	0,019
6	0,058	0,184	0,374	0,267	0,275	0,558	0,067	0,409
7	0,059	0,196	0,153	0,068	0,178	0,173	0,056	0,061
8	0,105	0,145	0,035	0,441	0,039	0,147	0,286	0,027
9	0,229	0,009	0,108	0,288	0,027	0,140	0,125	0,143
10	0,058	0,000	0,158	0,126	0,065	0,088	0,085	0,255
11	0,056	0,049	0,151	0,045	0,182	0,191	0,032	0,278
12	0,030	0,103	0,039	0,010	0,021	0,007	0,108	0,288
13	0,090	0,144	0,007	0,096	0,170	0,047	0,072	0,235
14	0,016	0,042	0,132	0,270	0,469	0,175	0,319	0,209
15	0,201	0,033	0,178	0,003	0,077	0,077	0,050	0,136
16	0,042	0,008	0,015	0,103	0,202		0,403	0,145
17	0,311	0,369	0,363	0,111	0,100	0,080	0,151	0,740
18	0,329	0,129	0,040	0,548	0,352	0,029	0,392	0,230
19	0,127	0,451	0,668	0,312	0,523	0,365	0,672	0,399
20	0,100	0,062	0,130	0,164	0,151	0,176	0,248	0,087
21	0,378	0,336	0,079	0,016	0,178	0,067	0,030	0,140
22	0,150	0,051	0,556	0,355				
23	0,001	0,149	0,060	0,076	0,199	0,132	0,109	0,220
24	0,009	0,027	0,192	0,785	0,496	0,029	0,066	0,162
25	0,031	0,001	0,218	0,008	0,015	0,049	0,098	0,277
26	0,032	0,093	0,158	0,079	0,037	0,054	0,082	0,012
27	0,114	0,006	0,057	0,042	0,012	0,086	0,075	0,042
28	0,148	0,004	0,029	0,107	0,053	0,147	0,051	0,088

Precision	1	3	5	7	8	9	10	11
1	0,068	0,122	0,193	0,100	0,102	0,130	0,246	0,135
2	0,034	0,112	0,157	0,093	0,155	0,114	0,099	0,120
3	0,126	0,058	0,115	0,058	0,145	0,319	0,132	0,232
4	0,025	0,071	0,069	0,058	0,143	0,477	0,153	0,142
5	0,021	0,127	0,140	0,100	0,428	0,213	0,156	0,093
6	0,026	0,179	0,132	0,055	0,263	0,079	0,112	0,070
7	0,019	0,087	0,175	0,266	0,170	0,275	0,039	0,217
8	0,089	0,045	0,169	0,326	0,191	0,092	0,052	0,138
9	0,088	0,119	0,076	0,525	0,172	0,542	0,157	0,151
10	0,031	0,176	0,071	0,151	0,166	0,127	0,124	0,118
11	0,031	0,148	0,102	0,346	0,118	0,209	0,158	0,102
12	0,079	0,072	0,118	0,142	0,169	0,086	0,022	0,149
13	0,166	0,212	0,102	0,066	0,108	0,394	0,130	0,175
14	0,034	0,123	0,150	0,119	0,323	0,704	0,132	0,160
15	0,047	0,051	0,040	0,030	0,104	0,140	0,126	0,179
16	0,097	0,074	0,074	0,041	0,603		0,346	0,106

17	0,092	0,134	0,192	0,215	0,410	0,548	0,489	1,169
18	0,093	0,119	0,207	0,116	0,492	0,280	0,140	0,105
19	0,044	0,171	0,234	0,123	0,329	0,256	0,406	0,129
20	0,074	0,100	0,130	0,081	0,077	0,240	0,144	0,107
21	0,097	0,099	0,068	0,216	0,637	0,126	0,195	0,206
22	0,154	0,175	0,180	0,150				
23	0,027	0,096	0,079	0,124	0,250	0,162	0,112	0,079
24	0,038	0,129	0,099	1,238	1,315	0,244	0,083	0,239
25	0,049	0,066	0,128	0,132	0,399	0,224	0,232	0,340
26	0,036	0,114	0,137	0,259	0,081	0,111	0,128	0,100
27	0,067	0,072	0,131	0,096	0,060	0,090	0,065	0,080
28	0,157	0,154	0,063	0,065	0,169	0,096	0,072	0,102

18 Annex 11 – Real car results

Test	Lap	Name	Age	Drive frequency	Yrs. Driving	Gender	Accuracy	Precision
Test 1	1	Driver 1	42	4	24	m	0,0313	0,0191
Test 2	2	Driver 1	42	4	24	m	0,0837	0,0225
Test 3	3	Driver 1	42	4	24	m	0,0346	0,0266
Test 4	1	Driver 5	33	4	15	m	0,0804	0,0359
Test 5	2	Driver 5	33	4	15	m	0,0476	0,0263
Test 6	3	Driver 5	33	4	15	m	0,0350	0,0158
Test 7	1	Driver 18	23	3	5	f	0,0714	0,0507
Test 8	2	Driver 18	23	3	5	f	0,0652	0,0563
Test 9	3	Driver 18	23	3	5	f	0,0544	0,0560
Test 10	1	Driver 23	26	3	8	m	0,0411	0,0255
Test 11	2	Driver 23	26	3	8	m	0,0411	0,0163
Test 12	3	Driver 23	26	3	8	m	0,0555	0,0382
Test 13	1	Driver 24	24	2	6	f	0,0851	0,0631
Test 14	2	Driver 24	24	2	6	f	0,0820	0,0589
Test 15	3	Driver 24	24	2	6	f	0,0820	0,0589
Test 16	1	Driver 25	26	2	8	m	0,0675	0,0405
Test 17	2	Driver 25	26	2	8	m	0,0440	0,0321
Test 18	3	Driver 25	26	2	8	m	0,0442	0,0186
Test 19	1	Driver 4	38	2	20	m	0,1461	0,0443
Test 20	2	Driver 4	38	2	20	m	0,0644	0,0760
Test 21	3	Driver 4	38	2	20	m	0,0339	0,0516
Test 22	1	Driver 26	26	2	8	f	0,2343	0,0773
Test 23	2	Driver 26	26	2	8	f	0,0987	0,0677
Test 24	3	Driver 26	26	2	8	f	0,0927	0,0397
Test 25	1	Driver 27	24	3	6	f	0,0402	0,0231
Test 26	2	Driver 27	24	3	6	f	0,0310	0,0194
Test 27	3	Driver 27	24	3	6	f	0,0391	0,0325
Test 28	1	Driver 9	40	4	20	m	0,0526	0,0395
Test 29	2	Driver 9	40	4	20	m	0,0285	0,0243
Test 30	3	Driver 9	40	4	20	m	0,0294	0,0257
Test 31	1	Driver 21	24	5	6	m	0,1116	0,0489
Test 32	2	Driver 21	24	5	6	m	0,0390	0,0328

Test 33	3	Driver 21	24	5	6	m	0,0305	0,0294
Test 34	1	Driver 28	24	2	6	f	0,1224	0,0635
Test 35	2	Driver 28	24	2	6	f	0,0737	0,0368
Test 36	3	Driver 28	24	2	6	f	0,1466	0,0487
Test 37	1	Driver 10	32	4	14	m	0,0637	0,0193
Test 38	2	Driver 10	32	4	14	m	0,0534	0,0535
Test 39	3	Driver 10	32	4	14	m	0,0590	0,0459

19 Annex 12 – Municipality/Highway society business model canvas

eMobility BM – Municipality/Higway Society as CPM				
KEY PARTNERS	**KEY ACTIVITIES**	**VALUE PROPOSITION**	**CUSTOMER RELATIONSHIPS**	**CUSTOMER SEGMENTS**
energy supplier	RFID vehicles targeting	**Street "owner"**	toll direct payment	traditional customers with ICE
infrastructure suppliers	IT systems management	dynamic charging along routes	RFID automatic payment	private EVs owners
electric mobility consultants	infrastructures maintenance	static fast charging areas availability	customer service by phone	other companies as EVs owners
IT systems provider	employees	"at least costant SOC" energy management system	RFID charging data transmission on board	other CPM (charging stations along routes)
distribution system operator	marketing campaigns	"toll + energy" billing	on board problem signals	TSO (V2G deals)
transmission system operator	consultants	special prices for transport companies with many EVs		
other CPM along routes	**KEY RESOURCES**	parking and service areas availability	**CHANNELS**	
	traditional highway infrastructures		higway customers points	
	dynamic charging infrastructures		RFID automatic billing	
	energy management system		web site	
	billing system (energy and toll)		energy direct delivery	
	maintenance vehicles fleet		charging information on board	
	marketing office			
	commercial office (energy and toll pricing)			
	toll and maintenance employees			
	infrastructure and IT engineers			

COST STRUCTURE	REVENUE STREAMS
energy purchasing	tolls
cost of infrastructures	fixed energy fares by distances and vehicle class
infrastructures maintenance	revenues from CPM for charging stations on routes
cost for IT systems (energy management and billing)	deals with transport companies for many vehicles
cost for employees	V2G deals
cost for consultants	